INFORMATION TO USERS

This manuscript has been reproduced from the microfilm master. UMI films the text directly from the original or copy submitted. Thus, some thesis and dissertation copies are in typewriter face, while others may be from any type of computer printer.

The quality of this reproduction is dependent upon the quality of the copy submitted. Broken or indistinct print, colored or poor quality illustrations and photographs, print bleedthrough, substandard margins, and improper alignment can adversely affect reproduction.

In the unlikely event that the author did not send UMI a complete manuscript and there are missing pages, these will be noted. Also, if unauthorized copyright material had to be removed, a note will indicate the deletion.

Oversize materials (e.g., maps, drawings, charts) are reproduced by sectioning the original, beginning at the upper left-hand corner and continuing from left to right in equal sections with small overlaps. Each original is also photographed in one exposure and is included in reduced form at the back of the book.

Photographs included in the original manuscript have been reproduced xerographically in this copy. Higher quality 6" x 9" black and white photographic prints are available for any photographs or illustrations appearing in this copy for an additional charge. Contact UMI directly to order.

UMI®

Bell & Howell Information and Learning
300 North Zeeb Road, Ann Arbor, MI 48106-1346 USA
800-521-0600

Analysis of Time-Dependent Effects on Segmental Prestressed Concrete Curved Box-Girder Bridges

Ahmed S. Debaiky

A Thesis

in

School for Building

Civil Engineering Program

Presented in Partial Fulfilment of the Requirements
for the Degree of Master of Applied Science at

Concordia University

Montreal, Quebec, Canada

June 1997

ABSTRACT

Analysis of Time-Dependent Effects on Segmental Prestressed
Concrete Curved Box-Girder Bridges

Ahmed S. Debaiky

Curved concrete box-girder bridges are basic elements of today's modern highway system. These bridges are normally built in stages over relatively long periods of time. In each stage of construction, units or segments of the bridge are cast or placed in their required positions and tied together by post-tensioned prestressing tendons. During the construction process, the structure undergoes changes in geometry, in statical system, and in distribution and/or magnitude of external loads and prestressing. This leads to continuous variations in the stresses and deformations. Creep and shrinkage of concrete and relaxation of prestressed steel magnify these effects during construction and over the service life of the structure. Development of the time-dependent effects in curved bridges depends heavily on the restraint provided at the supports.

In the present thesis, a numerical technique is introduced and a computer program is developed for the time-dependent analysis of segmentally erected curved prestressed box-girder bridges and other structures. The program is capable of predicting the response of such structures throughout their various stages of construction and service load history. The analysis accounts for the effects of concrete creep and shrinkage, prestressed steel relaxation, differences in age between concrete segments, sequence of construction and changes in geometry and support conditions. Deviations in the positions of new segments

due to the deformation of completed part of the structure needed to calculate formwork adjustment are accounted for in the analysis.

The procedure is based on the displacement method of analysis where multi-node variable cross-section beam elements curved in space, as well as conventional prismatic straight elements, are used to model bridges of arbitrary geometry. Prestressed tendons can have any profile in the space and can be prestressed, restressed or removed at any construction stage. Prestress losses due to friction and anchor setting are automatically evaluated by the program. A Step-by-Step approach is used to model the construction processes and to calculate the time-dependent effects at any instant during and after construction.

Several verification problems are presented to validate the computer program. A three-span continuous curved bridge example is analyzed to demonstrate the applicability of the program. A study on the effects of skew support alignments on the development of time-dependent stresses and deformations in prestressed concrete curved bridges is carried out.

To The Greatest Parent in the world

and The Most Loving Uncles, Mimi and Osama

Acknowledgment

It is a pleasure to the author to present his deep and sincere gratitude to **Dr. M. M. El-Badry**. Throughout the period of this research he was truly committed to the supervision and guidance of the author. His determination for a solid and perfect work performance is the corner stone behind the quality of the research presented.

Also, the financial support provided by the Natural Science and Engineering Council of Canada, NSERC, and by Concordia University is deeply acknowledged.

The author would like to acknowledge the support of two fine gentlemen. **Dr. Hany Abdallah** and **Mr. Mohamed Khedr** were most encouraging, helpful and supportive. They simply represent the quality of people one can find once in the life time.

To my friends, **Dr. M. Abdel Rahman, Dr. N. El-Sheemy, A. El-Agroudy, B. El-Ariss** and **R. El-Hacha** and their families, true and heartily thanks are due for their care and help.

The support and inspiration from my friends A. Ibrahim, Alaa, Marco and M. Aglaan is also greatly appreciated.

Table of Contents

THREE: Analysis of Variable Stress Regimes

FOUR: Analysis of Prestressed Curved Segmental Structures

List of Figures

List of Tables

List of Symbols

A	=	*cross-section area of a member*
$A_{y'}$ and $A_{z'}$	=	*reduced shear areas in local y and z directions*
A_{ps}	=	*cross-section area of prestressed tendon*
$[B]$	=	*strain-displacement matrix of curved element*
$\{\bar{D}\}$ and $\{D\}$	=	*vectors of local and global nodal displacements*
$[D]$	=	*elasticity matrix*
E_c and $\bar{E}_c$	=	*modulus of elasticity and aged-adjusted modulus of elasticity*
E_s	=	*modulus of elasticity of prestressed steel*
$e_{s,y'}$ and $e_{s,z'}$	=	*local eccentricities of shear centre in cross-section*
$e_{y'}$ and $e_{z'}$	=	*local eccentricities of prestressing tendon*
F_n	=	*force or reaction at degree of freedom n*
$\{F\}$	=	*vector of consistent nodal loads*
$\{\Delta F'\}_1$	=	*time-dependent change in fixed-end forces at Node 1 in straight elements*
f'_c	=	*characteristic strength of concrete*
f_{cm}	=	*mean compressive strength of concrete*
f_{ptk}	=	*yield stress of prestressed steel*
$[H]$	=	*transformation matrix*
h_o	=	*notional member size*
$J_{x'}$, $I_{y'}$ and $I_{z'}$	=	*torsional constant and principal moments of inertia*
$[k_e]$	=	*member stiffness matrix*

$[\bar{k}]_1$ = *age-adjusted stiffness matrix for straight element corresponding to 6 D.O.F. at Node 1*

k = *constant for steel relaxation depends on prestressed steel type*

$[L]$ = *transformation matrix for straight elements*

$M_{x'}$ = *torsional stress about local axis*

$M_{y'}$ and $M_{z'}$ = *bending stresses about local axes*

N = *normal stress in local direction*

$N(\zeta)$ = *interpolation shape function*

n = *magnitude of principal normal vector (curvature) to a point on a prestressed tendon*

$\{\hat{n}\}$ = *vector of principal normal to a point on a prestressed tendon*

R = *radius of curvature of prestressed tendon*

RH = *relative ambient humidity*

$r(t, t_o)$ = *relaxation function of concrete*

r_n = *nodal deformation at degree of freedom n*

s = *coefficient for creep and shrinkage depends on cement type*

$P(\zeta)$ = *prestressing force at any point along a prestressing tendon*

$\Delta\bar{P}_i$ = *prestrssing force loss due to increment of nodal displacements*

$[T]$ = *transformation matrix*

t = *time*

$V_{y'}$ and $V_{z'}$ = *shear stresses in local directions*

$q(\zeta)$ = *magnitude of the distributed load*

u = *cross-section perimeter*

$\{u\}$ = *vector of nodal displacements in global directions*

x_i, y_i *and* z_i = *global coordinates on a node*

α_i, β_i and γ_i = *angles between prestressing tendon and local axes of the member at any point*

β = *prescribed nodal displacement*

$\beta_c(t, t_o)$ = *function describes development of creep with time*

$\beta_{cc}(t)$ = *function describes development of concrete strength with time*

β_H = *function to account for the effect of relative humidity and member size on development of creep with time*

$\beta_s(t, t_o)$ = *function describes development of shrinkage with time*

$\{B\}_t$ = *strain-displacement matrix of a prestressing tendon*

γ_c = *correction factor for curing effect on creep*

γ_{cs} = *correction factor for curing effect on shrinkage*

Δ = *increment (applied to several parameters)*

$\Delta\varepsilon_o$, $\Delta\theta_{x'}$, $\Delta\psi_{y'}$ and $\Delta\psi_{z'}$ = *increment of strain components at a cross-section*

$\{\Delta d\}_1$ = *vector of nodal displacements in local directions at Node 1 for straight elements*

$\{\Delta F_{pr}\}$ = *vector of equivalent nodal forces due to prestressed steel relaxation*

$\{\varepsilon\}$ = *vector of generalized nodal strains in curved element*

ε_{cso} = *notional shrinkage coefficient of concrete*

η = *coefficient for steel relaxation depends on steel quality*

$\theta_{z'x}$, $\theta_{z'y}$, and $\theta_{z'z}$ = *angles between local z axis of a prismatic element and the global x, y, and z axes*

λ = *ratio of initial to tensile stress in prestressed steel tendon*

$\{\lambda_{x'}\}$, $\{\lambda_{y'}\}$, and $\{\lambda_{z'}\}$ = *vectors of direction cosines between local member axes and the global x, y, and z axes*

$\{\lambda_{cn}\}$ = *vector of unit principal normal to a point on a prestressed tendon*

$\{\lambda_t\}$ = *vector of unit tangential to a point on a prestressed tendon*

σ_{pso} = *initial stress in prestressed steel*

$\Delta\sigma_{pr}$ and $\Delta\bar{\sigma}_{pr}$ = *intrinsic and reduced relaxation of prestressed steel*

$\{\sigma\}$ = *vector of generalized local stresses*

Φ = *angle describes orientation of curved member cross-section*

ϕ_{RH} = *creep coefficient as a function of relative humidity and member size on notional creep coefficient*

ϕ_o = *notional creep coefficient*

$\phi(t, t_o)$ = *concrete creep coefficient at time t when loaded at time* t_o

ϕ_u = *ultimate creep coefficient*

χ = *aging coefficient of concrete*

χ_r = *reduction factor for prestressed steel relaxation*

Ω = *ratio used in for steel relaxation as in Equation* (2.14)

ζ = *natural curvilinear coordinate*

CHAPTER ONE

Introduction and Literature Review

1.1 General

In highway bridge construction there has been a strong trend towards the use of longer, multi-span bridges. This trend has developed as a result of reasons related to the economy, availability of space and complexity of natural and artificial obstruction. Among the various types of bridges, curved bridges have become much more desirable than ever.

Use of prestressing in bridges is a vital component as they are subjected to high internal forces and stresses. The main purpose of prestressing is to counteract the effects of dead and live loads, i.e, to produce opposite bending and torsional moments and to minimize the deflection of different spans of the bridge.

Segmental construction is one of the most popular techniques for building prestressed concrete bridges. One advantage of this technique is elimination of false work and temporary supports by adopting the cantilever construction method which results in no objection to traffic or water way beneath the bridge.

Multi-span straight or curved bridges are usually constructed over a long period of time during which the structure experiences continuous changes in the statical system and in support, loading and environmental conditions. Because of these conditions, the deformations and internal forces within a constructed part of the bridge change dramatically and, in some cases, can be greater in value than in the completed bridge. Accurate evaluation of stresses and deformations in each construction stage is essential in

order to maintain safety levels and to ensure the required alignment of the bridge. The long term behavior of the structure after completion of construction is highly affected by the method and sequence of construction.

Among the various parameters that affect the long term behaviour of bridge structures, the time-dependent properties of concrete and prestressed steel have the greatest effects on the bridge behaviour during and after construction. Changes in deflection and stresses are strongly affected by creep and shrinkage of concrete and relaxation of prestressed steel. The rate of creep, shrinkage and relaxation is generally high during the early ages of concrete and stressed steel and decreases continually with time under the same environmental conditions.

Time-dependent effects on structural behaviour differ from one statical system to another. For example, in a determinate structure, creep and shrinkage result in redistribution of strains and stresses within individual sections meaning a decrease in the compression in concrete and in the tension in steel. In statically indeterminate structures, additional changes in stresses and in the reactions will develop producing continuous variation of internal forces along the bridge with time. In a continuous curved structure, the restraint on the direction of movement provided at each support has a significant effect on the magnitude of the time-dependent internal forces produced in such structures. Relaxation of prestressed steel means a decrease of stress with time under constant (initial) strain, and hence, a continuous loss of prestressing force.

A number of numerical techniques and computer programs is available in the literature for the time-dependent analysis of segmental prestressed structures. However, a very limited number of these programs deals with the analysis of curved bridges and only

in a simplified manner.

1.2 Objective and Scope

The main objective of this research is to develop a numerical procedure and a computer program for the analysis of the time-dependent behaviour of segmentally erected curved prestressed concrete box-girder bridges. The analysis gives the instantaneous and time-dependent changes in the displacements, in the support reactions and in the internal forces from which the strains and stresses at various sections of the structure can be calculated. The analysis accounts for the effects of sequence of construction, loading and prestressing and changes in the statical system and support conditions.

The numerical procedure is based on the displacement (stiffness) method of strucutral analysis. The structure is idealized as a space frame assembled of multi-node curved elements and/or prismatic straight elements modelling the concrete segments. The prestressing tendons are also modelled as multi-node curved elements and can thus have any profile in the space. The multi-node curved element utilized in the present analysis is the one developed by Jirousek (1981). The element can have a minimum of three nodes and a maximum of six nodes. Material properties and age of concrete can vary from one element to another. This idealization can thus be suitable for modelling bridges with arbitrary alignment built in stages.

The analysis is done step-by-step for which the time is divided into intervals, the start of each coincides with an event such as addition of new concrete segments, application or removal of loads or prestressing, or changes in support conditions. In each interval, two analyses are performed; the first gives the instantaneous effects at the beginning of the interval and the second is for the time-dependent changes over the length

of the interval. The increments of displacements, reactions and internal forces calculated in any interval are stored to be used for the next time-intervals and are added to the previous values to give updated totals, thus giving the history of the bridge behaviour during and after construction.

Prediction of the time-dependent properties of concrete, namely, the modulus of elasticity, creep coefficient and shrinkage strain, is based on the recommendations of either the CEB-FIP model Code (1990) or the ACI Committee 209 (1992).

The analysis procedure is implemented in the computer program TD-SFRAME: Time-Dependent Analysis of Space FRAMEs (Debaiky and El-Badry, 1997). The program is an extension of program SFRAME developed by Maher (1985) in his studies on control of torsional moments produced by prestressing in curved bridges. TD-SFRAME is suitable for the time-dependent analysis of a wide range of prestressed structures constructed in stages.

1.3 Outline of the Thesis

In the following sections of this chapter, the concepts of analysis of horizontally curved structures will be reviewed. The effects of time-dependent deformations on the behaviour of curved structures will be briefly discussed. The previous work related to the analysis of segmentally erected prestressed structures will be reviewed. A brief description of the most commonly used methods of analysis of creep of concrete is given. The advantages and shortcomings of each method will be briefly discussed.

In Chapter 2, the material properties of concrete and prestressed steel pertaining to the time-dependent analysis are discussed and the relevant expressions adopted in the present investigation for prediction of time variations of these properties are given.

In Chapter 3, the step-by-step procedure employed in this thesis for the analysis of time-dependent stresses and strains under variable stress regimes is explained. The numerical procedure for prediction of the displacements, reactions and internal forces in segmentally erected curved prestressed concrete box-girder bridges is presented in Chapter 4. The validity of the proposed method of analysis and the applicability of the computer program are demonstrated in Chapter 5 by comparison with experimental data and with the results of analytical methods and by the analysis of three-span continuous segmentally constructed prestressed box-girder bridge with arbitrary alignment in plan. A study on the effects of restraints provided by the supports on the time-dependent behaviour of continuous curved bridges is also carried out in Chapter 5.

Finally, a summary of the investigation, the conclusions reached and recommendations for further research are given in Chapter 6.

1.4 General Concepts of Analysis of Curved Structures

Modern curved bridge systems which have been developed and constructed over the past few decades can be categorized into two different types: open-section type and closed-section type. Figures 1.1 and 1.2 show examples of cross sections of the two types. In open-section type, the internal forces consist of bending and torsional moments as well as warping stresses varying over the longitudinal axis of the bridge. When the transverse distortion of the cross-sections is prevented, e.g. by means of transverse diaphragms, transverse bimoment (warping torsion) develops. The existence of warping is significant and can never be ignored (Bell and Hiens, 1970). Thin-walled members subjected to torsion fall also in this category.

In the closed-section type, warping stresses and transverse distortion of the cross-

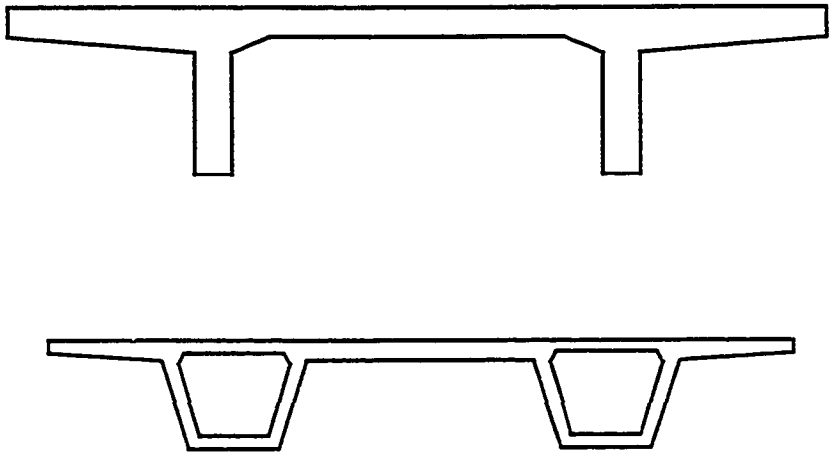

Figure 1.1 **Examples of Open Bridge Cross-Sections**

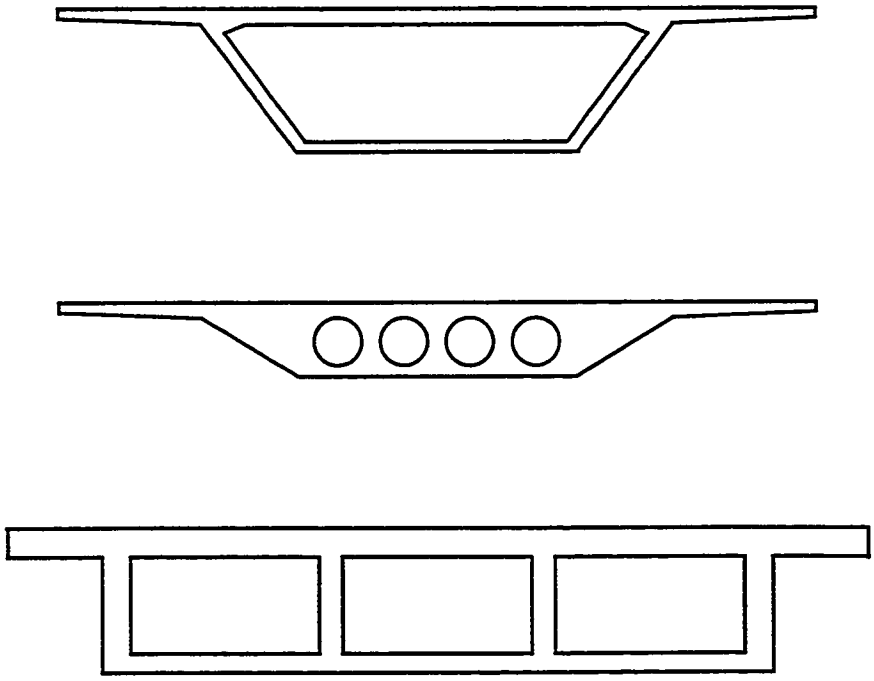

Figure 1.2 **Examples of Closed Bridge Cross-Sections**

section have relatively small values and can thus be ignored under the following conditions:

a) The cross-section consists of a closed shape, Figure 1.2 or single girder. No openings in the deck or bottom slab are present.

b) Plane sections along the longitudinal axis remain plane after deformations. This is the physical meaning of no warping of the cross-section.

c) Cross-section can be condensed to a single node, i.e. compacted form. This prevents occurrence of transverse distortion.

For box-girder cross-section, the second condition is usually satisfied even for bridges with relatively high slenderness (Span/Width) ratios. The span is defined as the distance between inflection points of bending moment due to dead load only while the width is the distance between the webs. A value of 4 is usually recommended as a limiting ratio (Maher 1985). This ratio is usually utilized in most modern bridges especially those with single box sections. For this type of bridges, a space frame analysis can be considered sufficient.

Menn (1990) presented simplified equations for calculating internal forces in curved bridges. The equations of Menn, although very useful for practising engineers, are not general as they cover only special cases of loading and geometry. Menn recommended that a simplified frame analysis be used to tackle curved bridge problems when applicable. He also stated that even for computing the transverse stresses in the cross section, a second step investigation that gives accurate results compared to a finite element analysis can be done separately.

Several investigations have shown that analysis of a curved bridge as a group of

linear beam elements using elastic frame theory gives results of reasonable accuracy with a considerable reduction in computational time and storage. Traditional methods of structural analysis such as virtual work, the flexibility method and the stiffness method have been utilized by many researchers (Engel, 1967, Reddy and Tuma, 1967, and Bazant and El-Nimeiri, 1974) to analyse structures with curved elements simplified as linear beam elements. The stiffness method of analysis is adopted in the present research as detailed Chapter 4.

1.5 Choice of Curved Beam Elements

During the past few decades, an extensive research work was carried out by many researchers to obtain the best performing model of curved elements. The first attempt was made by Timoshenko and Gere (1961) who introduced a differential equation for a solid curved element. The theory was limited by the condition that warping stresses are ignored and also was limited to two types of uniform loading. Valsov (1961) formulated generalized differential equations including warping. The proposed equations were limited to horizontally curved beams only. The mathematical complexity of these equations precludes their use in practical design or advanced research work.

A group of basic curved beam elements were developed from the direct stiffness method. El-Amin and Brotton (1976), Thornton and Master (1977), Hsu, Fu and Schelling (1990) introduced new formulations for horizontally curved circular beam elements which include warping degree of freedom. Wang and Merrill (1988) derived general stiffness coefficients for curved beams of either cyclodial, catenary, elliptic or sine arc segments. Unfortunately, the above beam elements, when used to model structures with variable or double curvature or with varying surface superelevation, a relatively fine discretization of

the structure is needed to obtain satisfactory results.

A totally different approach to the analysis of curved structures was followed by Bazant and El-Nimeiri (1974). The curved geometry was modelled as a series of straight two-node elements with skew ends. The element nodal degrees of freedom include, in addition to the traditional six degrees of freedom, a longitudinal warping and transverse distortion of the cross section. The element can have only straight segments of prestressing tendons between the nodes. In comparison with the Jirousek multi-note isoparametric element adopted for the present study, the element of Bazant and El-Nimeiri, in spite of having skew ends, is not suitable for modelling complex and practical variation of geometry in space.

Ferguson and Clark (1979) introduced a three dimensional isoparametric beam element which is superior to the above mentioned elements in its capability to be of any arbitrary geometry in space rather than in plane and to have variable cross-sectional area. On the other hand, the element cross-section must be of a rectangular shape which limits the applicability of the element to model most of the modern bridges. Jirousek and Bouberguig and Saygun (1979) concluded that the element also fails to represent the transverse shear or torsion response of curved bridges. This is due to the fact that the commonly used shear correction factor cannot accurately tune both behaviours at the same time.

The multi-node isoparametric element adopted for the present study was firstly introduced by Jirousek (1981) as a member of a family of isoparametric curved elements of a general, compact cross section. The formulation of the element is based on beam theory and takes into account both the transverse shear deformation and the shift in shear

centre location. The element can be defined by a minimum of three nodes and a maximum of six nodes and can thus be used to model any arbitrary geometry in space. The cross section can be of any shape (provided the user will be able to define its properties of reduced shear area and location of shear canter). The cross-section geometry can also vary from one node to another. Superelevation of any bridge deck can be described using the cross section orientation that may vary along the bridge length. The element can include prestressing tendons of any arbitrary layout described by cable eccentricities defined with respect to the local axes at individual cross sections. It was proven by Maher (1985) that the element provides exact results when appropriate order of nodes is chosen with matching load types. This, in addition to the above-mentioned geometric flexibility of the element, makes it the most appropriate available element for the present research.

1.6 Method of Prestressing Calculation

In order to develop a practical and feasible computer code that can analyze curved bridges or similar structures, the computation of prestressing effects on different elements should be accounted for. Calculation of equivalent forces should be automatically done by the program. The traditional way of providing these forces as input data is a tedious task because of the complexity of prestressing tendon layout and sequence of stressing.

Lin (1963) was the first to introduce the "Load Balancing Method" to calculate the equivalent uniform load parallel to the plane of the tendon. It was shortly after when Rozvany (1963) concluded that the method is only accurate for shallow beams, or in other words, for tendons with large radius of curvature. In other cases of deep beams or tendons with sharp curvature, radial forces should be considered as the equivalent load.

In recent years, Van Zyl (1978) used the skew-ended two node straight element

developed by Bazant and El Nimeiri (1974). The elements only allow tendons with straight segments between the two nodes, thus any cable profile can be discretized into chain of straight segments where equivalent loads to each segment are calculated separately at the nodes only.

El-Badry (1988) employed a concrete straight element which can be of variable cross-section along its length and can contain prestressing tendons of any practical profile between the two end nodes or covering a partial length between any two sections within the element. Such an advanced element can be the optimum choice for any two dimensional analysis.

In the multi-node curved element of Jirousek (1981) selected for the current study, a prestressing tendon is defined by local eccentricities of the tendon point at each nodal cross-section. The definition of cable eccentricities is quite practical and allows any universal layout of the cable to be considered. In addition, the equivalent nodal forces are computed directly from the original cable profile and the prestressing force rather than from equivalent distributed load. This makes the Jirousek element the most appropriate element for modelling bridges of arbitrary geometry and dimensions. Details of modelling the prestressing tendons within the curved concrete element will be given in Chapter 4.

1.7 Displacements due to Prestressing, Temperature, Creep and Shrinkage in Horizontally Curved Bridges

Horizontal movements of supports can result in curved bridges due to the following effects:

1. Prestressing forces, including the effects of creep
2. Shrinkage strain and temperature variations

3. Horizontal external loads due to wind, earthquakes and braking forces

In this section, the magnitude and direction of the horizontal movements that can be expected at the supports due to the effects of prestressing, creep, shrinkage and temperature are discussed.

1.7.1 Prestressing and Creep

Consider a horizontally curved concrete cantilever beam as shown in Figure 1.3. Assume that the beam is stressed with a co-axial prestressing cable producing a concentric force at every section along the beam length. Under the effect of this prestressing, every point in the beam tends to move towards the fixed support along the curved length of the beam, or in other words, in the direction of the tangent to the curve at any point (Figure 1.3a). The radius of curvature of the beam in this case will remain unchanged while the central angle, α_o, will decrease. For a beam with variable cross section and prestressing force, the total displacement that takes place at the free end of the cantilever (point B) is given by:

$$\delta_{P(B)} = \frac{1}{E} \cdot \int_0^S \frac{P(s)}{A(s)} dS \qquad (1.1)$$

where E, P, A and S are the modulus of elasticity, the prestressing force, the cross sectional area and the curved length of the beam, respectively. The concrete strain at any point is:

$$\varepsilon = \frac{\delta_{P(B)}}{S} \qquad (1.2)$$

The central angle in this case will change to $\alpha = \alpha_o(1 + \varepsilon)$. Creep of concrete will have a similar effect as the prestressing force.

1.7.2 Shrinkage and Temperature Change

With a temperature change or shrinkage, each point on the beam will move along

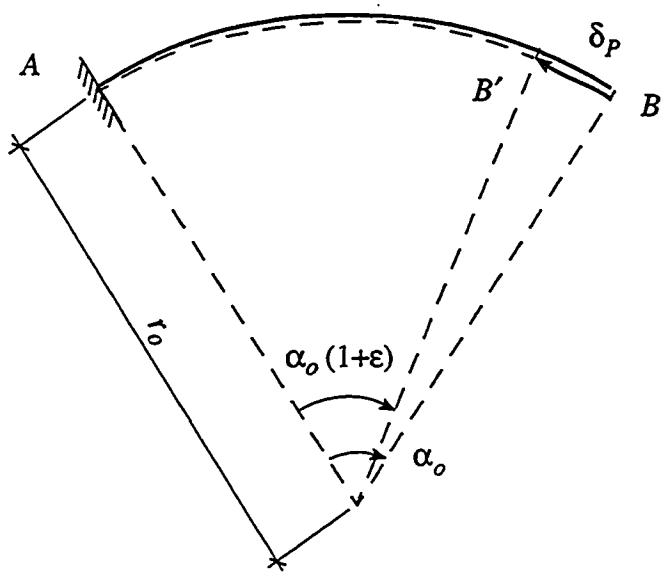

(a) Co-Axial Prestressing and Creep

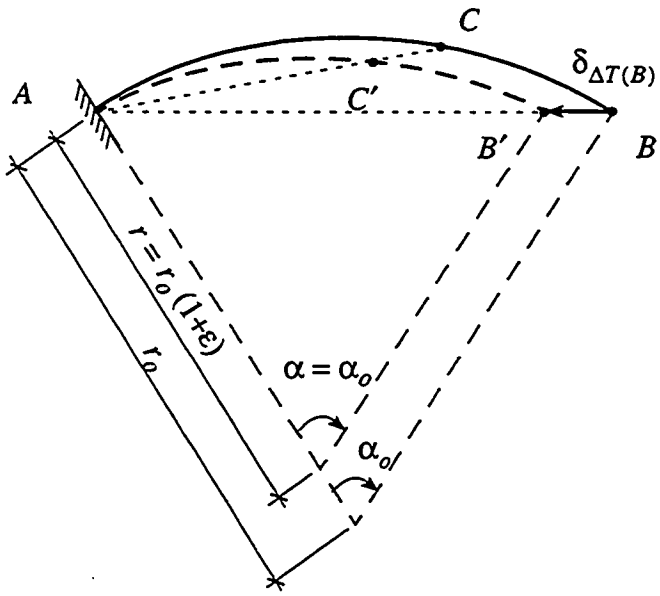

(b) Temperature Drop or Shrinkage

Figure 1.3 **Longitudinal Displacements of Horizontally Curved Beam due to Different Effects.**

the straight line between its original position and the fixed end (Figure 1.3b). In this manner, the central angle of the beam remains unchanged while the radius increases with an increase in temperature and decreases with shrinkage or with a drop in temperature. For the beam in Figure 1.3b, the total displacement of the free end of the cantilever (point B) due to a change in temperature, ΔT, is given by

$$\delta_{\Delta T(B)} = \alpha \cdot \Delta T \cdot L \tag{1.3}$$

where α is the coefficient of thermal expansion and L is the length of the chord AB. The movement due to shrinkage can be also calculated from Equation 1.3 by replacing $\alpha \cdot \Delta T$ by shrinkage strain, ε_{cs}.

The beam radius will thus change to the value $r = r_o(1 + \varepsilon)$, with $\varepsilon = \alpha \cdot \Delta T$ or ε_{cs}. A positive value of ε is used for an increase in temperature while a negative value is used for shrinkage or a temperature drop.

1.7.3 Forces Developed When Free Movements are Prevented

Free movements at the supports in curved bridges can not normally be allowed because of the wind forces. Also, at the expansion joint, movement should not deviate substantially from the tangent to the bridge axis.

If the bearings do not allow free movements in all directions, horizontal forces are developed and have to be resisted by the superstructure and substructure. Such forces are important for the design of the bearings and the substructure; however, they are normally neglected in the design of the superstructure. It should be noted, however, that the forces induced by preventing the movement due to temperature develop in their full magnitude. On the other hand, the forces induced from shrinkage are reduced by creep and the forces introduced by initial prestressing are reduced by the prestress loss only.

For alignment of the bearings, the deformation due to temperature is often the governing factor. For this reason, the bearings are normally aligned to allow movement in the direction to or from the fixed bearing. However, this is not a strict rule. If a bridge is very highly prestressed, the deformations due to prestressing may be of the same order of magnitude as those due to shrinkage and temperature. In this case, the alignment of the bearing should be studied carefully before a decision is made. In Chapter 5 of this thesis, an investigation is conducted into the effects of alignment of the bearings on the time-dependent behaviour of curved bridges.

1.8 Segmental Construction: History and Previous Investigations

The use of longer span bridges which became the most popular trend in the past three decades has raised a new construction problem. Construction of such bridges using conventional precast prestressed concrete bridge girders became impossible because of the maximum transportable weight and/or length of these girders. The development of precast segmental construction was the only solution that could combine the advantages of both precasting and post-tensioning concepts. Segmental construction was also used to build cast-in-situ type of bridge. Different methods were introduced under the concept of segmental construction. Launching of elements or segments is carried out using one of the following four methods: balanced cantilever, span-by-span, progressive placing and incremental launching. According to Ziadat (1988), each of the previous methods is best suited for a different range of typical spans and total bridge length as shown in Table 1.1

Table 1.1 **Characteristics of Different Segmental Construction Methods**

Segmental Construction Method	Total bridge length(m)	Typical span length(m)	Approx.% of total
Balanced Cantilever	> 1000	50 - 240	75
Span-by-Span	1500 - 2000	30 - 60	15
Progressive Placing	300 - 400	25 - 55	5
Incremental Launching	250 - 350	25 - 55	5

Because of the relatively young age of segmental construction techniques, only few detailed investigations into the behavior of segmentally erected bridges have been published to date. The very first study was carried out by Scordelis (1966) in which simply supported box-girder bridges were investigated. The analysis was later extended to multi-span bridges (Scordelis, 1967). This work of Scordelis was limited only to straight bridges and did not consider time-dependent effects on such structures.

A series of reports, published by the University of Texas at Austin, USA, on research directed by Breen (1969-1975), covered problems relating to segmental cantilever bridges (see for example, Brown, Burns and Breen, 1974). These reports summarized design procedures and criteria and investigated construction problems. A very powerful product of the research effort was a computerized incremental analysis procedure for segmental construction. The program was verified by Kashima and Breen (1975) who built and tested a model of Christi Bridge constructed in the USA. Time-dependent deformations were not taken into account in this investigation.

Tadros, Ghali and Dilger (1980) developed a computer program for prediction of long-term stresses and deformations in segmentally erected structures including the time-dependent effects. The program is recognized for taking into account the variation of

material properties and the changes of structural system during the construction period. Also, the program was developed to solve for the redistribution of internal stresses after continuity is established. Following a different approach, Abdel Halim (1982) employed the finite element method to predict the behavior of segmental post-tensioned concrete bridges through their elastic, plastic and failure stages. All the materials involved in the structure such as concrete, prestressed and non-prestressed steel were modelled. A numerical solution using both iterative and incremental techniques was developed to predict the redistribution of stresses between the three materials at post-cracking non-linear stages. The results were compared to an experimental segmental bridge model built for this purpose and tested up to failure. The two above-mentioned computer programs are limited to plane frame analysis.

Several other investigations on the behaviour of planer segmentally erected bridges include those by Ketchum (1986), Ziadat (1988), Kim (1990) and Abdel Karem (1991). These investigations were limited to the linear stage of structural behaviour. No significant differences between them can be highlighted, except for the one by Kim where a probabilistic study was conducted to predict confidence limits for long-term deflections and internal forces.

The most recent research work dealing with segmental construction was that carried out by El-Badry and Ghali (1989) as part of investigation into serviceability of concrete structures. A computer program for plane structures was developed which performs non-linear analysis of structures. The concrete member can be made up of different layers each installed at different time as in cast-in-place box-girder bridges. The analysis recognizes both prestressed and non-prestressed steel. Prestressed tendons can be

of any layout. Analysis of the cross-section is carried out in both the non-cracked and cracked stages. Time-dependent parameters are introduced by built-in functions or can be specified by the user. The program is considered the most powerful program ever developed for the analysis of two dimensional structures.

1.9 Methods of Creep Analysis of Structural Members

The mathematical prediction of creep effects in concrete structures is a complex problem even with the use of simplified linear forms of creep laws. Several methods of creep analysis were developed and used successfully during the past thirty years, with each having its own advantages and hence suited certain cases of applicability.

1.9.1 The Rate of Creep Method

The basis of this method was firstly established by Glanville (1930) when he concluded from experiments on young concrete that at any age of concrete, t, the rate of creep is independent of the age of application of the load. The mathematical formulation was later developed by Whitney (1932) and was applied to complex problems by Dischinger (1937). The assumption of the constant rate of creep means that creep curves are parallel for all ages of load application. This means that creep decreases very rapidly with increasing age at loading. Thus, creep deformations under increasing stresses are underestimated.

1.9.2 The Rate of Flow Method

This method was introduced by England and Illston (1965) to overcome the deficiencies of the Rate of Creep method. They proposed to represent the creep function as the sum of three components: elastic, delayed elastic (recoverable) and flow (irrecoverable) strains. Delayed elastic strain was recognized to be independent of age at

loading and reaches an ultimate value much faster than flow strain. Also, as a simplification of the method, the variation of the elasticity modulus was ignored.

This method is appreciated for its dramatic improvement over the Rate of Creep method since it properly predicts creep recovery of young concrete. However, the proposed creep function was noticed to incorrectly predict the creep of virgin concrete when loaded at later time after hardening.

1.9.3 Improved Dischinger Method

As a conclusion from the Rate of Flow method, the delayed elastic strain develops much faster than the flow component. In order to allow a simple analytical treatment for that effect, Nielsen (1970) proposed to add the delayed elastic part to the instantaneous elastic part, and then to treat the flow component in the same way as the total creep in the Rate of Creep method. The advantage of this method lies in the relatively simple analytical treatment and the good accuracy for simple practical problems in which the time after application of the load exceeds about three months. On the other hand, for old concrete, creep is underestimated as in the Rate of Flow method.

1.9.4 The Principle of Superposition of Virgin Creep Curves

The principle of superposition has been generally accepted as applicable to concrete. McHenry (1943) and Maslov (1940) modified Boltzmann's principle of superposition to include the effect of aging of concrete. Correctly interpreted, this principle means that strains produced at any time t by a stress increment applied at age $t' < t$ are independent of the effects of any stress applied earlier or later. In other words, creep curves of virgin concrete can be superimposed.

For increasing stresses and for slightly decreasing stresses, superposition of virgin

creep curves gives good agreement with experimental data, but for complete removal of load, the recovery is overestimated to some extent. However this should not be considered as a serious setback since such a case of sudden full unloading is not common in practice. The mathematical derivation of the method leads to an integration (as will be detailed in Chapter 3), which cannot be solved in a closed form, and thus, a numerical technique was developed for that purpose known as the Step-by-Step method.

1.9.5 Solution Using the Step-by-Step Approach

The Step-by-Step approach is completely general in that it can deal with any creep function and any prescribed stress or strain history. The method will be used in Chapter 3 to determine the so called "relaxation" or "aging" coefficient. This method can be used for problems with an arbitrarily prescribed stress or strain history. For the purpose of the analysis, the total time is sub-divided into a number of time steps whose length should increase with time. However, if a sudden change of stress or strain occurs within the prescribed history, a time interval of zero duration should be introduced such that the creep function for that interval, $\phi(t_j, t_j)$, degenerates to $1/E(t_j)$. The notation used for the Step-by-Step numerical analysis is defined in Figure 1.4. For best results under continuously varying stress, the time intervals Δt_j should be chosen such that their lengths are approximately equal on the log-time scale. Also for the same case, there is a number of different ways to calculate the strain due to a stress increment (or decrement) $\Delta\sigma_j$. The alternative ways are summarized in the following:

1. The stress increment $\Delta\sigma_j$ is assumed to be applied at the middle of the jth interval. The elastic strain component is calculated at that time with $E(t_j)$, and creep is determined from time t_j onwards. At the end of the jth interval, the strain increment is:

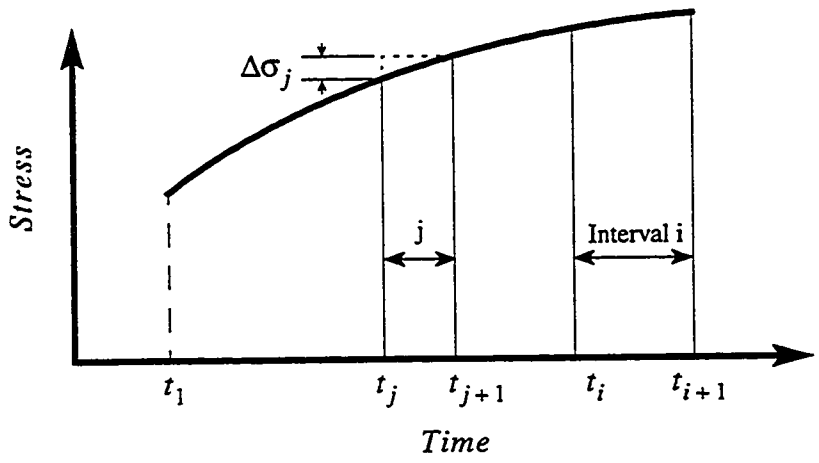

Figure 1.4 **Definition of Time Intervals and Stress Increments for the Step-by-Step Method**

$$\Delta\varepsilon_j = \frac{\Delta\sigma_j}{E(t_j)}[1 + \phi(t_{j+1}, t_j)] \tag{1.4}$$

2. In the Second method, the stress increment is assumed to be applied at the beginning of the jth interval and half of the stress increment is assumed to produce creep during the full length of the time interval. With these assumptions, the strain within the time interval j:

$$\Delta\varepsilon_j = \frac{\Delta\sigma_j}{E(t_{j-1})}\left[1 + \frac{1}{2}\phi(t_{j+1}, t_{j-1})\right] \tag{1.5}$$

3. The third method employs the trapezoidal rule where the elastic and creep properties for time interval are the average of those at the beginning and the end of the interval so that:

$$\Delta\varepsilon_j = \frac{\Delta\sigma_j}{2}\left[\frac{1 + \phi(t_{j+1}, t_{j-1})}{E(t_{j-1})} + \frac{1}{E(t_{j+1})}\right] \tag{1.6}$$

4. Finally, if relatively large time intervals are considered, Simpson's rule may be used to obtain accurate results as:

$$\Delta\varepsilon_j = \frac{\Delta\sigma_j}{6}\left[\frac{1 + \phi(t_{j+1}, t_{j-1})}{E(t_{j-1})} + 4\frac{1 + \phi(t_{j+1}, t_j)}{E(t_j)} + \frac{1}{E(t_j)}\right] \tag{1.7}$$

All the four mentioned methods are easily programmed for evaluation by computer and they all yield accurate results if a sufficient number of time steps is used. For the analysis presented in this thesis, the second method will be partially adopted. A major modification will be made to this method as the stress will be assumed to be applied at the beginning of any interval. The contribution of the so called "Aged-Adjusted Effective Modulus" will simplify the analysis as well as produce more accurate results.

1.9.6 Trost-Bazant Method (Aged-Adjusted Effective Modulus)

A practical method for directly computing the strain under a varying stress, or stress under a constant or varying strain, was developed by Trost (1967) and later improved by Bazant (1972), who called his method the "Aged-Adjusted Effective Modulus Method". This introduces the concept of an "aging" coefficient. The basic idea of the method is to modify the resultant strain (or stress) that develops during any time step due to time-dependent effects. The strain that induces this stress is treated in the method of superposition as if it were introduced suddenly at certain instant within the time step which is not true. The actual situation is that this strain develops gradually and hence it produces smaller stress. This method was initiated to cater for this difference. A detailed explanation of this method along with its implementation into the Step-by-Step method is given in Chapter 3.

1.9.7 Comparison of Different Methods for Creep Analysis

In Figure 1.5, a comparison of the different methods for creep analysis is shown (Neville, Dilger and Brooks, 1983). The strain due to a variable stress history is calculated using the aforementioned creep methods. The results show that the Rate of Creep method generally overestimates the strain produced while in the Improved Dischinger method, creep is underestimated for old concrete. The method of Superposition is believed to be the most suitable one for the analysis of variable stress problem. For increasing or decreasing stress, superposition of virgin creep curves gives good agreement with experimental data, however, for complete removal of load from the concrete, the recovery is slightly overestimated. This is not considered a serious deficiency because the case of sudden complete unloading is not common in practice.

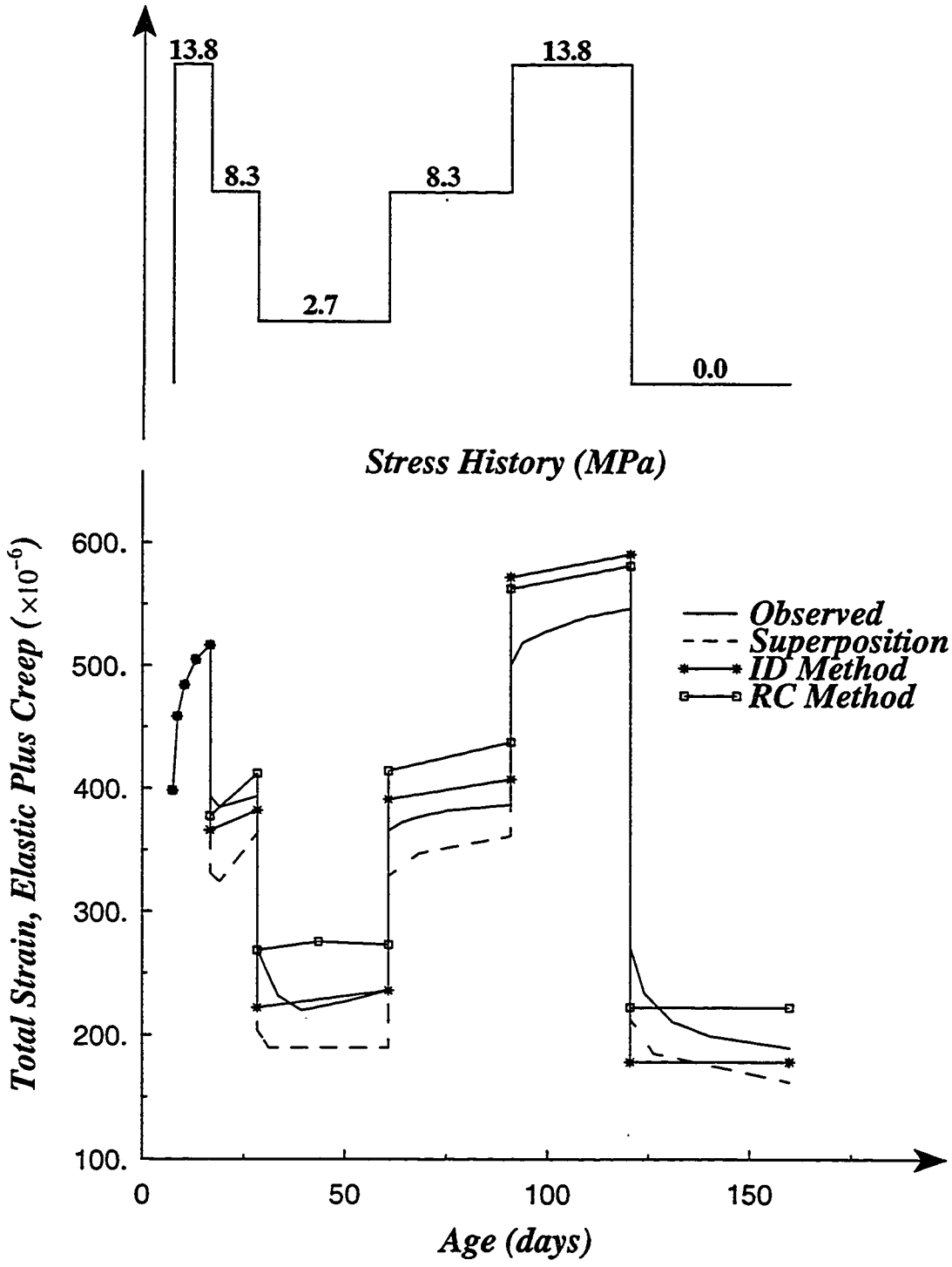

Figure 1.5 **Comparison of Strain Calculated from a Variable Stress History by Different Creep Prediction Methods.**

CHAPTER TWO

Basic Relations and Materials Properties

2.1 Introduction

The analysis of time-dependent stresses and deformations in prestressed structures requires one important set of information related to the properties of concrete and prestressed steel. The variation with time of properties such as the concrete strength, its modulus of elasticity and creep and shrinkage properties as influenced by the concrete mix, the size and shape of the concrete member, the age at first loading and the duration of load and the humidity and temperature of the surrounding atmosphere must be known for realistic prediction of the time-dependent effects. The development of prestressed steel relaxation with time is also required. This information is best obtained from results of tests conducted on specimens made of materials used in the actual structure and subjected to conditions similar to those to which the structure will be subjected. Because of the long period of time required to obtain such test results, for each structure, reliable methods and equations for prediction of the aforementioned properties of concrete and prestressed steel are available in the literature and are suitable for incorporation in computer programs for the required analysis. The most commonly used sources for prediction of these properties are the CEB-FIP Model Code (1990) and the ACI Committee 209 (1992).

In this chapter, the behaviour characteristics of concrete and prestressed steel under service conditions are briefly reviewed. Analytical expressions for prediction of the magnitude of their properties and their variation with time are also given.

2.2 Strain Components in Concrete Structures

Under sustained loading, the total strain in concrete is composed of two components: instantaneous strain and time-dependent strain. The instantaneous strain is the elastic strain that takes place immediately after application or removal of external load or prestressing force; its magnitude depends primarily on the magnitude of the load and

the modulus of elasticity, E_c at the time of loading. Time-dependent strains falls into two categories: stress-dependent strains known as "Creep", and stress-independent strains known as "Shrinkage".

2.2.1 Creep of Concrete

Creep of any material in general is defined as the increase of strain with time under constant sustained stress. Creep of concrete is recognized to be compound of two components (England and Illiston, 1965):

i) Delayed elastic creep (recoverable creep): This part of creep develops rapidly after application of load with a decaying rate to reach a limiting value in a short period. This limiting value changes slightly with the age of concrete at loading. In its report, CEB-FIP (1978) established the fact that the time of recovery after unloading differs from the time of development after loading. This delayed elastic creep strain is known to be independent of temperature and relative humidity.

ii) Creep flow (irrecoverable creep): This part has no limiting value and develops at a lower rate than the first part. It is also highly affected by the surrounding environmental conditions such as ambient temperature and relative humidity. Furthermore, the creep flow can be divided into three components, namely, basic flow, rapid flow and drying flow (Rüsch et al., 1973). The three components were found to be temperature dependent, but only the first two components are humidity dependent. Thus the creep flow can be treated as one sum only under the condition of constant humidity ratio.

2.2.2 Shrinkage of Concrete

Shrinkage of concrete is the decrease in its volume under zero stress due to loss of moisture. This change in volume of concrete occurs gradually with time starting from the moment of termination of curing of concrete. The rate of shrinkage decreases with time till it reaches a limiting value depending on the mix components, ambient temperature and relative humidity. The development of concrete shrinkage and its ultimate value increase proportionally with water/cement ratio as the loss of mix moisture will be greater. An

increase in relative humidity or decrease in temperature produces less shrinkage for the same reason. The effect of aggregate as linking material that restrains cement paste results in less shrinkage.

2.3 Prediction Models by Engineering Societies

2.3.1 Concrete Properties According to CEB-FIP (1990) Model

The relationships recommended by CEB-FIP (1990) for predicting the variation with time of the elasticity modulus, E_c, the creep coefficient, ϕ, and the shrinkage strain of concrete, ε_{cs}, are briefly described below.

i) Modulus of Elasticity:

The development of the modulus of elasticity with time t is estimated by:

$$E_c(t) = E_c(28)\sqrt{\beta_{cc}} \tag{2.1}$$

where

$$\beta_{cc} = exp[s(1-\sqrt{28/t})] \tag{2.2}$$

where t is the age of concrete and

s = coefficient depending on the type of cement

$$s = \begin{cases} 0.38 & \text{for slowly hardening cement SL} \\ 0.25 & \text{for normally or rapid hardening cement N, R} \\ 0.2 & \text{for rapid hardening, high strength cement RS} \end{cases}$$

In Equation 2.1, $E_c(28)$, is the elasticity modulus of concrete at age of 28 days. For normal-weight concrete, $E_c(28)$ is given by:

$$E_c(28) = 21500\ \sqrt[3]{(f_{cm}/f_{cmo})} \quad \text{(MPa)} \tag{2.3}$$

where f_{cm} is the mean compressive strength of concrete at age 28 days and f_{cmo}= 10 MPa.

ii) Creep Coefficient:

Although the CEB-FIP (1990) model recognizes the fact that creep is composed of three components as defined by Rüsch et al. (1973), the effect of these components are lumped in one function. Accordingly, the creep coefficient $\phi(t, t_o)$ can be calculated as

$$\phi(t, t_o) = \phi_o \beta_c(t, t_o) \tag{2.4}$$

where

ϕ_o = notional creep coefficient given by Equation 2.5;

β_c = coefficient describing the development of creep with time after loading, see Equation 2.10;

t = age of concrete (in days) at the time considered;

t_o = age of concrete (in days) at the time of loading.

The notional creep coefficient can be estimated from:

$$\phi_o = \phi_{RH} \beta(f_{cm}) \beta(t_o) \tag{2.5}$$

with

$$\phi_{RH} = 1 + \frac{1 - \frac{RH}{100}}{0.1(\sqrt[3]{h_o})} \tag{2.6}$$

$$\beta(f_{cm}) = \frac{16.8}{\sqrt{f_{cm}}} \tag{2.7}$$

$$\beta(t_o) = \frac{1.0}{0.1 + t_o^{0.2}} \tag{2.8}$$

and

$$h_o = \frac{2A_c}{u} \tag{2.9}$$

In the above equations

f_{cm} = mean compressive strength of concrete (MPa);

RH = relative humidity of the ambient atmosphere;

h_o = notional thickness of the member (mm);

A_c = cross section area;

u = perimeter in contact with the atmosphere.

The development of creep with time is given by the function:

$$\beta_c(t, t_o) = \left[\frac{(t - t_o)}{\beta_H + (t - t_o)}\right]^{0.3} \tag{2.10}$$

with

$$\beta_H = 1.5h_o[1 + (0.012 \times RH)^{18}]^{0.3} + 250 \quad \leq 1500 \text{ days} \tag{2.11}$$

The CEB-FIP (1990) recommendations give additional functions to account for the effect of both elevated and reduced temperature and the effect of type of cement used. When prevailing temperature is higher or lower than 20 degrees Celsius, the effect of temperature on the maturity of concrete is accounted for by using adjusted age t_T in lieu of t_o or t in all the equations presented above. The adjusted age is given by:

$$t_T = \sum_{i=1}^{n}\left[\Delta t_i \exp\left(13.65 - \frac{4000}{273 + T(\Delta t_i)}\right)\right] \tag{2.12}$$

where Δt_i is the number of days in which a temperature $T(\Delta t_i)$ prevails for period i.

For the effect of concrete type, the age of concrete at loading, t_o, should also be adjusted and is given by:

$$t_o = t_{o,T}\left(\frac{9}{2 + (t_{o,T})^{1.2}} + 1\right)^{\alpha} \tag{2.13}$$

where $t_{o,T}$ is the adjusted age of concrete according to Equation 2.12 and

α = coefficient depending on the type of cement

$$= \begin{cases} -1.0 & \text{for slowly hardening cement SL} \\ 0 & \text{for normally or rapid hardening cement N, R} \\ 0.1 & \text{for rapid hardening, high strength cement RS} \end{cases}$$

iii) Shrinkage of Concrete:

The prediction model for shrinkage gives the average free time-dependent deformation of a plain concrete structural member exposed to a dry or moist environment after curing. The model is valid for ordinary normal weight concrete, moist cured at normal temperature no longer than 14 days and exposed to mean relative humidity $\geq 40\%$ at mean temperature between 5 to 30 ^{o}C.

The free strain due shrinkage (or swelling) can be evaluated by:

$$\varepsilon_{cs}(t, t_s) = \varepsilon_{cso}\beta_s(t, t_s) \tag{2.14}$$

where

ε_{cso} = notional shrinkage coefficient given by Equation 2.15;

β_s = coefficient describing the development of shrinkage with time; see Equation 2.19;

t = age of concrete (in days) at the time considered;

t_s = age of concrete (in days) at the time of termination of curing.

The notional shrinkage coefficient is given by:

$$\varepsilon_{cso} = \varepsilon_s(f_{cm})\beta_{RH} \tag{2.15}$$

with

$$\varepsilon_s(f_{cm}) = [160 + \beta_{sc}(90 - f_{cm})] \cdot 10^{-6} \tag{2.16}$$

where

β_{sc} = coefficient depending on the type of cement

$$= \begin{cases} 4 & \text{for slowly hardening cement SL} \\ 5 & \text{for normally or rapid hardening cement N, R} \\ 8 & \text{for rapid hardening, high strength cement RS} \end{cases}$$

$$\beta_{RH} = \begin{cases} -1.55 \times \beta_{SRH} & \text{for } 40\% \leq RH < 99\% \\ 0.25 & \text{for } RH \geq 99\% \end{cases} \tag{2.17}$$

where

$$\beta_{SRH} = 1 - \left(\frac{RH}{100}\right)^3 \tag{2.18}$$

The development of shrinkage with time is given by the function

$$\beta_s(t, t_s) = \sqrt{\frac{(t - t_s)}{\beta_{SH} + (t - t_s)}} \tag{2.19}$$

with

$$\beta_{SH} = 0.035 \times h_o^2 \tag{2.20}$$

where RH, f_{cm}, h_o are the same as stated earlier.

2.3.2 Concrete Properties According to ACI (1992) Model

The equations suggested by the ACI Committee 209 (1992) for prediction of the variation with time of the elasticity modulus of concrete, the creep coefficient and the shrinkage strain are given below.

i) Modulus of Elasticity:

The development of the modulus of elasticity with time t can be estimated by:

$$E_c(t) = E_c(28)\sqrt{\frac{t_o}{\alpha + \beta t_o}} \quad \text{(MPa)} \tag{2.21}$$

where the coefficients α and β are constants depending on the type of cement and curing used. For cement Type I, $\alpha = 4$ and $\beta = 0.85$ and for cement Type III, $\alpha = 2.3$ and $\beta = 0.92$.

In Equation 2.21, $E_c(28)$ is the modulus of elasticity of concrete at age 28 days. For normal-weight concrete, $E_c(28)$ can be estimated by:

$$E_c(28) = 4730\sqrt{f'_c} \quad \text{(MPa)} \tag{2.22}$$

with f'_c is the compressive strength of concrete at age 28 days in MPa.

ii) Creep Coefficient:

Creep coefficient, $\phi(t, t_o)$ at time t for age at loading t_o, is given by:

$$\phi(t, t_o) = \phi_u \frac{(t-t_o)^{0.6}}{10+(t-t_o)^{0.6}} \quad (2.23)$$

where ϕ_u is the ultimate creep coefficient given by;

$$\phi_u = 2.35\gamma_c \quad (2.24)$$

where γ_c is a correction factor, given as the product of several multipliers depending on the ambient relative humidity, average thickness of the member or its volume/surface ratio (V/S) and on temperature. For relative humidity of 40 percent, average thickness of 150 mm and V/S ratio of 1.5 in temperature of 21^oC, all the multipliers are equal to unity. In this case γ_c may be calculated as a function of the age at loading t_o:

$$\gamma_c = 1.25t_o^{-0.188} \quad (2.25)$$

or

$$\gamma_c = 1.113t_o^{-0.188} \quad (2.26)$$

Equations 2.25 and 2.26 are for moist-cured concrete and for steam-cured concrete (1-3) days respectively. The two equations give $\gamma_c \cong 1.0$ when $t_o = 7$ and 3 days, respectively.

iii) Shrinkage of Concrete:

The free shrinkage of concrete can be calculated as:

$$\varepsilon_{cs}(t, t_o) = (\varepsilon_{cs})_u \frac{(t-t_o)}{b+(t-t_o)} \quad (2.27)$$

where b is a constant depending on the method of curing and equals to 35 for moist-cured concrete and to 55 for steam-cured concrete.

In Equation 2.27, $(\varepsilon_{cs})_u$ is the ultimate free shrinkage corresponding to t_∞ (assumed equals 10,000 days) and is given by

$$(\varepsilon_{cs})_u = -780\times10^{-6}\gamma_{cs} \quad (2.28)$$

where γ_{cs} is a correction factor given as the product of a number of multipliers which depend on the same factors mentioned earlier for γ_c. The correction factor γ_{cs} equals 1.0 when the period of the initial moist curing is 7 days, the relative humidity of the ambient

air is 40 percent, the average thickness is 150 mm or V/S ratio is 37.5 mm.

The free shrinkage between any two ages t_o and t can be calculated as the difference of shrinkage for the periods $(t-7)$ and (t_o-7) as:

$$\varepsilon_{cs}(t, t_o) = \varepsilon_{cs}(t, 7) - \varepsilon_{cs}(t_o, 7) \qquad (2.29)$$

Equation 2.27 is applicable for each of the two terms in Equation 2.29. In a similar way, it can be employed to calculate $\varepsilon_{cs}(t, t_o)$ for steam-cured concrete.

2.3.3 Comparison Between Prediction Models

Figures 2.1 and 2.2 show a comparison between the CEB-FIP and ACI prediction models for elasticity modulus, creep coefficient and shrinkage strain. The creep coefficients plotted in Figures 2.2a for ages at load application of 3, 28, 120, 365, and 1400 days. Shrinkage strain given in Figure 2.2b are calculated for periods starting at ages 7, 14, 28, and 90 days. As Figure 2.2 indicates, creep and shrinkage values estimated by the two models differ considerably, particularly for concrete loaded at early ages. The ACI model generally predicts lower creep and higher shrinkage than does the CEB-FIP model. It can also be noted from Figure 2.2a that the rate of creep (i.e. the slope of the creep curve) predicted by the CEB-FIP model is higher than that given by the ACI method. This difference can have a significant effect on the analytical results of structures constructed in stages. Similar observations were made by El-Badry (1988) when comparing the CEB-FIP (1978) model and ACI (1982) method.

In an attempt to evaluate the relative reliability of the various creep prediction methods available in the literature until 1982, Müller and Hilsdorf (1982) made a comparison between the predicted values and the experimental results. They found that, despite the considerable difference between the results of the CEB-FIP (1978) and the ACI (1982) methods, the comparison with experimental findings showed consistent reliability. The mean coefficient of variation between test data and predicted values was found to be about 25% for both methods.

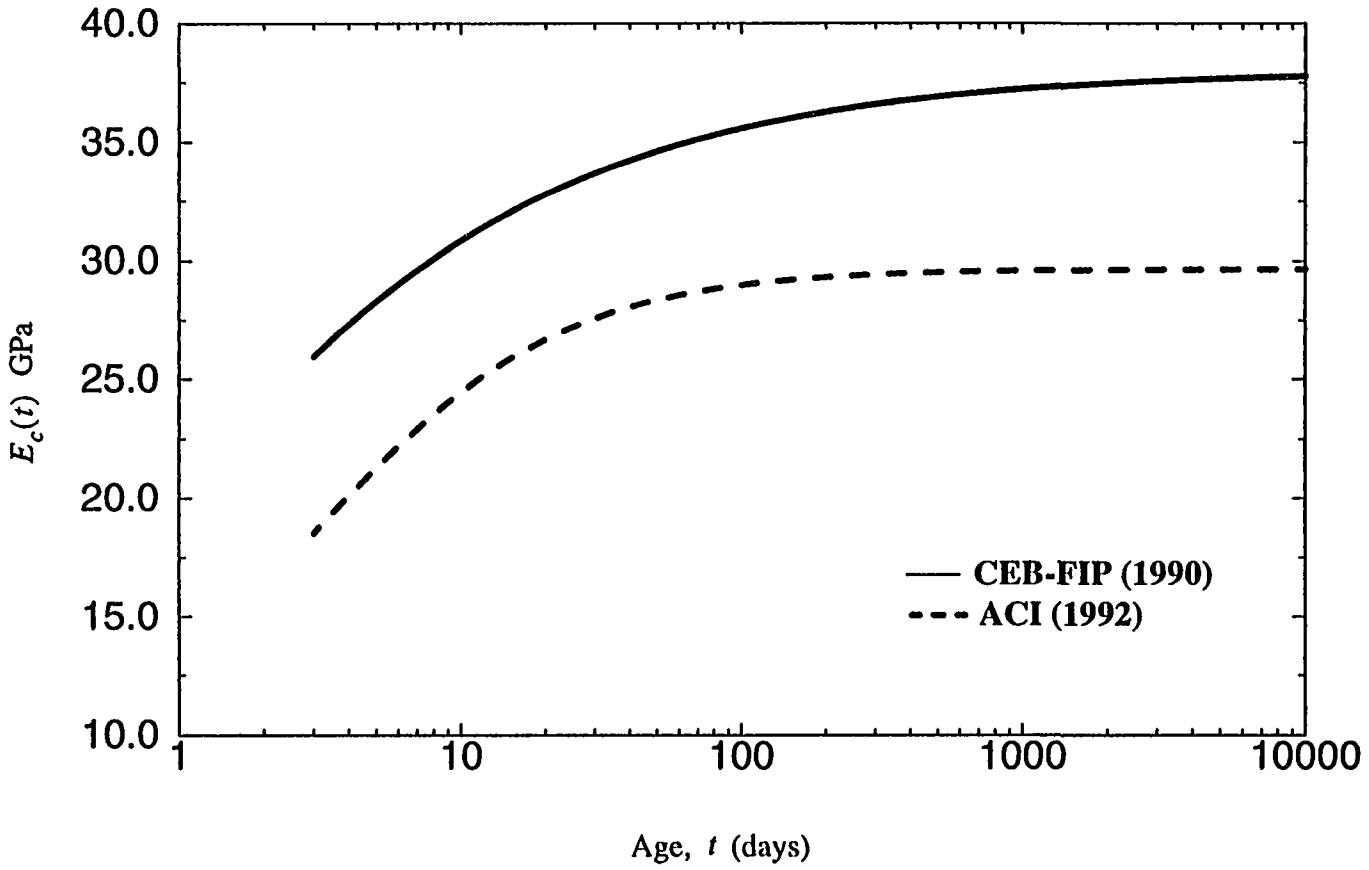

Figure 2.1 **Development of Modulus of Elasticity of Concrete with Time**

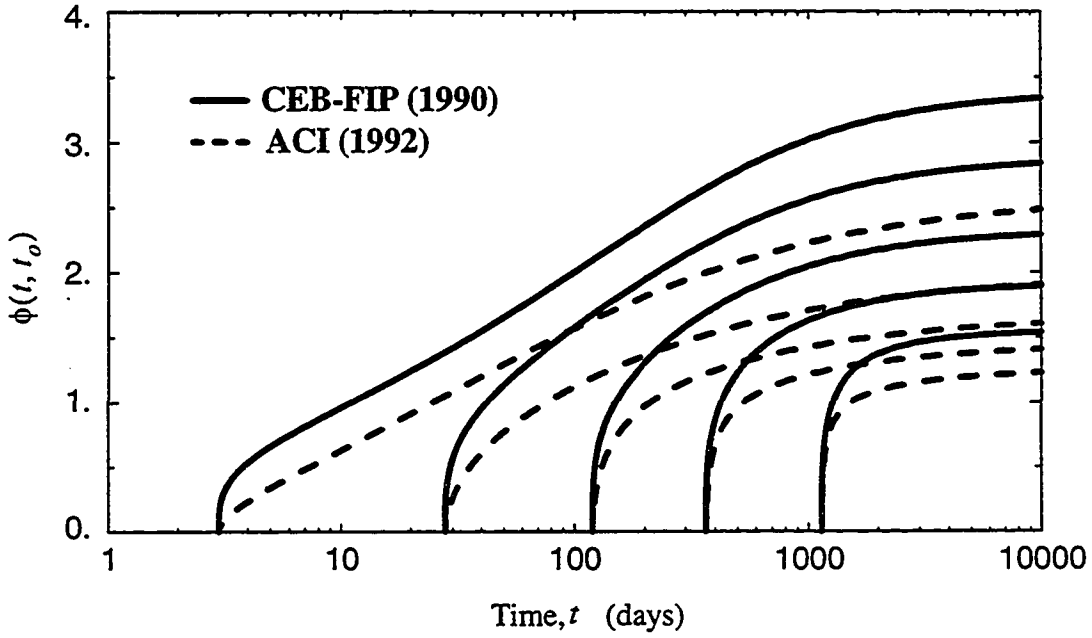

(a) Creep Coefficient

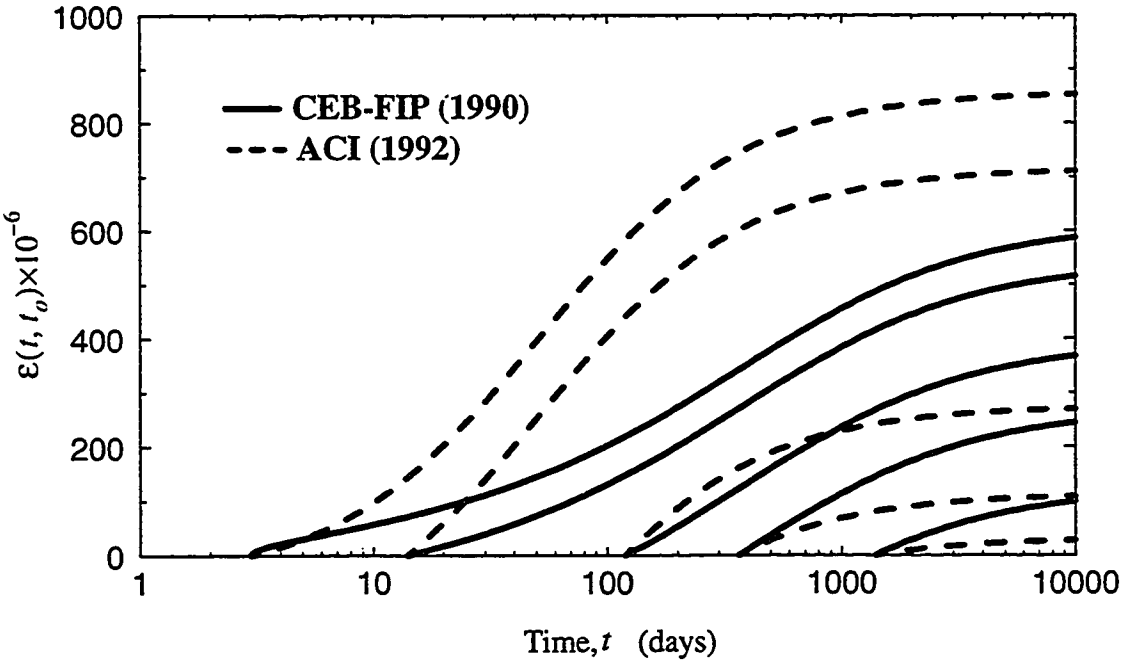

(b) Shrinkage Strain

Figure 2.2 **Comparison Between the ACI (1992) and the CEB-FIP (1990) Models for Prediction of Creep Coefficient and Shrinkage Strains** (Theoretical thickness = 150 mm, Relative humidity = 40%).

Müller and Hilsdorf (1982) concluded from their study that none of the prediction methods they investigated can be considered accurate ant that much more experimental work is required before a prediction model which accurately accounts for the various factors that affect creep and shrinkage of concrete can be established. They suggested that at the design stage, particularly in cases where creep and shrinkage have a great effect on the behavior of a structure, variations in creep and shrinkage coefficients of at least ±20 percent should be considered in the analysis. In this manner, upper and lower bounds for stresses and deformations in the structure can be obtained.

2.4 Relaxation of Prestressed Steel

Relaxation of prestressed steel is basically defined as the decrease in stress with time under constant strain. This phenomena can be considered similar to creep of concrete. Steel relaxation can be determined experimentally by stretching a tendon and maintaining its length after tensioning, and hence the strain, constant and then measuring the reduction in stress with time. The relaxation obtained by this method is called intrinsic relaxation, $\Delta\sigma_{pr}$, since it is measured regardless of the actual condition of the tendon when installed within the concrete structure. The amount of intrinsic relaxation depends upon the steel type and the level of the initial stress in the tendon.

Based on the experimental results provided by the CEB-FIP (1978), Ghali and Trevino (1985) suggested the following formula for evaluation of intrinsic relaxation

$$\Delta\sigma_{pr} = -k\eta\sigma_{pso}\left(\frac{\sigma_{pso}}{f_{ptk}} - 0.4\right) \tag{2.30}$$

where

σ_{pso} = initial tendon stress;

f_{ptk} = characteristic tensile strength of prestressed steel;

k = constant depending on steel type

= 1.5 for stress-relieved steel

= 2/3 for low relaxation steel

η = factor depending on duration $(t - t_o)$ of the steel relaxation (in hours)

$$= \begin{cases} \frac{1}{16}\ln\left(\frac{t-t_o}{10}+1\right) & (t-t_o) \le 1000 \\ \left[\frac{(t-t_o)}{0.5\times10^6}\right]^{0.2} & 1000 \le (t-t_o) \le 0.5\times10^6 \\ 1 & (t-t_o) \ge 0.5\times10^6 \end{cases} \qquad (2.31)$$

The above Equation 2.31 is applicable only when $\sigma_{pso} \ge 0.4 f_{ptk}$. It must be noted that for any time interval $(t_i - t_j)$, with $t_j > t_o$ the intrinsic relaxation is

$$\Delta\sigma_{pr}(t_i,t_j) = \Delta\sigma_{pr}(t_i - t_o) - \Delta\sigma_{pr}(t_j - t_o) \qquad (2.32)$$

2.5 Reduced Relaxation

In a prestressed concrete member, a prestressing tendon experiences continuous drop in its initial stress and decrease in its length with time due to creep and shrinkage of the surrounding concrete. Thus, the actual relaxation is expected to be smaller than the intrinsic value. Ghali, Sisodiya and Tadors (1974) employed a step-by-step approach to account for the effect of the variation of initial stress level on the value of steel relaxation. Ghali and Trevino (1985) developed a reduction coefficient χ_r, based on Equations 2.30 and 2.31 to be used as a multiplier to the intrinsic relaxation to obtain a reduced relaxation value, $\Delta\bar{\sigma}_{pr}$; thus

$$\Delta\bar{\sigma}_{pr} = \chi_r \Delta\sigma_{pr} \qquad (2.33)$$

where

$$\chi_r = e^{(-6.7 + 5.3\lambda)\Omega} \qquad (2.34)$$

with

$$\lambda = \frac{\sigma_{pso}}{f_{ptk}} \qquad (2.35)$$

and

$$\Omega = \frac{\Delta\sigma_{ps} - \Delta\sigma_{pr}}{\sigma_{pso}} \qquad (2.36)$$

where $\Delta\sigma_{ps}$ is the total prestress loss due to the combined effects of creep, shrinkage and relaxation. Since this value is not known before the analysis is done, an initial value of χ_r must be assumed and then modified later by iteration using Equations 2.36 and 2.34. The procedure should be repeated until the difference in two consecutive values of χ_r is insignificant. Ghali and Favre (1994) suggested a value for χ_r equals 0.7 to be assumed initially. For simplicity of the analysis presented in this thesis, the assumed value for χ_r will be maintained throughout the analysis.

CHAPTER THREE

Analysis of Variable Stress Regimes

3.1 Introduction

While most of the experimental data or empirical expressions for prediction of concrete creep are based on constant stress conditions, stresses in reinforced and prestressed concrete structures may change either suddenly or gradually with time. Creep under variable stress conditions makes the time-dependent analysis of concrete structures more complex. Several approximate methods have been suggested in the literature to simplify such an analysis. The most commonly used methods are the effective modulus method by Faber (1927), the rate of creep method by Glanville (1930), the method of superposition by McHenry (1943), the rate of flow method by England and Illston (1965) where creep was firstly divided into three components, namely, elastic creep, delayed elastic and flow creep, and Trost's approach (1967) for strain history problem (relaxation type) which was later modified by Bazant (1972) in his method known as the "Age-adjusted effective modulus method". All methods are based on the assumption that creep is proportional to the applied stress, utilize the creep-time relations derived from constant stress tests (e.g. Equation 2.4 or 2.23), and employ the principle of superposition.

The above methods have been briefly discussed in Chapter 1 of this thesis, and extensively reviewed and their merits and drawbacks discussed by several researchers including Bazant and Najjar (1973), Rao (1976), Neville et al. (1983) and many others. Among the various methods, the superposition of virgin creep curves (the step-by-step method) and the age-adjusted effective modulus method have been shown to predict creep of concrete most closely. In addition, combination of these two methods makes them the most suitable procedure available for the analysis of time-dependent effects on concrete structures built in stages. The two methods will be utilized in the present investigation for

the analysis of time-dependent stresses and strains of segmentally erected prestressed curved concrete bridges. Therefore, a brief discussion of the two methods is given below. The discussion, however, will be limited in this chapter to the effects of normal stresses and strains. Torsional effects which are more pronounced in curved structures can be treated in a similar manner as will be discussed in Chapter 4.

3.2 Principle of Superposition

The principle of superposition was first introduced by McHenry (1943); it implies that the total strain induced by a number of stress increments applied at different ages is equal to the sum of the strains due to each stress increment considered separately. To demonstrate the practical application of this principle, consider four identical specimens be loaded as follows (see Figure 3.1):

-Specimen (1): loaded at time t_1 with a sustained stress of constant magnitude σ.

-Specimen (2): loaded at time t_2 with a sustained stress of constant magnitude σ.

-Specimen (3): loaded at time t_1 with a constant stress σ sustained until time t_2 and then loaded with additional stress σ.

-Specimen (4): loaded at time t_1 with a constant stress σ which is subsequently removed at time t_2.

According to the principle of superposition, the strain in specimen (3) at any time later than t_2 is equal to the sum of the strains in specimens (1) and (2). Also the strain in specimen (4) at any time later than t_2 is equal to the difference of the strains in specimens (1) and (2). Thus

$$\varepsilon_3(t) = \varepsilon_1(t) + \varepsilon_2(t) \qquad t > t_2 \qquad (3.1)$$

$$\varepsilon_4(t) = \varepsilon_1(t) - \varepsilon_2(t) \qquad t > t_2 \qquad (3.2)$$

The previous conclusions are illustrated in Figure 3.1.

The strain at any time due to constant stress σ applied at time $t > t_o$ can be expressed as:

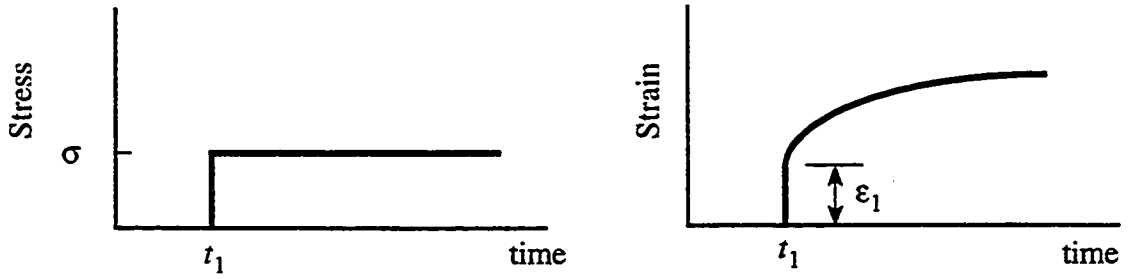

(a) Specimen (1)

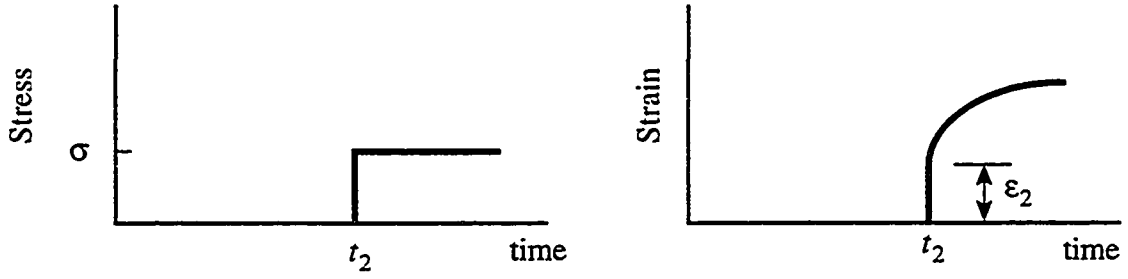

(b) Specimen (2)

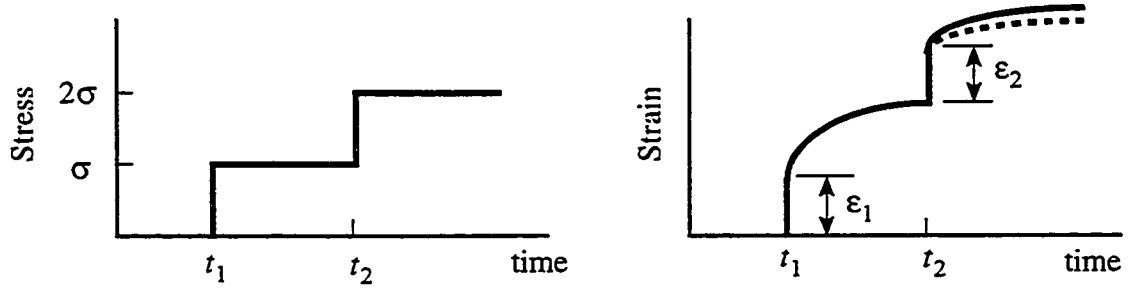

(c) Specimen (3)

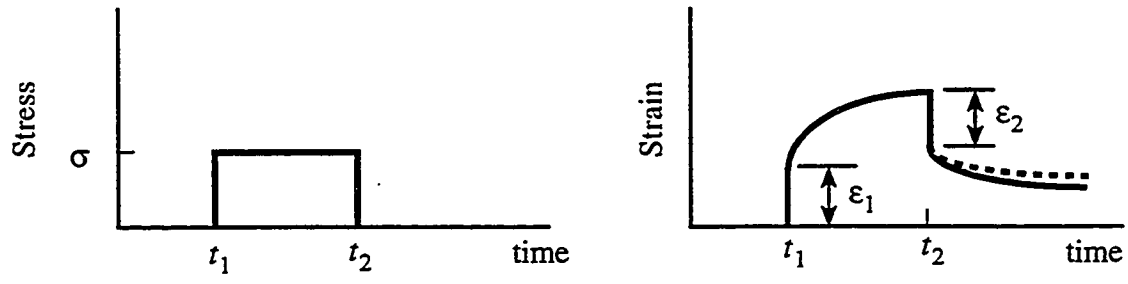

(d) Specimen (4)

Actual Strain

Theoretical Strain

Figure 3.1 **Stress-Strain Relation for Different Stress History**

$$\varepsilon(t) = \frac{\sigma_c(t_o)}{E_c(t_o)} [1 + \phi(t, t_o)] \qquad t > t_o \qquad (3.3)$$

where $\phi(t, t_o)$ is the creep coefficient between times t and t_o and $E_c(t_o)$ is the modulus of elasticity of concrete at the instant of loading.

Thus, when the stress is introduced in steps such that stress increments are applied at instants t_i, with $i = 1, 2, \ldots, n$, the total strain at time $t > t_n$ is given by:

$$\varepsilon(t) = \sum_{i=1}^{n} \frac{\Delta\sigma_c(t_i)}{E_c(t_i)} [1 + \phi(t, t_i)] \qquad t > t_n \qquad (3.4)$$

where n is the total number of stress increments.

For a continually varying stress, the total strain at time t is

$$\varepsilon(t) = \int_{t_o}^{t} \frac{1 + \phi(t, \tau)}{E_c(\tau)} \cdot \frac{\partial\sigma_c(\tau)}{\partial\tau} d\tau \qquad (3.5)$$

where τ is an intermediate instant between t and t_o.

Experiments conducted by Ross (1958) and England and Illston (1965) to examine the validity of the principle of superposition indicated that under increasing stresses, superposition overestimates the actual creep (Figure 3.1c). Even when the stress is suddenly and completely removed, the creep recovery obtained by superposition is always greater than the actual values (Figure 3.1d). The reason for this is that the principle of superposition ignores the following two facts:

(i) Creep caused by a stress applied to a virgin concrete is greater than creep caused by a stress of the same magnitude applied to previously loaded concrete.

(ii) Upon removal of stress, creep recovery is smaller than creep of virgin concrete loaded at the same age at which the recovery specimen is unloaded.

In practice, however, complete unloading is uncommon and small or gradual decrease of stress closely agrees with superposition of virgin concrete curves.

The major drawback of superposition is that it requires a large number of

experimental data or creep curves. However, the use of empirical equations for prediction of creep, similar of those given in Section 2.3, may overcome this problem.

3.3 Step-by-Step Approach

An analytical evaluation of the integral in Equation 3.5 is difficult to obtain unless approximations are introduced to the variation of ϕ, E_c and σ with time. Numerical solutions are therefore desirable; of these, a step-by-step procedure proved to be the most efficient. Such a procedure is completely general as it can be used with any creep function and any prescribed stress and strain histories that vary in an arbitrary fashion. The step-by-step analysis can be used to calculate the strain at any time when the stress history is prescribed, or to predict the stress if the variation of strain is known.

Assume that the stress in concrete varies over a period of time between t_o and t as shown in Figure 3.2. For the purpose of the analysis, the period $(t - t_o)$ is divided into a number of time intervals whose length should increase with the age of concrete. For best results, under continuously varying stress, the time intervals Δt_i should be chosen such that their lengths are approximately equal on the log-time scale (Bazant, 1972). Assume that the stress is divided into increments introduced instantaneously at the middle of the intervals. Equation 3.4 can be used to calculate the strain at time $t_{i+\frac{1}{2}}$, the end of interval i, as:

$$\varepsilon_c\left(t_{i+\frac{1}{2}}\right) = \sum_{j=1}^{i} \frac{\Delta\sigma_j}{E_c(t_j)} \left[1 + \phi\left(t_{i+\frac{1}{2}}, t_j\right)\right] \tag{3.6}$$

where t_j is the middle of interval j and $\Delta\sigma_j$ is the stress increment applied at t_j. Equation 3.6 can be written as:

$$\varepsilon_c\left(t_{i+\frac{1}{2}}\right) = \frac{\Delta\sigma_i}{E_c(t_i)} \left[1 + \phi\left(t_{i+\frac{1}{2}}, t_i\right)\right] + \sum_{j=1}^{i-1} \frac{\Delta\sigma_j}{E_c(t_j)} \left[1 + \phi\left(t_{i+\frac{1}{2}}, t_j\right)\right] \tag{3.7}$$

Thus

$$\Delta\sigma_i = \frac{E_c(t_i)}{1 + \phi\left(t_{i+\frac{1}{2}}, t_i\right)} \left\{\varepsilon_c\left(t_{i+\frac{1}{2}}\right) - \sum_{j=1}^{i-1} \frac{\Delta\sigma_j}{E_c(t_j)} \left[1 + \phi\left(t_{i+\frac{1}{2}}, t_j\right)\right]\right\} \tag{3.8}$$

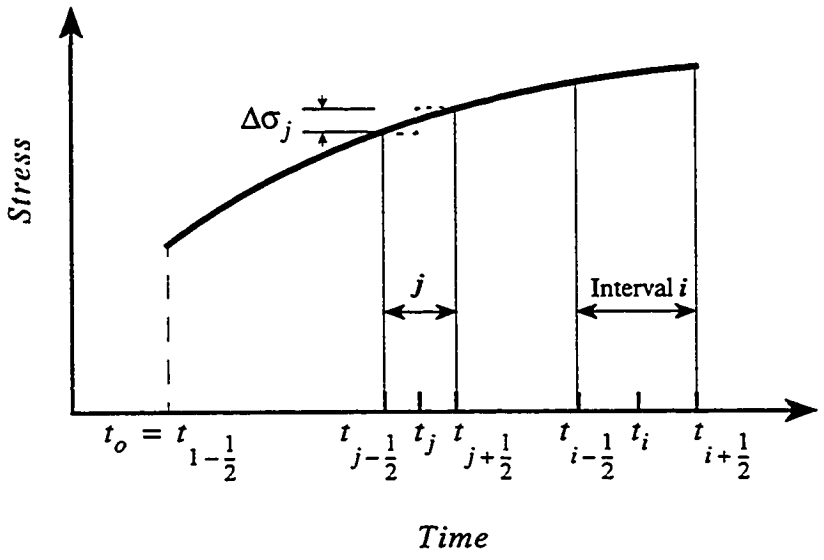

Figure 3.2 **Definition of Time Intervals and Stress Increments for the Step-by-Step Analysis.**

which can be used when the strain history is known to determine the stress $\sigma\left(t_{i+\frac{1}{2}}\right)$ at the end of interval i from the stress increments calculated for all the previous intervals, noting that

$$\sigma_c\left(t_{i+\frac{1}{2}}\right) = \sigma_c\left(t_{i-\frac{1}{2}}\right) + \Delta\sigma_i \tag{3.9}$$

where $t_{i-\frac{1}{2}}$ is the beginning of interval i. Successive application of Equations 3.7 to 3.9 for each time interval gives the variation of the stress with time.

The step-by-step analysis just described has been the basis of a number of computer programs developed by several researchers to study the behaviour of different structures under the time-dependent effects of creep, shrinkage and steel relaxation. Examples of theses programs are those developed by Kabir (1976) to study the behaviour of concrete panels, slabs and shells, by Tadros, Ghali and Dilger (1979) for the analysis of structures built in stages, by Khalil (1979) for the analysis of cable-stayed bridges, by Van Zyl (1978) for the analysis of curved prestressed segmental bridges and by El-Badry (1988) for the analysis of serviceability of a wide range of concrete structures.

In the present investigation, the above step-by-step procedure will be utilized for the analysis of the time-dependent effects in segmentally erected curved prestressed concrete bridges. In this analysis the time intervals will be chosen with their starts coinciding with the instants of occurrence of new events such as addition or removal of new members or prestressing tendons, application of loads or change in support conditions (see Figure 3.3). The limits of time intervals can also be selected at the instants when the behaviour of the structure in terms of the stresses, strains and deformations is required. In each time interval, the material properties are assumed to be constant. The change in strain due to creep of concrete will be calculated using the age-adjusted effective modulus method (to be discussed in subsequent sections). In this manner the analysis requires a small number of intervals and, thus, the storage required for the stress history will be reduced.

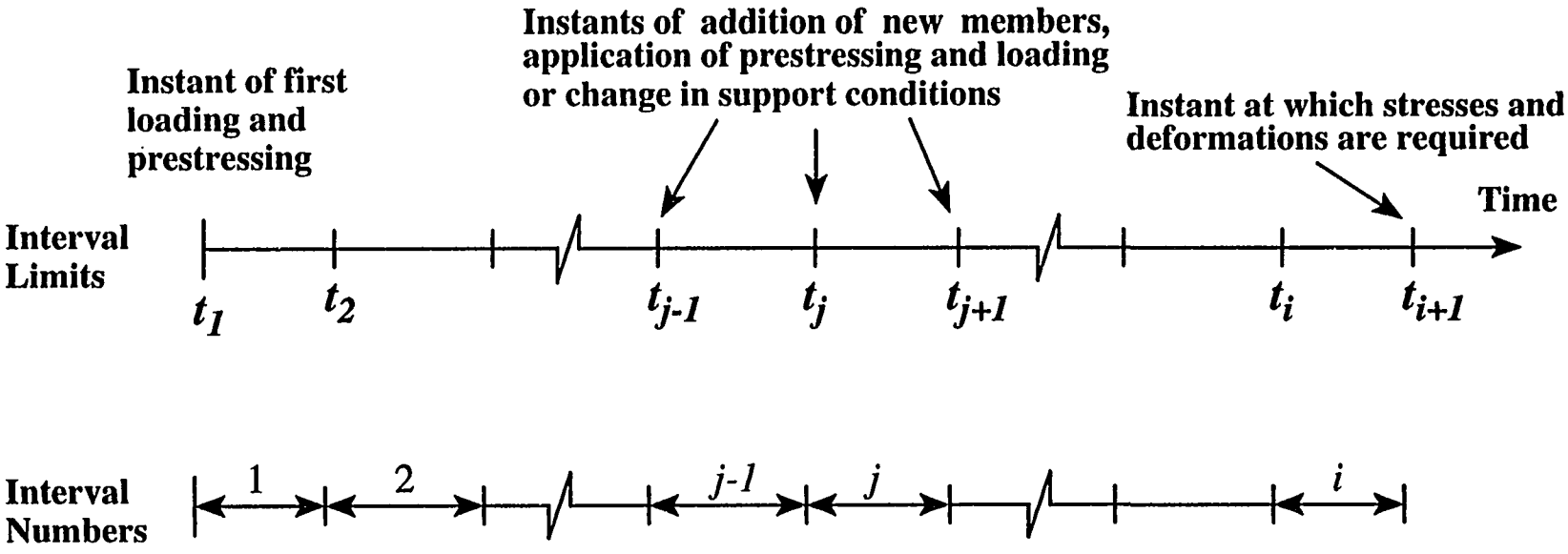

Figure 3.3 **Division of Time into Intervals for the Step-by-Step Analysis**

3.4 Concrete Response to Time-varying Stress Pattern

3.4.1 Relaxation of Concrete

When a concrete specimen is subjected at time t_o to an instantaneously imposed strain ε_o which is subsequently sustained, the instantaneous induced stress decreases continually with time. This phenomenon is known as relaxation of concrete. The variation of stress with time can be expressed as:

$$\sigma_c(t) = \varepsilon_o \cdot r(t, t_o) \tag{3.10}$$

where $r(t, t_o)$ is a relaxation function defined as the stress at time t induced by a unit strain imposed at time t_o and sustained thereafter. The relaxation function r depends on the duration $(t - t_o)$ and the creep coefficient $\phi(t, t_o)$. Figure 3.4 shows the variation of concrete stress with time for a constant sustained strain. As can be seen, $r(t, t_o)$ is smaller than $E_c(t_o)$.

The variation of $r(t, t_o)$ with time can be determined from the step-by-step analysis described in the previous section by putting $\varepsilon_c\left(t_{i+\frac{1}{2}}\right)$ in Equation 3.7 equal to unity for all intervals. Thus, the relaxation of concrete $r\left(t_{i+\frac{1}{2}}, t_o\right)$ at the end of interval i is given by:

$$r\left(t_{i+\frac{1}{2}}, t_o\right) = \frac{E_c(t_i)}{1 + \phi\left(t_{i+\frac{1}{2}}, t_i\right)} \left\{1 - \sum_{j=1}^{i-1} \frac{\Delta r_j}{E_c(t_j)} \left[1 + \phi\left(t_{i+\frac{1}{2}}, t_j\right)\right]\right\} \tag{3.11}$$

with

$$\Delta r_j = r\left(t_{j+\frac{1}{2}}, t_o\right) - r\left(t_{j-\frac{1}{2}}, t_o\right) \tag{3.12}$$

Figure 3.5 shows the variation of the relaxation function with time for certain creep data.

3.4.2 Aging Coefficient of Concrete

For a concrete subjected to a gradually increasing stress between t_o and t, (Figure 3.6a), the total strain, instantaneous plus creep, at time t is calculated as:

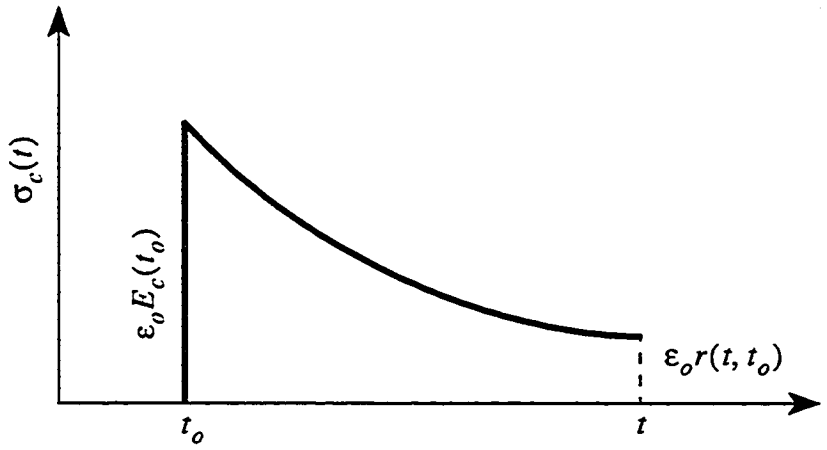

Figure 3.4 **Strain in Concrete with Time under Constant Sustained Stress**

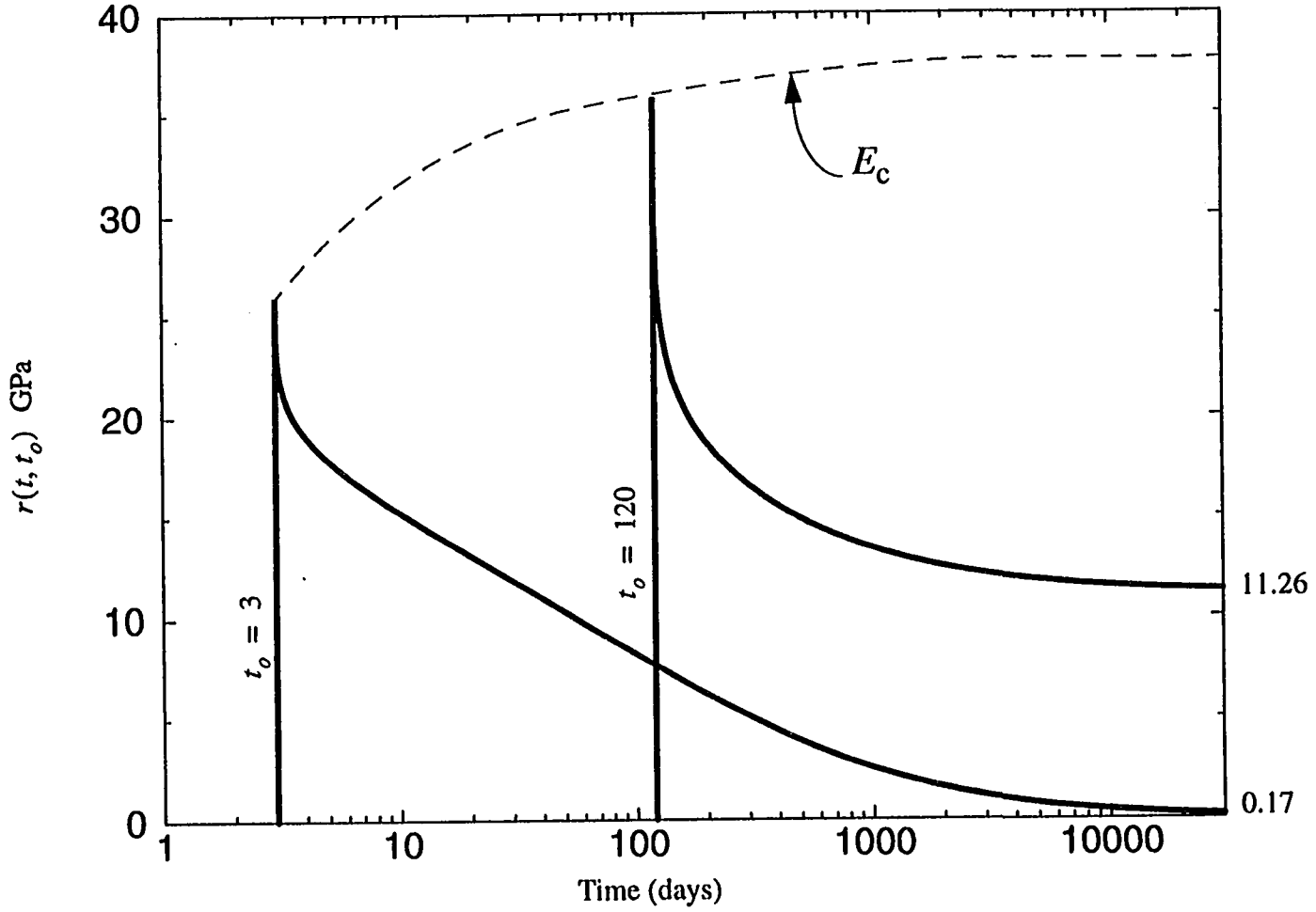

Figure 3.5 **Relaxation Function *r(t,to)* with Time**

(for f_{ck} = 30 MPa, RH = 50%, h_o = 400 mm).

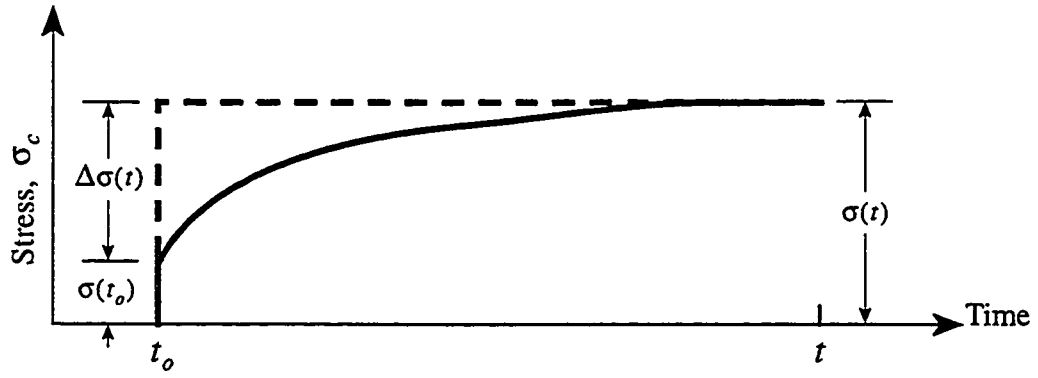

(a) Stress History

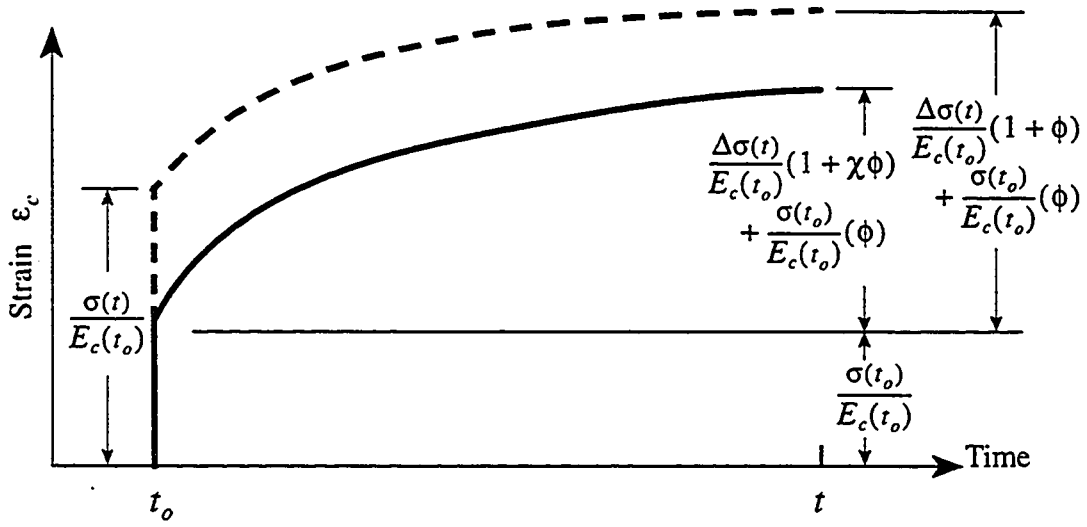

(b) Strain History

Figure 3.6 **Strain Development due to Variable Stress**

$$\varepsilon_c(t) = \sigma_c(t_o)\left[\frac{1+\phi(t,t_o)}{E_c(t_o)}\right] + \int_{\sigma_c(t_o)}^{\sigma_c(t)} \frac{1+\phi(t,\tau)}{E_c(\tau)} \cdot d\sigma_c(\tau) \qquad (3.13)$$

It is essential to realize that the stress pattern shown by the solid curve in Figure 3.6a produces creep at time t with a lower value in comparison to a stress of equal magnitude but applied in its full magnitude at time t_o (shown by the dotted line in Figure 3.6a). This is depicted in Figure 3.6b. Thus, in order to simplify evaluation of the integral in Equation 3.13, the gradually applied stress $\Delta\sigma(t, t_o)$ can be treated as if it were introduced in its full magnitude at time t_o and the resulting ultimate value of creep can be multiplied by a reduction factor $\chi(t, t_o)$ to account for the effect of the stress variation on creep. Thus,

$$\varepsilon_c(t) = \sigma_c(t_o)\,\frac{1+\phi(t,t_o)}{E_c(t_o)} + \Delta\sigma_c(t,t_o)\,\frac{1+\chi\phi(t,t_o)}{E_c(t_o)} \qquad (3.14)$$

In this Equation $\chi(t, t_o)$ is referred to as the "aging coefficient"; its value varies between 0.0 and 1.0 (Bazant, 1972).

The first term in Equation 3.14 represents the total strain at time t due to initial stress $\sigma_c(t_o)$ introduced at time t_o and sustained without change until time t, whereas the second term represents the total strain due to the stress change, which could be an increase or a decrease, introduced gradually between t_o and t.

In a relaxation problem, the strain $\varepsilon_c(t)$ is constant at any time and equal to $\varepsilon_c = \sigma_c(t_o)/E_c(t_o)$. Thus, the stress history can be expressed as:

$$\Delta\sigma_c(t,t_o) = \sigma_c(t) - \sigma_c(t_o) \qquad (3.15)$$

$$= \varepsilon_c \cdot r(t,t_o) - \sigma_c(t_o) \qquad (3.16)$$

$$= \varepsilon_c \cdot r(t,t_o) - \varepsilon_c \cdot E_c(t_o) \qquad (3.17)$$

$$= \varepsilon_c\,[r(t,t_o) - E_c(t_o)] \qquad (3.18)$$

Thus, Equation 3.14 can be rewritten as:

$$\varepsilon_c = \varepsilon_c\ [1+\phi(t,t_o)] + \varepsilon_c\ [r(t,t_o) - E_c(t_o)]\ \frac{1+\chi\phi(t,t_o)}{E_c(t_o)} \tag{3.19}$$

from which χ can be expressed as:

$$\chi(t,t_o) = \frac{1}{1-r(t,t_o)/\phi(t,t_o)} - \frac{1}{\phi(t,t_o)} \tag{3.20}$$

3.4.3 Age-Adjusted Effective Modulus of Concrete

The analysis for any concrete structure under service loads involves two repetitive steps, namely, instantaneous and time-dependent. For the second step of analysis, the free strain due to creep and shrinkage of concrete develops gradually over the period under consideration. Equation 3.14 that predicts the free strain can be rewritten as

$$\varepsilon_c(t) = \sigma_c(t_o) \cdot \frac{1+\phi(t,t_o)}{E_c(t_o)} + \frac{\Delta\sigma_c(t)}{\bar{E}_c(t,t_o)} \tag{3.21}$$

where

$$\bar{E}_c(t,t_o) = \frac{E_c(t_o)}{1+\chi\phi(t,t_o)} \tag{3.22}$$

which is referred to as the "Age-adjusted effective modulus of elasticity", firstly introduced by Trost (1967) then refined by Bazant (1972). The age-adjusted modulus of concrete defined by Equation 3.22 can be considered a measure of softening of concrete within the time period $(t-t_o)$ due to gradual development of stress with time. The use of this age-adjusted effective modulus simplifies any time-dependent analysis to a direct elasticity problem. It can be used in an analysis by the displacement method to evaluate the time-dependent stiffness matrices of individual concrete elements and the forces necessary to restrain the free strain which would develop due to creep and shrinkage of concrete and hence calculate the fixed-end forces needed for the analysis as will be explained in the next chapter.

3.5 Instantaneous Stresses and Strains

As will be discussed in Chapter 4, the analysis of concrete structures built in stages is performed step-by-step, for which the time is divided into intervals, each of finite length. In each interval, the displacement (stiffness) method of analysis is utilized to determine instantaneous and time-dependent changes in nodal displacements and support reactions and, hence, deformations and stress resultants (internal forces) and corresponding stresses and strains at different sections of individual members of the structure. The instantaneous changes at the start of each time interval may result from addition or removal of members, external loads or prestressing cables, or from changes in support conditions. For such an analysis, the concrete modulus of elasticity corresponding to the age of concrete at the beginning of the time interval, say interval i, must be used. In each cross section, the analysis results in three internal force increments, ΔN, $\Delta M_{y'}$ and $\Delta M_{z'}$, which produce normal stresses and strains in the cross-section. The instantaneous change in strain at any point (y', z') in the cross-section is given by

$$\Delta\varepsilon(t_i) = \Delta\varepsilon_o(t_i) + \Delta\psi_{y'}(t_i) \cdot z' + \Delta\psi_{z'}(t_i) \cdot y' \tag{3.23}$$

where ε_o is the average strain at the section centroid and $\psi_{y'}$ and $\psi_{z'}$ are the curvatures about the principal y' and z' axes, respectively:

$$\Delta\varepsilon_o(t_i) = \frac{\Delta N}{E_c(t_i)A}$$

$$\Delta\psi_{y'}(t_i) = \frac{\Delta M_{y'}}{E_c(t_i) \cdot I_{y'}} \quad ; \Delta\psi_{z'}(t_i) = \frac{\Delta M_{z'}}{E_c(t_i) \cdot I_{z'}} \tag{3.24}$$

in which A, $I_{y'}$ and $I_{z'}$ are the transformed cross-sectional area and moment of inertia about the y' and z'-axes, respectively, and $E_c(t_i)$ is the modulus of elasticity of concrete at time t_i.

Figure 3.7 shows the positive directions of ΔN, ΔM_y, and ΔM_z, acting on a cross-section. The instantaneous change in stress in concrete at time t_i can thus be calculated as

$$\Delta\sigma_c(t_i) = E_c(t_i) \cdot \Delta\varepsilon_c(t_i) \tag{3.25}$$

3.6 Time-Dependent Stresses and Strains

The analysis of time dependent changes in stresses and strains in composite section (concrete and prestressed steel) due to creep, shrinkage and relaxation follows the basic concepts of the displacement (stiffness) method. The free strain that may develop during a certain time interval due to creep and shrinkage of concrete is firstly restrained by artificial restraining forces acting at each cross section. For equilibrium, these forces are subsequently eliminated by applying equal and opposite forces at the centroid of the cross section. Evaluation of the restraining forces will be discussed in details in Section 4.5. Relaxation of prestressed steel is treated as an initial stress problem. Restraining forces are also evaluated at the nodes and then applied in a reversed direction on the elements in the same manner as before.

After obtaining all nodal forces due to the time-dependent parameters, the stiffness analysis is carried out to calculate the increment of the nodal displacements due to these effects.

3.6.1 Hypothetical Free Strain Due to Creep and shrinkage

Let $t_1, t_2, \ldots$ represent the instants at which new events take place during or after a multi-stage construction of a concrete structure. The symbol $\Delta\sigma_c(t_j)$ represents a stress increment introduced at time t_j and sustained without change in magnitude up to time t.

Since the analysis of the structure will be performed step-by-step, the stress history

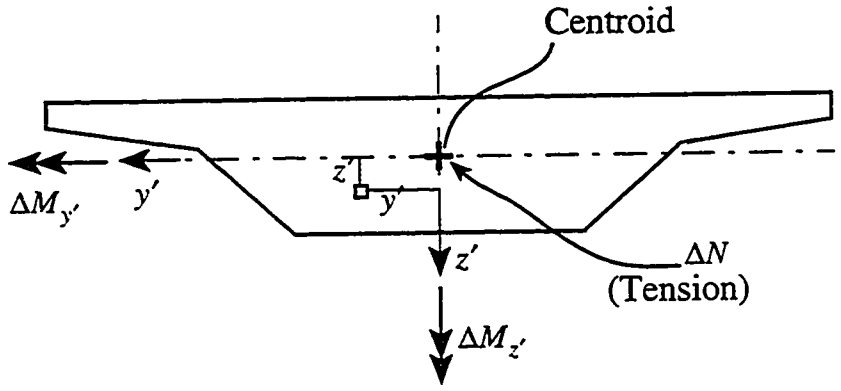

Figure 3.7 **Positive Directions of y', z', ΔN, $\Delta M_{y'}$ and $\Delta M_{z'}$ in a Cross-Section of a Space Frame Element.**

at any instant for all the previous time steps will be known and stored. For any time interval i between t_i and t_{i+1}, the creep strain $\Delta\varepsilon_c(t_{i+1}, t_i)_{free}$ due to a stress increment $\Delta\sigma_c(t_j)$ applied instantaneously at an earlier instant t_j equals:

$$\frac{\Delta\sigma_c(t_j)}{E_c(t_j)}[\phi(t_{i+1}, t_j) - \phi(t_i, t_j)] \tag{3.26}$$

A stress increment $\Delta\sigma_c(t_{j+1}, t_j)$, introduced gradually between t_j and t_{j+1}, can be treated as if it were introduced instantaneously in its full value at some time t_e between t_j and t_{j+1} (Ghali and Favre, 1994) such that

$$\frac{1 + \phi(t_{j+1}, t_e)}{E_c(t_e)} = \frac{1 + \chi\phi(t_{j+1}, t_j)}{E_c(t_j)} \tag{3.27}$$

where χ and ϕ are the aging and creep coefficients, respectively. The value t_e can be determined by trial. Equation 3.27 means that if the stress increment $\Delta\sigma_c(t_{j+1}, t_j)$ were introduced at time t_e and kept constant up to time t_{j+1}, it would produce a total strain (instantaneous plus creep) equals that developed when the increment is introduced gradually between time t_j and t_{j+1}. Thus, the creep strain that develops during interval i can be expressed as

$$\frac{\Delta\sigma_c(t_{j+1}, t_j)}{E_c(t_e)}\ [\phi(t_{i+1}, t_e) - \phi(t_i, t_e)] \tag{3.28}$$

El-Badry (1988) showed that a very slight difference exists between the quantity $[\phi(t_{i+1}, t_j) - \phi(t_i, t_j)]/E_c(t_j)$ and $[\phi(t_{i+1}, t_e) - \phi(t_i, t_e)]/E_c(t_e)$. Thus, the time t_e can be replaced by t_j for simplicity. The strain increment that develops during the interval $(t_{i+1} - t_i)$ due to the combined effects of instantaneous and gradually applied stresses can thus be expressed as:

$$\frac{\Delta\sigma_c(t_j)+\Delta\sigma_c(t_{j+1},t_j)}{E_c(t_j)}\ [\phi(t_{i+1},t_j)-\phi(t_i,t_j)] \tag{3.29}$$

If at the instant t_i an external loading or a sudden effect takes place producing a stress increment $\Delta\sigma_c(t_i)$, the corresponding creep strain that develops during the interval i is given by

$$\frac{\Delta\sigma_c(t_i)}{E_c(t_i)}\cdot\phi(t_{i+1},t_i) \tag{3.30}$$

The shrinkage strain develops during the same interval is $\Delta\varepsilon_{cs}(t_{i+1},t_i)$

Thus, the total free strain that develops during interval i due to creep and shrinkage taking into account the stress history in all previous intervals can be written as:

$$\Delta\varepsilon_c(t_{i+1},t_i)_{free}=\sum_{j=1}^{i-1}\left\{\frac{\Delta\sigma_c(t_j)+\Delta\sigma_c(t_{j+1},t_j)}{E_c(t_j)}[\phi(t_{i+1},t_j)-\phi(t_i,t_j)]\right\}+$$
$$\frac{\Delta\sigma_c(t_i)}{E_c(t_i)}\cdot\phi(t_{i+1},t_i)+\Delta\varepsilon_{cs}(t_{i+1},t_i) \tag{3.31}$$

The free strain obtained by this equation will be restrained at each cross section for each element and a set of equivalent nodal forces will be developed as described in Section 4.5.

CHAPTER FOUR

Analysis of Prestressed Curved Segmental Structures

4.1 Introduction

In this chapter, a numerical procedure is presented and a computer program is described for the analysis of segmentally erected curved prestressed concrete box-girder bridges. The analysis accounts for the effects of creep and shrinkage of concrete and relaxation of prestressed steel, for the effects of construction sequence and change of geometry and support conditions, and for the effects of movement of supports. The analysis gives the history of instantaneous and time-dependent changes in displacements, in support reactions and in statically indeterminate internal forces (or stress resultants).

The procedure is based on the displacement method of strucutral analysis and is implemented in a computer program TD-SFRAME (Debaiky and El-Badry, 1997) which is suitable for the analysis of curved structures with arbitrary geometry in space. In the following sections, the assumptions concerning idealization of the structure are given and the formulation of the curved elements used in modelling the concrete segments and the prestressing tendons, as well as the details of the analysis are presented.

4.2 Modelling of the Structure

In the present analysis, a curved concrete bridge is idealized as an assemblage of multi-node curved beam elements and/or three-dimensional prismatic straight elements depending on the alignment of the bridge. A curved concrete element can be defined in space by a minimum of three and a maximum of six nodes and can be of variable cross-

sections described at the nodes (Figure 4.1). The nodes coincide with the centroids of the cross sections and are defined by three global coordinates. A bridge segment can be modelled by a single or multiple concrete elements. Prestressing tendons within curved concrete elements can be of any profile in space and are defined by local eccentricities at each cross-section (node). However, each end of a prestressing tendon must be located in an end section of a concrete element. The formulation of the multi-node curved concrete element is based on the assumption that both warping and transverse deformation of the cross-section are ignored. Thus, only six degrees of freedom are associated with each node. Contribution of post-tensioned tendons to the stiffness of the structure is included in the analysis only after the instantaneous effects of prestressing are calculated. A straight concrete element is defined by two end nodes. The element must be of a constant cross-section. Orientation of the elements with respect to the global system of axes can be of any desired pattern. For each concrete section, six area properties must be given as data; these are the area and the effective shear area of the cross-section, its second moment of area about the two local axes, y' and z' and the torsional constant with respect to the local x'-axis of the element.

Material properties such as the moduli of elasticity of concrete and prestressed steel, and the creep and aging coefficients and shrinkage strain of concrete for each time interval can be either defined by the user or automatically generated by the program using equations recommended by the CEB-FIP code (1990) or the ACI Committee 209 (1992) as explained in Chapter 2. Stress relaxation of prestressed steel with time can also be given or generated.

Formulation of the elements allows for all types of externally applied loads.

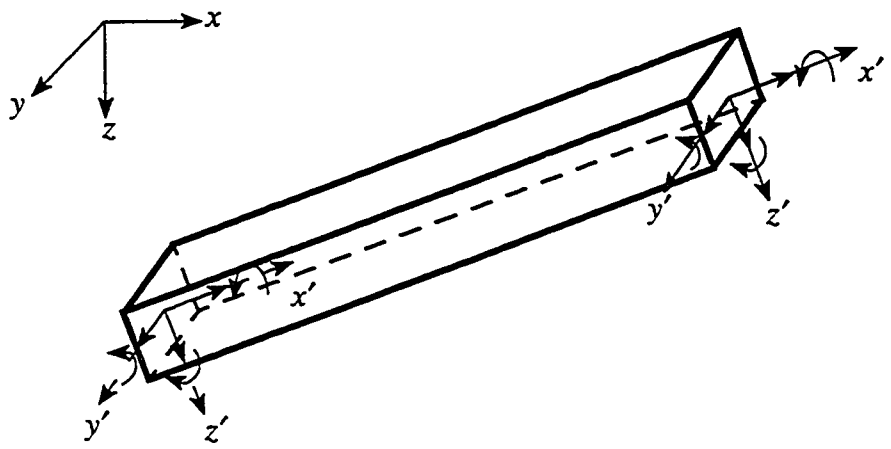

(a) **Local Axes and Nodal Degrees of Freedom for Straight Prismatic Element**

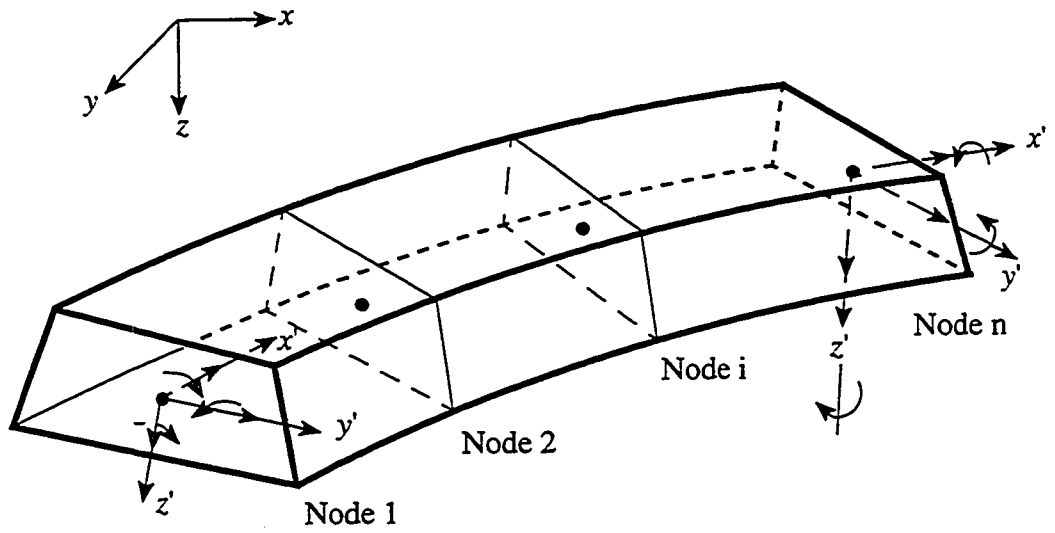

(b) **Local Axes and Nodal Degrees of Freedom for Multi-Node Curved Element of Jirousek**

Figure 4.1 **Available Beam Elements in the Computer Program TD-SFRAME**

Concentrated forces or couples can be addressed at any node with respect to the global coordinates. Distributed loads can vary from one node to another to account for the variable distribution of own weight and superimposed loads along the bridge length. Self weight of the concrete elements is considered as external loads and must be given by the analyst as input to the computer program.

Formulation of the curved isoparametric elements to model concrete segments and prestressing tendons is given in detail in the following sections. The stiffness formulation of straight elements will not be presented in this chapter as it can be found in any textbook on structural analysis (see for example Ghali and Neville, 1989).

4.3 Isoparametric Element Formulation

4.3.1 Element Geometry

The global and local coordinate system of the multi-node isoparametric element of Jirousek (1981) are shown in Figure 4.1b. The element may contain from three to six nodes located on the beam centroidal axis. A three-node element describes a quadratic curve in space and a six-node element describes a quintic curve. For an isoparametric element a natural curvilinear coordinate, ξ, can be defined; where ξ varies from -1 at the first element node to +1 at the element end node. The global coordinates of any point on the element centroidal axis are defined as:

$$\begin{Bmatrix} x(\xi) \\ y(\xi) \\ z(\xi) \end{Bmatrix} = \sum_{i=1}^{n} N_i(\xi) \cdot \begin{Bmatrix} x_i \\ y_i \\ z_i \end{Bmatrix} \tag{4.1}$$

where n is the total number of nodes in the element and $N_i(\xi)$ is the shape function given by:

$$N_i(\xi) = \frac{(\xi-\xi_1)(\xi-\xi_1)\ \cdots\ (\xi-\xi_{i-1})(\xi-\xi_i)\ \cdots\ (\xi-\xi_n)}{(\xi_i-\xi_1)(\xi_i-\xi_1)\ \cdots\ (\xi_i-\xi_{i-1})(\xi_i-\xi_i)\ \cdots\ (\xi_i-\xi_n)} \quad (4.2)$$

4.3.2 Displacement Function

The displacements u, v, w, θ_x, θ_y and θ_z, in the global directions at any point on the centroidal axis of the element can be defined using the same shape function $N_i(\xi)$ as:

$$\begin{Bmatrix} u(\xi) \\ v(\xi) \\ w(\xi) \end{Bmatrix} = \sum_{i=1}^{n} N_i(\xi) \cdot \begin{Bmatrix} u_i \\ v_i \\ w_i \end{Bmatrix} \quad (4.3a)$$

and

$$\begin{Bmatrix} \theta_x(\xi) \\ \theta_y(\xi) \\ \theta_z(\xi) \end{Bmatrix} = \sum_{i=1}^{n} N_i(\xi) \cdot \begin{Bmatrix} \theta_{xi} \\ \theta_{yi} \\ \theta_{zi} \end{Bmatrix} \quad (4.3b)$$

4.3.3 Coordinate Transformation

The local and global components of displacements are related as follows

$$\begin{Bmatrix} u' \\ v' \\ w' \end{Bmatrix} = [T] \cdot \begin{Bmatrix} u \\ v \\ w \end{Bmatrix} \quad (4.4a)$$

$$\begin{Bmatrix} \theta'_x \\ \theta'_y \\ \theta'_z \end{Bmatrix} = [T] \cdot \begin{Bmatrix} \theta_x \\ \theta_y \\ \theta_z \end{Bmatrix} \quad (4.4b)$$

where the primed terms refer to the local axes and the unprimed terms refer to the global axes. The previous relations can be rewritten in the implicit expression:

$$\{u'\} = [H] \cdot \{u\} \tag{4.5}$$

where

$$[H] = \begin{bmatrix} [T] & [0] \\ [0] & [T] \end{bmatrix} \tag{4.6}$$

Since the element is a non-prismatic space element, the transformation matrix can never be uniquely defined by the global coordinates of element nodes only. Several techniques can be used to provide the information required to generate this matrix. A common approach is to use the direction cosines of the local y' or z' axes with respect to the global axes. However, it is not possible to interpolate the nodal direction cosines to any required point on the beam. For this reason, an alternative approach is adopted. The angle Φ between the local y' axis and the global xy plan is defined at each node (Figure 4.2). The angle at any point along the beam can be computed by interpolating between the nodal values. Thus:

$$\Phi(\zeta) = \sum_{i=1}^{n} N_i(\zeta) \cdot \Phi_i \tag{4.7}$$

Given the value $\Phi(\zeta)$, the transformation matrix $[T]$ can be defined at any point as

$$[T] = \begin{bmatrix} \lambda_{x'x} & \lambda_{x'y} & \lambda_{x'z} \\ \lambda_{y'x} & \lambda_{y'y} & \lambda_{y'z} \\ \lambda_{z'x} & \lambda_{z'y} & \lambda_{z'z} \end{bmatrix} = \begin{bmatrix} \{\lambda_{x'}\} \\ \{\lambda_{y'}\} \\ \{\lambda_{z'}\} \end{bmatrix} \tag{4.8}$$

where $\{\lambda_{x'}\}$ is the vector of direction cosines of the local x'-axis with respect to the global axes. The vectors $\{\lambda_{y'}\}$ and $\{\lambda_{z'}\}$ are similarly defined. The vector $\{\lambda_{x'}\}$ is given by:

$$\{\lambda_{x'}\} = \frac{\{\hat{t}\}}{t} \tag{4.9a}$$

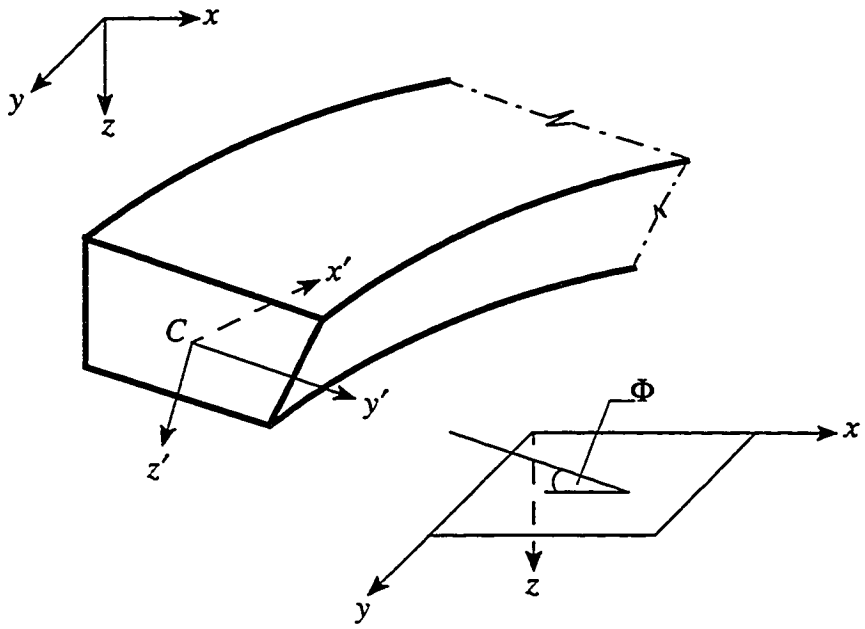

Figure 4.2 **Description of Orientation of Cross Section for Jirousek Multi-Node Element** (General Case)

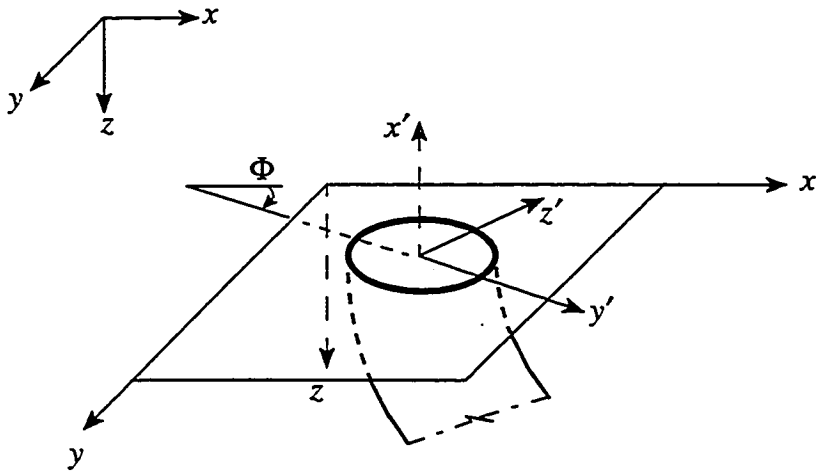

Figure 4.3 **Definition of the Angle Φ When the Cross Section Lies in the Global xy Plane** (Special Case)

where

$$\{\hat{t}\} = \begin{Bmatrix} t_x \\ t_y \\ t_z \end{Bmatrix} = \sum_{i=1}^{n} \frac{dN_i}{d\zeta} \begin{Bmatrix} x_i \\ y_i \\ z_i \end{Bmatrix} \tag{4.9b}$$

and

$$t = \sqrt{t_x^2 + t_y^2 + t_z^2} \tag{4.9c}$$

Computation of $\{\lambda_{y'}\}$ depends upon the orientation of the member cross section. When t_x and t_y are not simultaneously equal to zero, $\{\lambda_{y'}\}$ is given by:

$$\lambda_{y'z} = \sin\Phi \tag{4.10a}$$

$$\lambda_{y'y} = \frac{-b \pm \sqrt{b^2 - 4ac}}{2a} \tag{4.10b}$$

with +ve when $t_x > 0$ and -ve when $t_x < 0$.

In the above equations

$$a = t_x^2 + t_y^2$$

$$b = 2t_y t_z \sin\Phi$$

and

$$c = t_z^2 \sin^2\Phi - t_x^2 \cos^2\Phi$$

$$\left.\begin{array}{ll} \text{If} \quad t_x \neq 0, & \lambda_{y'x} = -\frac{1}{t}(t_y \lambda_{y'y} + t_x \lambda_{y'z}) \\ \text{If} \quad t_x = 0, & \lambda_{y'x} = \pm\sqrt{\cos^2\Phi - (\lambda_{y'y})^2} \end{array}\right\} \tag{4.11}$$

with +ve when $t_y < 0$ and -ve when $t_y > 0$.

When $t_x = 0$ and $t_y = 0$, the cross section is parallel to the global xy plane (Figure 4.3). In this case, Φ must be redefined as the angle between the local y' axis and the

global x axis. Thus

$$\left.\begin{aligned} \lambda_{y'x} &= \cos\Phi \\ \lambda_{y'y} &= \cos\Phi \\ \lambda_{y'z} &= 0 \end{aligned}\right\} \qquad (4.12)$$

With the vectors $\{\lambda_{x'}\}$ and $\{\lambda_{y'}\}$ computed, the third vector of direction cosines, $\{\lambda_{z'}\}$, can be calculated from the vector (cross) product of the first two.

4.3.4 Cross-Section Properties

The isoparametric element used in the analysis has the following features:

- capability of modelling any compact cross section.
- element geometry in space can be of any arbitrary shape.
- cross section properties can vary from one cross section to another.
- shear centre can differ from the gravity centre which allows to model box girder bridges.

The above features are on the other hand limited to some extent due to the following two facts:

- Warping deformations are not modelled in the element formulation.
- Cross section must be normal to the element centroidal axis, i.e. skew sections are not considered.

For formulation of the element stiffness matrix the following quantities are required:

(1) Cross section area, A.

(2) Reduced shear areas, $A_{y'}$ and $A_{z'}$.

(3) Torsional constant, $J_{x'}$.

(4) Principal moments of inertia, $I_{y'}$ and $I_{z'}$.

(5) Local eccentricities of the section shear centre, $e_{s,y'}$ and $e_{s,z'}$.

(6) The angle, Φ, between the local axis and the global xy plan.

The above values are specified at the nodes and are interpolated to give the respective quantities at any section along the member using the shape functions as follows:

$$X(\zeta) = \sum_{i=1}^{n} N_i(\zeta) \cdot X_i \tag{4.13}$$

where $X(\zeta)$ is any of the above nine quantities.

It should be mentioned here that the analysis presented in this thesis is mainly concerned with post-tensioned prestressing. Therefore, when calculating the instantaneous effects of prestressing, the area of ducts of prestressing cables should be excluded at the time of calculating the area properties of the concrete cross-section. However, it is assumed that grouting of these ducts is done shortly after prestressing and, thus, their areas should be accounted for when performing the time-dependent analysis.

4.3.5 Strain-Displacement Relation

At any cross section, the vector of generalized strains is

$$\{\varepsilon\} = \begin{Bmatrix} u'_{c,x'} \\ v'_{s,x'} - \theta'_{z'} \\ w'_{s,x'} + \theta'_{y'} \\ \theta'_{x,x'} \\ \theta'_{y,x'} \\ \theta'_{z,x'} \end{Bmatrix} \tag{4.14}$$

where the subscripts c and s refer to the centroidal axis and shear centre respectively; x' denotes differentiation with respect to the normal to the cross-section.

The above strain-displacement relationship considers the shear deformations (as

the second terms in 2nd and 3rd components of strain)

The generalized stress resultants are obtained using the generalized strains and the elasticity matrix $[D]$ as:

$$\{\sigma\} = [D] \cdot \{\varepsilon\} \tag{4.15}$$

where

$$\{\sigma\} = \begin{Bmatrix} N_{x'} \\ V_{y'} \\ V_{z'} \\ M_{x'} \\ M_{y'} \\ M_{z'} \end{Bmatrix} \tag{4.16}$$

and

$$[D] = \begin{bmatrix} EA & & & & & \\ & GA_{y'} & & & & \\ & & GA_{z'} & & & \\ & & & GJ_{x'} & & \\ & & & & EI_{y'} & \\ \text{Elements not} & & & & & EI_{z'} \\ \text{shown are zeros} & & & & & \end{bmatrix} \tag{4.17}$$

In Equation 4.16, $N_{x'}$ is the axial force, $V_{y'}$ and $V_{z'}$ are the shear forces in the local y' and z'-directions, respectively, $M_{x'}$ is the torsional moment about a longitudinal axis through the shear centre, and $M_{y'}$ and $M_{z'}$ are the bending moments about the local y' and z'-axes, respectively.

The components of the strain vector above are functions of local displacements in the local coordinate system which are obtained from the global displacements in Equation 4.4. The terms v'_s and w'_s represent the relative translation of the shear centre due to

twisting of the cross-section (Figure 4.4) and calculated as follow:

$$\begin{Bmatrix} v'_s \\ w'_s \end{Bmatrix} = \begin{Bmatrix} v'_c \\ w'_c \end{Bmatrix} + \theta'_x \cdot \begin{Bmatrix} -e_{s,z'} \\ e_{s,y'} \end{Bmatrix} \tag{4.18}$$

In order to generalize the element formulation, mapping between the element actual coordinates and the natural coordinate ζ is required as in any element based on the isoparametric formulation. A scaling factor, known as the Jacobian must be defined. Invoking the chain rule results in:

$$\frac{d}{dx'} = \frac{d\zeta}{dx'} \cdot \frac{d}{d\zeta} = \frac{1}{t} \cdot \frac{d}{d\zeta} \tag{4.19}$$

where t is a transformation factor defined by Equation 4.9.

Using of the transformation matrix $[T]$ and the shape functions N_i and then differentiating of nodal displacements to obtain the strain components, leads to the following strain-displacement relation:

$$\{\varepsilon\} = [B] \cdot \{u\} \tag{4.20}$$

where $\{u\}$ is the vector of nodal displacements, and

$$[B] = \frac{1}{t} \cdot \left[\begin{matrix} \left[\begin{matrix} \left[\frac{dN_1}{d\zeta}[T] \right]_{3\times 3} & \left[\begin{matrix} 0 \\ -tN_1\{\lambda_{z'}\} - \frac{dz_{s'}}{d\zeta} N_1\{\lambda_{x'}\} - \frac{dN_1}{d\zeta} e_{s,z'}\{\lambda_{x'}\} \\ tN_1\{\lambda_{y'}\} + \frac{dy_{s'}}{d\zeta} N_1\{\lambda_{x'}\} + \frac{dN_1}{d\zeta} e_{s,y'}\{\lambda_{x'}\} \end{matrix} \right]_{3\times 3} \\ \left[0 \right]_{3\times 3} & \left[\frac{dN_1}{d\zeta}[T] \right]_{3\times 3} \end{matrix} \right]_{i=1} & \left[\begin{matrix} \\ \\ \\ \\ \\ \\ \end{matrix} \right]_{6\times 6} \cdots \end{matrix} \right]_{i=2} \tag{4.21}$$

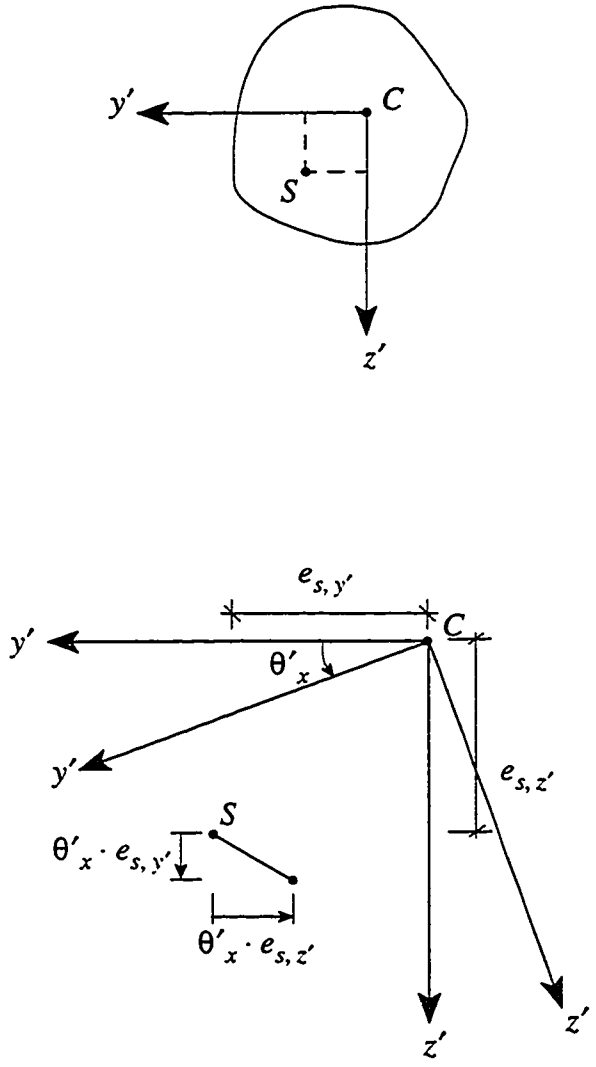

Figure 4.4 **Relative Translation of Shear Centre due to Twisting of the Cross-Section**

4.3.6 Element Stiffness Matrix

Establishing isoparametric element stiffness matrix follows the standard finite element formulation which leads to:

$$[k] = \int_0^l [B]^T \cdot [D] \cdot [B] \cdot dl \tag{4.22}$$

or

$$[k] = \int_{-1}^{1} [B]^T \cdot [D] \cdot [B] \cdot t d\zeta \tag{4.23}$$

The above integration is determined numerically using Gauss quadrature technique. The order of integration depends on the order of the shape functions used to build the strain-displacement matrix [B]. In Equation 4.23, the highest order of any term equals to $N_i N_j$ where N is the shape function. As mentioned earlier, the isoparametric element may contain three to six nodes. In case of five-node element, the shape function N_i will be quartic and the product $N_i N_j$ will be of the eighth order. The numerical integration using Gaussian quadrature technique requires n integration points to exactly integrate a function of order $2n$-1. Thus, to evaluate the eighth order function five points are required which is the same as the number of nodes.

The conclusion drawn from the above discussion is implemented into program TD-SFRAME and the number of integration points is automatically chosen equal to the number of nodes of the isoparametric element.

4.3.7 Consistent Nodal Load Vector

The consistent nodal load vector used in solving the stiffness solution is formed following the standard finite element method. In case of distributed loads or couples, the

load vector is given as:

$$\{F\} = \int_{-1}^{+1} \{N(\xi)\} \cdot q(\xi) \cdot t dt \qquad (4.24)$$

where $\{N(\xi)\}$ is the vector of nodal interpolation functions evaluated at the appropriate Gauss points and $q(\xi)$ is the magnitude of the distributed load at that point.

The Jirousek isoparametric element, by definition, adopts the same interpolation functions used in building the stiffness matrix to compute the consistent load vector. In case of a concentrated force or couple f at certain location within the isoparametric element, the consistent nodal load vector is similarly given by

$$\{F\} = \{N(\xi)\} \cdot f \qquad (4.25)$$

4.4 Effects of Prestressing

As mentioned earlier in the previous chapters, the current computer program TD-SFRAME is a modified version of Program SFRAME developed by Maher (1985) which is suitable only for the analysis of space frames under the instantaneous effects of external loads and prestressing. The program is extended in the present study to perform the analysis of structures constructed in stages accounting for the time-dependent effects of creep and shrinkage of concrete and relaxation of prestressed steel.

In SFRAME, the contribution of the prestressing tendons to the stiffness of the concrete structure was not considered. The effects of prestressing were accounted for, however, in the form of equivalent nodal and element forces. These forces were calculated as follows:

1) The instantaneous losses in prestressing forces at the time of jacking due to friction and anchor slip were calculated first considering that jacking can be from either or both ends of the tendon.

2) The nodal values of prestressing forces were computed in light of the above instantaneous losses.

3) The prestressing forces were considered as composed of two components, namely, anchorage and distributed forces. The anchorage forces are applied at the anchorage nodes as concentrated forces while the distributed load within the element is considered as composed of two orthogonal components, tangential and normal to cable local axis. The tangential component results from the variation of the cable force along its length (as a result of the losses) while the normal component is due to the curvature of the tendons in space.

In the present work, SFRAME is modified to include the contribution of the tendons to the stiffness of the structure and to include the time-dependent prestressing losses due to creep, shrinkage and relaxation in the analysis as discussed below.

4.4.1 Modelling of Prestressing Tendons

The formulation of the prestressing tendons stiffness follows the same basic concepts of the Jirousek isoparametric element. The tendon is assumed to be composed of multi-node (up to six nodes) segments. The tendon's nodes are correlated to the concrete element through nodal local eccentricities at each cross section of the concrete element. Since the isoparametric element adopted in the analysis provides accurate results at the nodes, the cable behaviour is expected to be satisfactory for the current research work.

For computation of the tendon stiffness and the forces due to prestressing, the tendon profile in space and its location with respect to the centroidal axis of the concrete element must be defined first. Figure 4.5 gives a general description of the prestressing

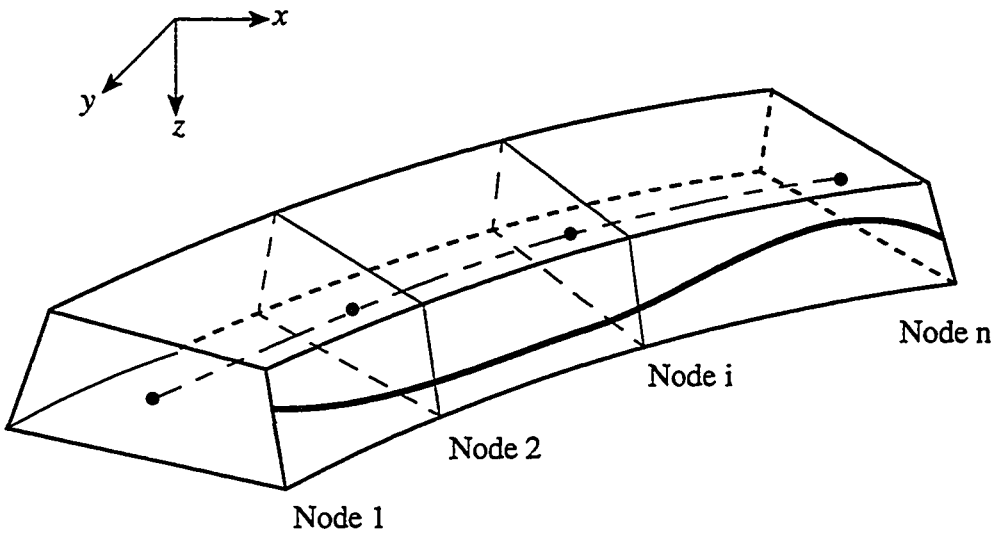

(a) **Permissible Cable Profile**

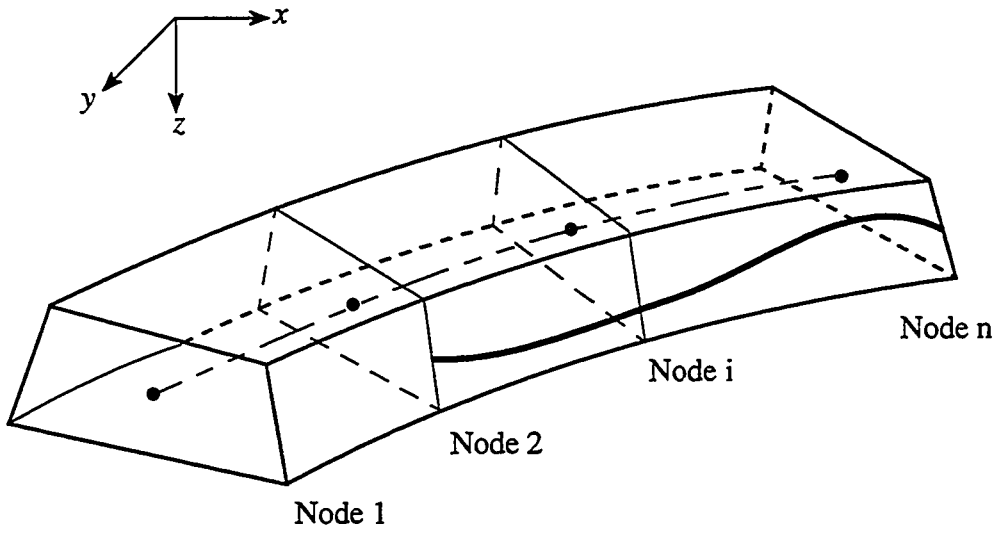

(b) **Invalid Cable Profile**

(Cable anchorage point does not coincide with the end cross-section of the Jirousek element)

Figure 4.5 **Cable Profile used with the Multi-Node Curved Element**

tendon profile within a curved concrete element. The tendon profile can be defined in space by the following relation given that the global coordinates of the tendon at the element nodal cross section are known:

$$\begin{Bmatrix} x_p \\ y_p \\ z_p \end{Bmatrix} = \sum_{i=1}^{n} N_i(\xi) \cdot \begin{Bmatrix} x_{pi} \\ y_{pi} \\ z_{pi} \end{Bmatrix} \tag{4.26}$$

The subscript p refers to the prestressing tendon and $N_i(\xi)$ is the same shape function used for the concrete curved element and is given by Equation 4.2. This requires that the anchorage of a tendon must lie within the cross-section of a Jirousek concrete element. Tendons with an anchorage lying within any intermediate section of a concrete element (Figure 4.5b) can not be considered in the present analysis.

In the computer program TD-SFRAME, the eccentricities of the cable with respect to the cross-section principal axes are given as input data at each node. The global coordinate can be calculated from these eccentricities (Maher, 1985).

4.4.2 Strain-Displacement Relation for Prestressing Tendons

At any cross section, the steel strain is

$$\varepsilon = u'_{t,x'} \tag{4.27}$$

where the subscript t refers to a prestressing tendon and x' is its longitudinal local axis. Thus, the steel stress is

$$\sigma_{st} = \varepsilon \cdot E_s \tag{4.28}$$

Since the analysis is concerned with the coordinates in global directions at the nodal points, the steel strain should be correlated to the nodal displacements. First, the displacement in the local direction at any point on the steel tendon is

$$u'_t = (u' + \theta_{y'} \cdot e_{z'} - \theta_{z'} \cdot e_{y'}) \cdot \cos\alpha$$
$$+ v'_t \cdot \cos\beta + w'_t \cdot \cos\gamma \qquad (4.29)$$

where

$$u' = \{\lambda_{x'}\} \cdot \sum_{i=1}^{n} N_i \cdot \begin{Bmatrix} u_i \\ v_i \\ w_i \end{Bmatrix} \qquad (4.30)$$

$$v'_t = v' - \theta_{x'}\, e_{z'} \qquad w'_t = w' + \theta_{x'}\, e_{y'} \qquad (4.31)$$

$$\theta_{y'} = \{\lambda_{y'}\} \cdot \sum_{i=1}^{n} N_i \cdot \begin{Bmatrix} \theta_{xi} \\ \theta_{yi} \\ \theta_{zi} \end{Bmatrix} \qquad \theta_{z'} = \{\lambda_{z'}\} \cdot \sum_{i=1}^{n} N_i \cdot \begin{Bmatrix} \theta_{xi} \\ \theta_{yi} \\ \theta_{zi} \end{Bmatrix} \qquad (4.32)$$

$$\begin{Bmatrix} \cos\alpha \\ \cos\beta \\ \cos\gamma \end{Bmatrix} = \sum_{i=1}^{n} N_i \cdot \begin{Bmatrix} \cos\alpha_i \\ \cos\beta_i \\ \cos\gamma_i \end{Bmatrix} \qquad (4.33)$$

In the above equations, $\cos\alpha$, $\cos\beta$ and $\cos\gamma$ are the direction cosines of the tendon at the point considered with respect to the local axes x', y' and z' of the concrete element, respectively (see figure 4.6); u', v', w', $\theta_{x'}$, $\theta_{y'}$ and $\theta_{z'}$ are the displacements in the local directions of the concrete element at the section which includes the tendon point under consideration (see Equations 4.4); u_i, v_i, w_i, θ_{xi}, θ_{yi} and θ_{zi} are the displacements in the global directions at node i. The vectors $\{\lambda_{x'}\}$, $\{\lambda_{y'}\}$ and $\{\lambda_{z'}\}$ are as defined in Subsection 4.3.3. The tendon eccentricities $e_{y'}$ and $e_{z'}$ at the point considered can be expressed as:

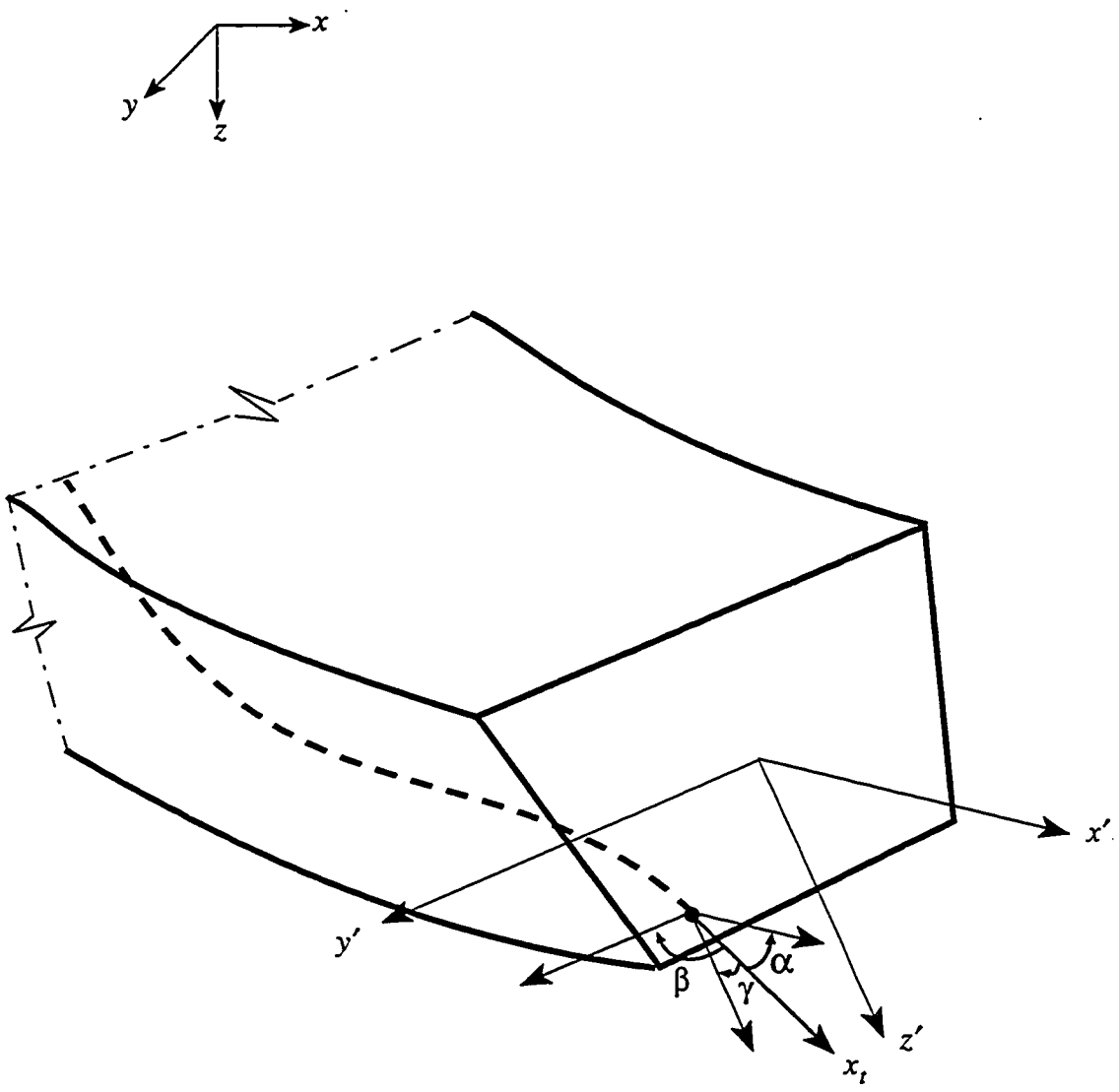

Figure 4.6 **Definition of the Angles between the Cable's Local Axis and Element Local axes**

$$e_{y'} = \sum_{i=1}^{n} N_i \cdot e_{y'i} \qquad e_{z'} = \sum_{i=1}^{n} N_i \cdot e_{z'i} \tag{4.34}$$

then

$$\frac{de_{y'}}{dx'} = \frac{1}{t} \cdot \sum_{i=1}^{n} \frac{dN_i}{d\zeta} \cdot e_{y'i} \qquad \frac{de_{z'}}{dx'} = \frac{1}{t} \cdot \sum_{i=1}^{n} \frac{dN_i}{d\zeta} \cdot e_{z'i} \tag{4.35}$$

Hence, the strain at that point is

$$\begin{aligned} u'_{t,x'} = \frac{d}{dx'} u'_t = {} & [u'_{x'} + (\theta'_{y',x'} \cdot e_{z'} + \theta_{y'} \cdot e'_{z',x'}) - (\theta'_{z',x'} \cdot e_{y'} + \theta_{z'} \cdot e'_{y',x'})] \cos\alpha \\ & + [v'_{x'} - (\theta'_{x',x'} \cdot e_{z'} + \theta_{x'} \cdot e'_{z',x'})] \cos\beta \\ & + [w'_{x'} + (\theta'_{x',x'} \cdot e_{y'} + \theta_{x'} \cdot e'_{y',x'})] \cos\gamma \end{aligned} \tag{4.36}$$

The strain-displacement relation is given by:

$$\{\varepsilon\} = \{B\}_t \cdot \{u\} \tag{4.37}$$

Using Equations 4.27 to 4.36, the strain-displacement matrix $\{B\}_t$ can be written as:

$$\{B\}_t = \frac{1}{t} \cdot \left[\left(\overset{i=1}{[\{A_1\}_{1\times 3} \vdots \{B_1\}_{1\times 3}]} \right) \left(\overset{i=2}{[\ ]_{1\times 6}} \right) \ldots \right] \tag{4.38}$$

where

$$\{A_1\} = \frac{dN_1}{d\zeta} \cdot \left(\{\lambda_{x'}\}\cos\alpha + \{\lambda_{y'}\}\cos\beta + \{\lambda_{z'}\}\cos\gamma \right)$$

$$\{B_1\} = \left[\{\lambda_{y'}\}\left(\frac{dN_1}{d\zeta} \cdot e_{z'} + N_1 \cdot \frac{de_{z'}}{d\zeta}\right) - \{\lambda_{z'}\}\left(\frac{dN_1}{d\zeta} \cdot e_{y'} + N_1 \cdot \frac{de_{y'}}{d\zeta}\right)\right]\cos\alpha$$

$$- \{\lambda_{x'}\}\left(N_1 \cdot \frac{de_{z'}}{d\zeta} + \frac{dN_1}{d\zeta} \cdot e_{z'}\right)\cos\beta + \{\lambda_{x'}\}\left(N_1 \cdot \frac{de_{y'}}{d\zeta} + \frac{dN_1}{d\zeta} \cdot e_{y'}\right)\cos\gamma \tag{4.39}$$

4.4.3 Prestressing Tendon Stiffness Matrix

As previously done for the stiffness matrix of the isoparametric concrete element, the prestressed steel tendon stiffness matrix is computed using the well known standard finite element integration given by

$$[k_t] = EA \cdot \int_0^l \{B\}_t^T \cdot \{B\}_t \cdot dl \tag{4.40}$$

Or

$$[k_t] = EA \cdot \int_{-1}^{1} \{B\}_t^T \cdot \{B\}_t \cdot t d\zeta \tag{4.41}$$

Once again, a numerical integration is used to evaluate the integration given above. The same Gaussian quadrature technique is used along with the same shape functions.

4.4.4 Prestressing Forces and Prestressing Load Vector

The prestressing force at any point along the tendon can be calculated by integration of the forces defined at each element node. Thus,

$$P(\xi) = \sum_{i=1}^{n} N_i(\xi) \cdot P_i \tag{4.42}$$

The tangential component of the prestressing force is expressed as

$$P_t = \frac{dP}{dl} = \frac{d\zeta}{dl} \cdot \frac{dP}{d\zeta} = \frac{1}{t} \cdot \frac{dP}{d\zeta} = \frac{1}{t} \cdot \sum_{i=1}^{n} \frac{dN_i}{d\zeta} P_i \tag{4.43}$$

where t is the magnitude of the vector tangent to the cable at the point under consideration and is calculated from Equations 4.9b and c replacing x_i, y_i and z_i by x_{pi}, y_{pi} and z_{pi} (Equation 4.26).

The normal component of the prestressing force is evaluated as

$$P_n = \frac{P}{R} = P \cdot n \tag{4.44}$$

where R is the radius of principal curvature of the tendon line in space at the point under consideration and equals the reciprocal of the magnitude of the principal normal vector n, Figure 4.7, which can be expressed in the unit vector form as

$$\{\lambda_n\} = \frac{\{\hat{n}\}}{n} \tag{4.45}$$

The global components of the distributed force at any point can now be obtained as

$$\{P\} = \begin{Bmatrix} P_x \\ P_y \\ P_z \end{Bmatrix} = P_t\{\lambda_t\} + P_n\{\lambda_n\} \tag{4.46}$$

where λ_t is calculated from Equations 4.9, replacing x_i, y_i and z_i by x_{pi}, y_{pi} and z_{pi}.

The load vector obtained is then transformed into local coordinates at the node under consideration and then used to obtain local concentrated moments as a result of tendon node eccentricities. The final load vector (forces and moments), is inversely transformed to the global coordinate system.

Finally, the corresponding equivalent nodal loads are computed using the standard finite element technique as

$$\{F\} = \int_{-1}^{1} \{N(\zeta)\} \cdot \{P(\zeta)\} \cdot t d\zeta \tag{4.47}$$

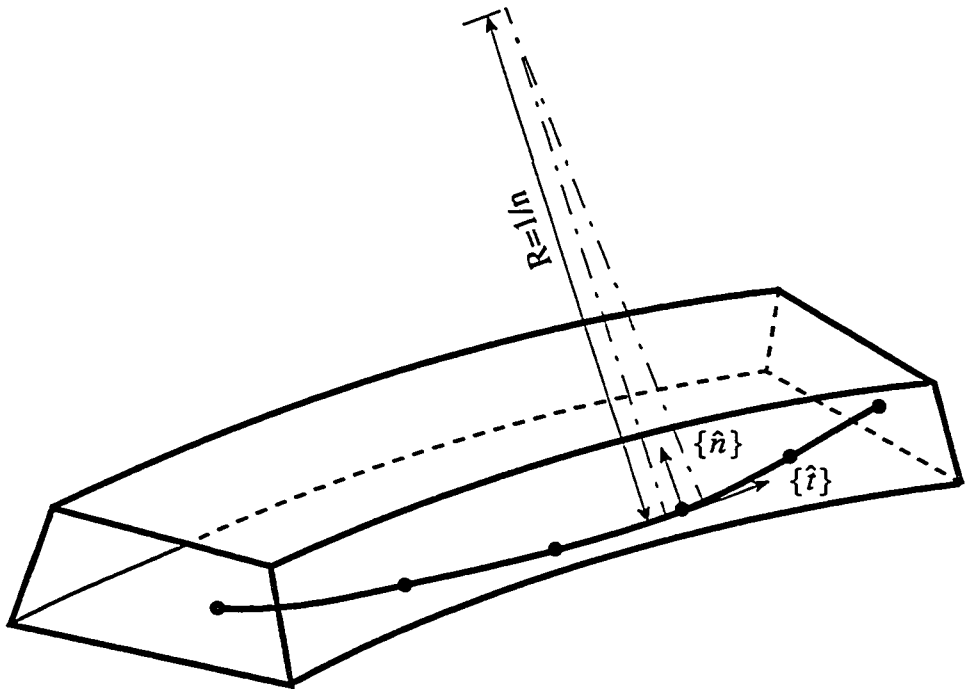

Figure 4.7 **Principal Normal and Tangent Vectors to the Tendon in Space**

4.5 Time-Dependent Stiffness Analysis

In section 3.6, the time-dependent strain due to creep and shrinkage of concrete was discussed. In reinforced or prestressed structures, the free strain induced by creep and shrinkage will be restrained by the reinforcement and redistribution of stresses between the concrete and the steel takes place. Time-dependent deformations of individual members also develop. In statically determinate structures, these deformations occur freely without restraint at the supports and, thus, changes in reactions or internal forces develop. In statically indeterminate structures, on the other hand, the time-dependent deformations are restrained by the supports or by adjacent members and changes in the support reactions and hence in internal forces develop. The displacement method of analysis described in the previous sections can be applied to determine the time-dependent changes in displacements, reactions and internal forces in statically indeterminate structures. For this purpose, the stiffness matrix of individual elements must be modified for each time interval by replacing the cross-section properties A, $I_{y'}$ and $I_{z'}$ by $\bar{A}$, $\bar{I}_{y'}$ and $\bar{I}_{z'}$, the area and moments of inertia about the centroidal y' and z' axes of an "age-adjusted" transformed section made up of concrete and the area of steel reinforcement multiplied by $E_s/\bar{E}_c(t_{i+1}, t_i)$; where $\bar{E}_c(t_{i+1}, t_i)$ is the age-adjusted modulus of elasticity of concrete in the time interval $(t_{i+1} - t_i)$ defined by Equation 3.22. The elasticity matrix $[D]$ of Equation 4.17 must also be modified by replacing E and G by $\bar{E}$ and $\bar{G}$.

A group of nodal forces are also required to artificially restrain the hypothetical free deformations at the ends of individual members. These nodal forces are to be summed up and applied at the nodes of the assembled structure in reversed directions in order to

calculate the time-dependent changes in nodal displacements and support reactions. Two different approaches are used in the prismatic straight elements and in isoparametric multi-node Jirousek elements.

4.5.1 Time-Dependent Restraining Forces in Straight Elements

Consider a typical space frame member as shown in Figure 4.1a. In order to calculate the fixed-end forces required to restrain the free deformations due to the time-dependent effects, assume that the member is fixed at one of its nodes, say Node 2, while the other end (Node 1) is free, as shown in Figure 4.8. During any time interval i between t_i and t_{i+1}, the time-dependent changes in fixed-end forces at the six degrees of freedom at Node 1 are:

$$\{\Delta F'(t_{i+1}, t_i)\}_1 = -[\bar{k}(t_{i+1}, t_i)]_1 \ \{\Delta d(t_{i+1}, t_i)\}_1 \tag{4.48}$$

where $\{\Delta d(t_{i+1}, t_i)\}_1$ represents the six displacements in the local directions at Node 1 with the member treated as a cantilever and subjected to the time-dependent effects within the period $(t_{i+1} - t_i)$. The elements of vector $\{\Delta d\}_1$ are given as:

$$\left.\begin{aligned} \Delta d_1 &= -\int_0^l \Delta\varepsilon_o(t_{i+1}, t_i)dx'; \\ \Delta d_2 &= -\int_0^l \Delta\Psi_{z'}(t_{i+1}, t_i)x'dx'; \qquad \Delta d_3 = -\int_0^l \Delta\Psi_{y'}(t_{i+1}, t_i)x'dx' \\ \Delta d_4 &= -\int_0^l \Delta\theta_{x'}(t_{i+1}, t_i)dx' \\ \Delta d_5 &= -\int_0^l \Delta\Psi_{y'}(t_{i+1}, t_i)dx'; \qquad \Delta d_6 = \int_0^l \Delta\Psi_{z'}(t_{i+1}, t_i)dx' \end{aligned}\right\} \tag{4.49}$$

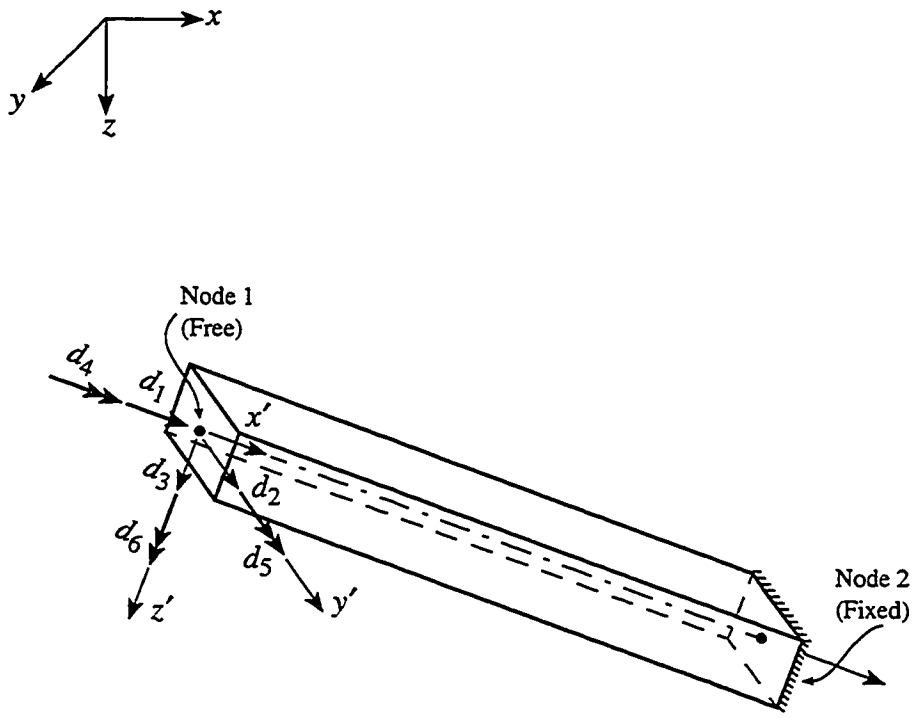

Figure 4.8 **Displacement at Node 1 of a Straight Prismatic Space Frame Element Treated as a Cantilever Fixed at Node 2.**

where $\Delta\varepsilon_o$, $\Delta\Psi_{y'}$, $\Delta\Psi_{z'}$ and $\Delta\theta_{x'}$ are, respectively, the free time-dependent changes in the average normal strain at the centroid and curvatures and angle of twist per unit length as calculated at different cross sections of the member by Equations 3.24 and 3.31 or similar equations as discussed in Section 3.6. In reinforced or prestressed concrete members, $\Delta\varepsilon_o$, $\Delta\Psi_{y'}$ and $\Delta\Psi_{z'}$ are calculated using the area properties of the age-adjusted transformed section. The integration in Equations 4.49 are evaluated numerically, assuming a parabolic variation of $\Delta\varepsilon_o$, $\Delta\Psi_{y'}$, $\Delta\Psi_{z'}$ and $\Delta\theta_{x'}$ between each three consecutive sections or a straight line variation of the same variables between each two sections.

In Equation 4.48, $[\bar{k}(t_{i+1}-t_i)]$ is a 6x6 age-adjusted stiffness matrix corresponding to the six degrees of freedom at Node 1 and is given by:

$$[\bar{k}]_1 = \begin{bmatrix} \frac{\bar{E}\bar{A}}{l} & & & & & \\ & \frac{12\bar{E}\bar{I}_{z'}}{l^3} & & & & \\ & & \frac{12\bar{E}\bar{I}_{y'}}{l^3} & & & \\ & & & \frac{\bar{G}\bar{J}}{l} & & \\ & & \frac{6\bar{E}\bar{I}_{y'}}{l^2} & & \frac{4\bar{E}\bar{I}_{y'}}{l} & \\ & \frac{6\bar{E}\bar{I}_{z'}}{l^2} & & & & \frac{4\bar{E}\bar{I}_{z'}}{l} \end{bmatrix} \quad \text{Symmetrical; Elements not shown are zeros} \qquad (4.50)$$

where $\bar{E}$ and $\bar{G}$ are the age-adjusted elasticity and shear moduli, respectively; and $\bar{A}$, $\bar{I}_{y'}$ and $\bar{I}_{z'}$ are the area and the moments of inertia of the age-adjusted cross-section of the

member.

Equation 4.48 gives the fixed-end forces at Node 1. The forces at Node 2 can be determined by equilibrium; thus, the twelve fixed-end forces can be expressed as:

$$\{\Delta F'\} = [L]^T \{\Delta F'\}_1 \tag{4.51}$$

where $[L]_{6\times 12}$ is given by:

$$[L] = \begin{bmatrix} 1 & & & -1 & & & & & & & & \\ & 1 & & & -1 & & & & & & & -l \\ & & 1 & & & & -1 & & & -l & & \\ & & & 1 & & & & -1 & & & & \\ & & & & 1 & & & & -1 & & & \\ & & & & & 1 & & & & & & -1 \end{bmatrix} \quad \begin{matrix} \text{Element not} \\ \text{shown are} \\ \text{zeros} \end{matrix} \tag{4.52}$$

The fixed-end forces given by Equation 4.51 are derived with respect to the local coordinate system. Before assemblage of the overall load vector, the forces $\{\Delta F'\}$ for all members must be transformed from the local to the global directions as follows:

$$\{\Delta F_m\} = [H]^T \{\Delta F'\} \tag{4.53}$$

where $\{\Delta F_m\}$ is the load vector in global coordinates for member m and $[H]^T_{12\times 12}$ is a transformation matrix given by

$$[H] = \begin{bmatrix} [T] & & & \\ & [T] & & \\ & & [T] & \\ & & & [T] \end{bmatrix} \quad \begin{matrix} \text{Matrices not shown} \\ \text{are null} \end{matrix} \tag{4.54}$$

in which $[T]_{3\times 3}$ is given by Equation 4.8 but with

$$\left.\begin{aligned}
&\lambda_{x'x} = (x_2 - x_1)/l \quad ; \quad \lambda_{x'y} = (y_2 - y_1)/l \quad ; \quad \lambda_{x'z} = (z_2 - z_1)/l \\
&\lambda_{z'x} = \cos\theta_{z'x} \quad ; \quad \lambda_{z'y} = \cos\theta_{z'y} \quad ; \quad \lambda_{z'z} = \cos\theta_{z'z} \\
&\lambda_{y'x} = \frac{1}{t}(\lambda_{z'y}\lambda_{x'z} - \lambda_{x'y}\lambda_{z'z}); \\
&\lambda_{y'y} = \frac{1}{t}(\lambda_{x'x}\lambda_{z'z} - \lambda_{z'x}\lambda_{x'z}); \\
&\lambda_{y'z} = \frac{1}{t}(\lambda_{z'x}\lambda_{x'y} - \lambda_{x'x}\lambda_{z'y})
\end{aligned}\right\} \quad (4.55)$$

where x, y and z are the global coordinates of the nodes; the subscripts 1 and 2 refer to the first and second nodes of the element, respectively; $\theta_{z'x}$, $\theta_{z'y}$ and $\theta_{z'z}$ are the angles between the local z'-axis and the global x, y and z axes; t is given by

$$t = \sqrt{\lambda_{y'x}^2 + \lambda_{y'y}^2 + \lambda_{y'z}^2} \quad (4.56)$$

4.5.2 Time-Dependent Restraining Forces in Isoparametric Curved Elements

The increments of free strain during a time interval $(t_{i+1} - t_i)$ at each nodal cross-section are restrained by the following restraining forces:

$$\left.\begin{aligned}
\Delta N_j &= \bar{E}\bar{A}_j \;\; \Delta\varepsilon_{o,j}(t_{i+1}, t_i) \\
\Delta M_{x',j} &= \bar{G}_i \bar{J}_{x',j} \;\; \Delta\theta_{x',j}(t_{i+1}, t_i) \\
\Delta M_{y',j} &= \bar{E} \bar{I}_{y',j} \;\; \Delta\Psi_{y',j}(t_{i+1}, t_i) \\
\Delta M_{z',j} &= \bar{E} \bar{I}_{z',j} \;\; \Delta\Psi_{z',j}(t_{i+1}, t_i)
\end{aligned}\right\} \quad (4.57)$$

These restraining forces are stored in a generalized stress resultant vector $\{\sigma_r\}$ at each node J:

$$\{\sigma_r\}_j = \left\{ \Delta N, \;\; 0, \;\; 0, \;\; \Delta M_{x'}, \;\; \Delta M_{y'}, \;\; \Delta M_{z'} \right\}_j \quad (4.58)$$

The equivalent nodal forces for each element are calculated directly from the nodal restraining forces as follows:

$$\{\Delta F'(t_{i+1}, t_i)\} = \int_{-1}^{1} [B]^T \{\sigma_r\} \, t d\zeta \tag{4.59}$$

where $$\{\sigma_r\} = \bar{E} \left\{ \bar{A}\Delta\varepsilon_o, 0, \; 0, \frac{J_{x'}\Delta\theta_{x'}}{2(1+\nu)}, \bar{I}_{y'}\Delta\Psi_{y'}, \bar{I}_{z'}\Delta\Psi_{z'} \right\} \tag{4.60}$$

where

$$\left.\begin{aligned} \bar{A} &= \sum_{j=1}^{n} N_j \, \bar{A}_j \quad ; \quad \Delta\varepsilon_o = \sum_{j=1}^{n} N_j \, \Delta\varepsilon_{j,o} \\ J &= \sum_{j=1}^{n} N_j \, J_j \quad ; \quad \Delta\theta_{x'} = \sum_{j=1}^{n} N_j \, \Delta\theta_{x',j} \\ \bar{I}_{y'} &= \sum_{j=1}^{n} N_j \, \bar{I}_{y',j} \quad ; \quad \Delta\Psi_{y'} = \sum_{j=1}^{n} N_j \, \Delta\Psi_{y',j} \\ \bar{I}_{z'} &= \sum_{j=1}^{n} N_j \, \bar{I}_{z',j} \quad ; \quad \Delta\Psi_{z'} = \sum_{j=1}^{n} N_j \, \Delta\Psi_{z',j} \end{aligned}\right\} \tag{4.61}$$

Numerical integration is required to evaluate the integration in Equation 4.59. Gauss quadrature is used with an order depending on the order of shape functions N_j.

4.5.3 Nodal Forces due to Prestress Losses

In prestressed concrete structures, a prestressing tendon experiences a continuous decrease in the tension force due to instantaneous and time-dependent effects. In multi-stage construction, a prestressing tendon undergoes instantaneous losses at the instant of new events such as addition of new loads, change of boundary condition, addition or removal of another tendon or changing the tension force of an existing tendon. These losses are referred to as elastic losses as they result from elastic deformations of the structure. During a period between any two consecutive instants, prestress losses take

place only due to the time-dependent deformations which result from creep and shrinkage of concrete and relaxation of prestressed steel.

To evaluate the losses in a prestressed tendon, either due to elastic or time-dependent deformations, the contribution of the tendon to the stiffness of the overall structure must be taken into consideration when performing the stiffness analysis of the completed part of the structure at any time during or after construction. This was discussed in Section 4.4 above.

In the present analysis, reduced relaxation of prestressed steel is computed for each tendon in the structure based on the time at which the initial tension is applied to the tendon. The decrease in the steel stress is converted to equivalent nodal forces using the conventional finite element formulation for initial stress problem. The equivalent forces can be expressed as (Cook, 1992):

$$\{\Delta F_{pr}(t_{i+1}, t_i)\} = \int_{-1}^{1} \{N(\xi)\} \ \{\Delta P(\xi)\} \ t d\xi \qquad (4.62)$$

where $\Delta P(\xi)$ represents the losses in the prestressing force at any cross-section and is equal to $A_{ps} \ \Delta\bar{\sigma}_{pr}$, with A_{ps} being the cross-sectional area of the tendon and $\Delta\bar{\sigma}_{pr}$ being the reduced relaxation in the period $(t_{i+1} - t_i)$ as calculated by Equation 2.33.

In the analysis of the time-dependent effects, the total losses in a prestressing tendon within any time interval due to the combined effects of creep, shrinkage and relaxation are calculated as:

$$\Delta P_{ps} = A_{ps} \ \Delta\bar{\sigma}_{pr} + \Delta\bar{P} \qquad (4.63)$$

Equation 4.63 gives the absolute value of the prestress losses. The term $\Delta\bar{P}$ is the

change in the prestressing force due to application of the nodal forces resulting from creep, shrinkage and relaxation on the structure.

4.6 Formwork Adjustment in Segmental Construction

The balanced cantilever method of construction has become widely used over the past few decades because of its flexibility in allowing long span bridges and those with arbitrary alignment to be built. In this construction method the piers are built first and then segments of the bridge deck are placed successively on both sides of the pier and tied together by post-tensioning forming a balanced cantilever at each pier. When two cantilevers from two consecutive piers meet near the middle of the span between the piers, a closure segment is used to complete the span. Additional prestressing tendons extending over a number of adjacent spans are also stressed to provide the amount of prestressing required by the design and to ensure continuity of the spans.

A cantilevered part of the structure consists of several segments, which can be of different ages constructed, loaded or prestressed at different instants of time during construction, this leads to significant time-dependent deformations due to creep, shrinkage and relaxation. These time-dependent deformations may cause considerable discontinuity (i.e., relative displacements) between the free ends of two meeting cantilevers. These relative displacements must be accurately predicted in order eliminate the discontinuity in the field by adjusting the formwork during construction either by jacking or by providing appropriate camber.

During construction, a segmentally built cantilever deforms continuously with time due to its self weight, prestressing and time-dependent effects. Thus, when a new segment is added, it will assume a position different from that originally intended. This deviated

position is a result of the displacements in space at the tip of the cantilever before the segment is added. Figure 4.9 shows the projection on the *xy*-plane of a two segment cantilever which may represent a part of a segmentally erected space frame. For clarity of presentation, the two segments are assumed to be modelled with two straight prismatic elements. Line *ABC* represents the projection of the desired undisplaced position of the cantilever. Line AB' represents the projection of Segment 1 after deformation and just before adding segment 2 to the structure. Thus, line $B'C'$ represents the projection of the deviated position of Segment 2 at the instant of its installation.

The step-by-step procedure which will be described in Section 4.9 gives the displacement increments that take place at the end of each stage of construction. Thus, at the end of stage 1, the displacements of node *B* will be known. Just before erection of Segment 2, node *C* will take the position C'. The displacements between *C* and C' can be calculated as follows:

$$\{d_C\} = \{d_B\} + [T]_{BC} \cdot \begin{Bmatrix} d_{x'} \\ d_{y'} \\ d_{z'} \end{Bmatrix}_C \tag{4.64}$$

$$\{\theta_C\} = \{\theta_B\} \tag{4.65}$$

where

$$\begin{Bmatrix} d_{x'} \\ d_{y'} \\ d_{z'} \end{Bmatrix}_C = \begin{Bmatrix} 0 \\ \theta_{z'(B)} \cdot l_{BC} \\ -\theta_{y'(B)} \cdot l_{BC} \end{Bmatrix} \tag{4.66}$$

$$\{\theta'\}_B = [T]_{BC} \cdot \{\theta\}_B \tag{4.67}$$

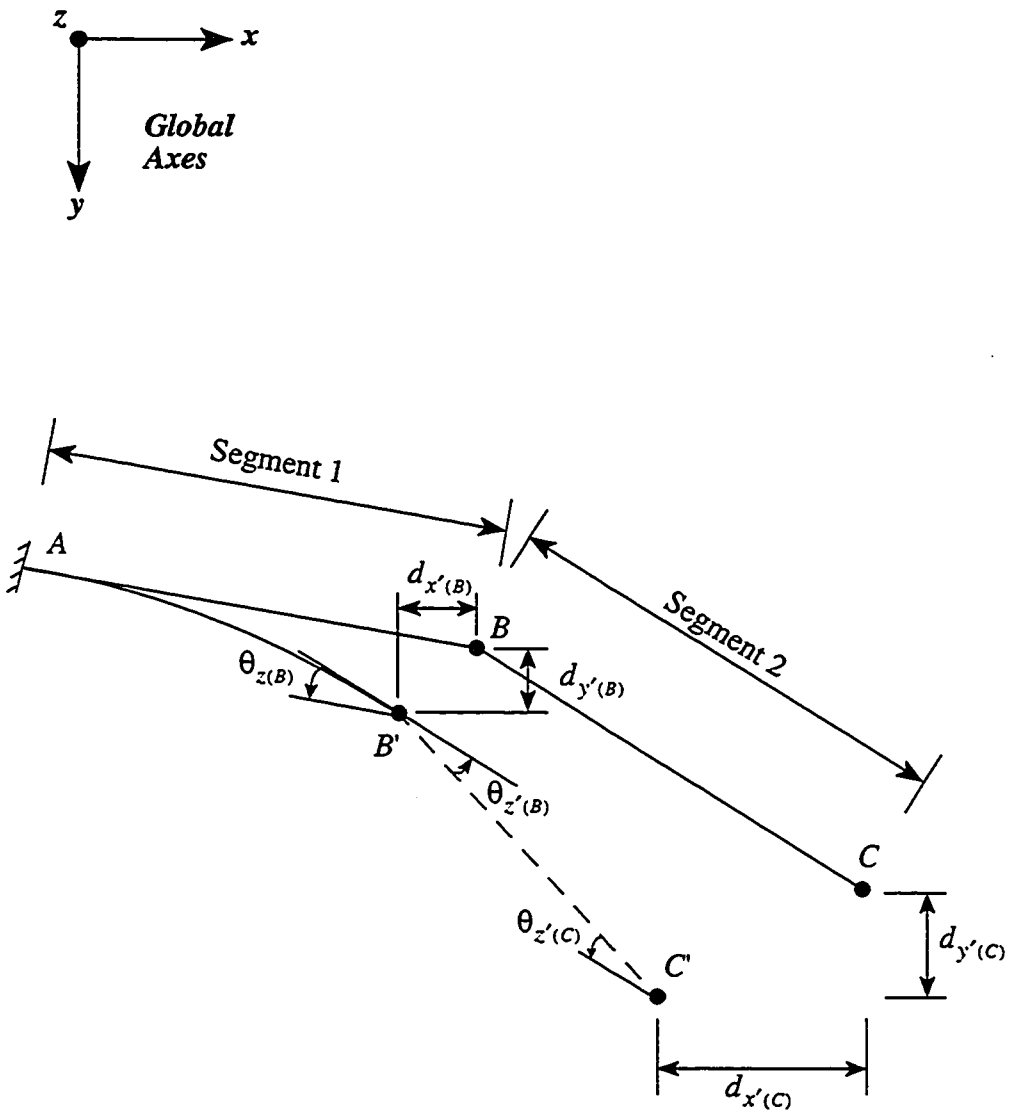

Figure 4.9 **Horizontal Displacements in Precast Segmentally Ereceted Elements**

In the above equations the primed symbols denote deformations related the local axes of the element BC whereas the unprimed symbols refer to displacements with respect to the global axes; l_{BC} is the length of the chord between nodes B and C. The transformation matrix $[T]_{BC}$ is given by Equation 4.8 for the Jirousek curved element and by Equation 4.55 for the straight prismatic element.

4.7 Effect of Changes in Boundary Conditions

In multi-stage and segmental constructions shoring or temporary supports are commonly used during some stages of construction. They are normally added at or removed from some locations to maintain deformations within certain limits or to prevent excessive internal forces. Temporary supports are more likely needed in curved than in straight bridges to provide stability of parts of the structure during construction.

In the balanced cantilever method of construction, a constructed part of the bridge deck can be kept cantilevering from the pier until it reaches the middle of the span or the location of a permanent support provided that the deformations of the cantilever are acceptable, otherwise, a temporary support must be used as in the case shown in Figure 4.10a for example. Just after removal of the temporary supports, the reaction components resisted by the supports must be applied in a reversed direction on the structure as shown in Figure 4.10b. Another similar situation arises when the rigid connection between the pier and the bridge deck is transformed into a hinged or a roller support after the spans are completed or the bridge is made continuous. Any unbalanced moments at the top of the pier must be applied at the support in a reversed direction. The effects of these changes in boundary conditions are automatically accounted for in the computer program TD-SFRAME developed for this research.

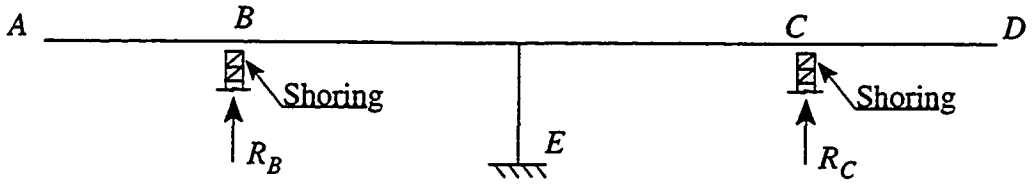

(a) Reactions at Temporary Supports

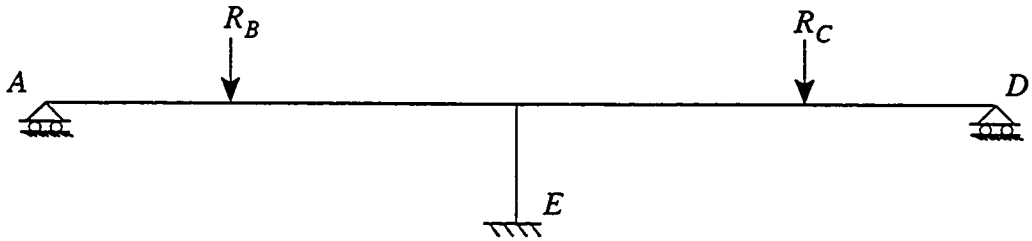

(b) Forces due to Removal of Temporary Supports

Figure 4.10 **Effect of Changes in Support Conditions**

4.8 Calculation of Reactions

In the program TD-SFRAME, boundary conditions are introduced to the stiffness matrix and the load vector of the structure using the penalty method. For a restrained degree of freedom n with a prescribed displacement β, the stiffness element K_{nn} is modified to:

$$K_{nn(modified)} = K_{nn} + H \tag{4.68}$$

where H is a large number calculated as

$$H = K_{nn} \times 10^6 \tag{4.69}$$

And the element R_n of the load vector is modified to:

$$R_{n(modified)} = R_n + H \cdot \beta \tag{4.70}$$

After solving the simultaneous equilibrium equations for the nodal displacements, the reaction F_n can be calculated as:

$$F_n = H \cdot (\beta - r_n) \tag{4.71}$$

where r_n is the nodal displacement associated with the degree of freedom n.

4.9 Analysis Routine

The time domain under consideration is divided into a finite number of intervals, for each interval the conventional displacement (stiffness) method is generally performed twice. First the structure is analyzed under the instantaneous effects that take place at the beginning of the time interval. These instantaneous effects can be due to addition or removal of an element, prestressing tendons, supports or boundary conditions. Concrete moduli of elasticity used are those calculated at the beginning of the interval. The analysis is performed for a second time to evaluate the effects of the time dependent changes in displacements, reactions and internal forces that take place during the time interval under

consideration. For this analysis, the age-adjusted effective moduli of elasticity are to be used in formulating element stiffness matrices and the vector of nodal forces required to restrain the hypothetical free deformations due to creep, shrinkage and relaxation.

In some cases, the user may wish to ignore the time dependent effects on the structure at any intermediate time interval. Here the length of the time interval is zero and only an instantaneous analysis is performed. Similarly, the user may need to calculate the time dependent effects on the structure at some specific time interval after completion of construction and no changes in loads or boundary conditions take place. Here, only a time-dependent analysis is performed.

For any time interval *i*, the instantaneous and time-dependent increments of nodal displacements, support reactions and member internal forces are determined in steps as follows:

1. Generate the element stiffness matrices of all members already existing or added to the structure at the beginning of interval *i*. The isoparametric finite element formulation presented in Subsections 4.3.1 to 4.3.6 are to be used for the curved elements and the conventional space frame element stiffness matrix is to be used for the straight prismatic elements. The concrete elasticity and shear moduli, *E* and *G*, used for establishing the stiffness matrices depend on the analysis required, instantaneous or time-dependent. Also, calculate the stiffness matrices of all the prestressing tendons already effective in the completed part of the structure using the equations given in Subsections 4.4.1 to 4.4.3. The system stiffness matrix is then established by assembling the individual stiffness matrices of all concrete and prestressing elements.

2. Calculate the system nodal force vector. For an instantaneous analysis, this vector consists of all external forces applied at the nodes plus the nodal forces equivalent to loads acting on the concrete elements and forces due to prestressing, all applied at the beginning of interval *i*. The equations given in Subsection 4.3.7 and 4.4.4 are to be used for this purpose. For a time-dependent analysis, the elements of the nodal force vector represent the forces required to restrain the hypothetical free deformations due to creep and shrinkage of concrete and relaxation of prestressed steel. These restraining forces are to be calculated for individual concrete straight or curved elements and prestressing tendons using the equations presented in Subsections 4.5.1 to 4.5.3.
3. Using the well known Gauss elimination technique, solve the system equilibrium equations to determine the increments of nodal displacements and support reactions. Add the increments to the existing values to obtain updated totals.
4. Use the displacement increments to calculate the changes in member end forces and internal forces (or stress resultants) at different sections as well as the changes in the prestressing forces. Add the changes to the previous values to calculate the total values at the end of interval *i*.

The above four steps are to be repeated for all time intervals until completion of the analysis. The procedure just described is implemented in the computer program TD-SFRAME. The logic of the program is illustrated in the flow chart of Figure 4.11. A detailed description of the input data required to run the program and the output printout is given in a user's manual (Debaiky and El-Badry, 1997). A listing of the program is also provided. The program is developed to run on both IBM personal computers and SUN Workstations.

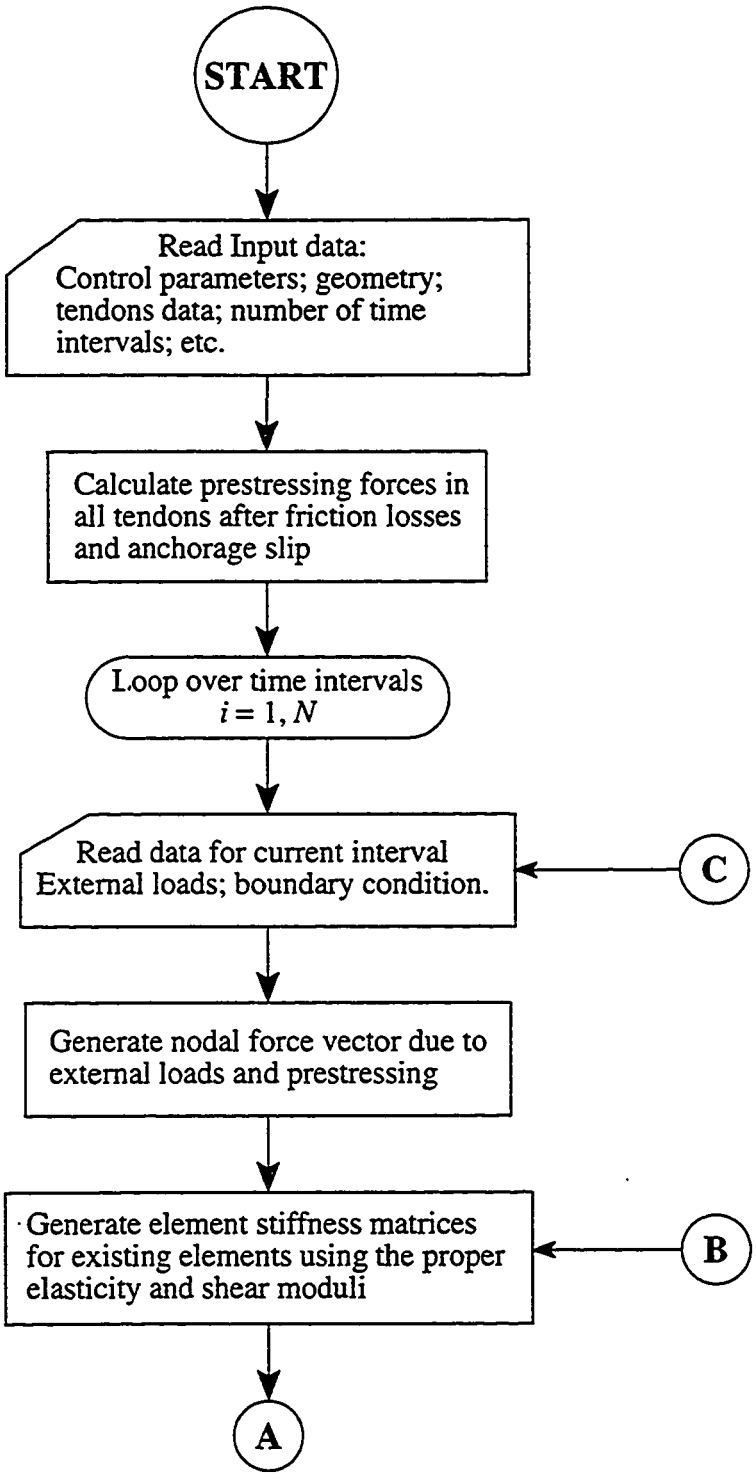

Figure 4.11 **Flow Chart for Computer Program TD-SFRAME**

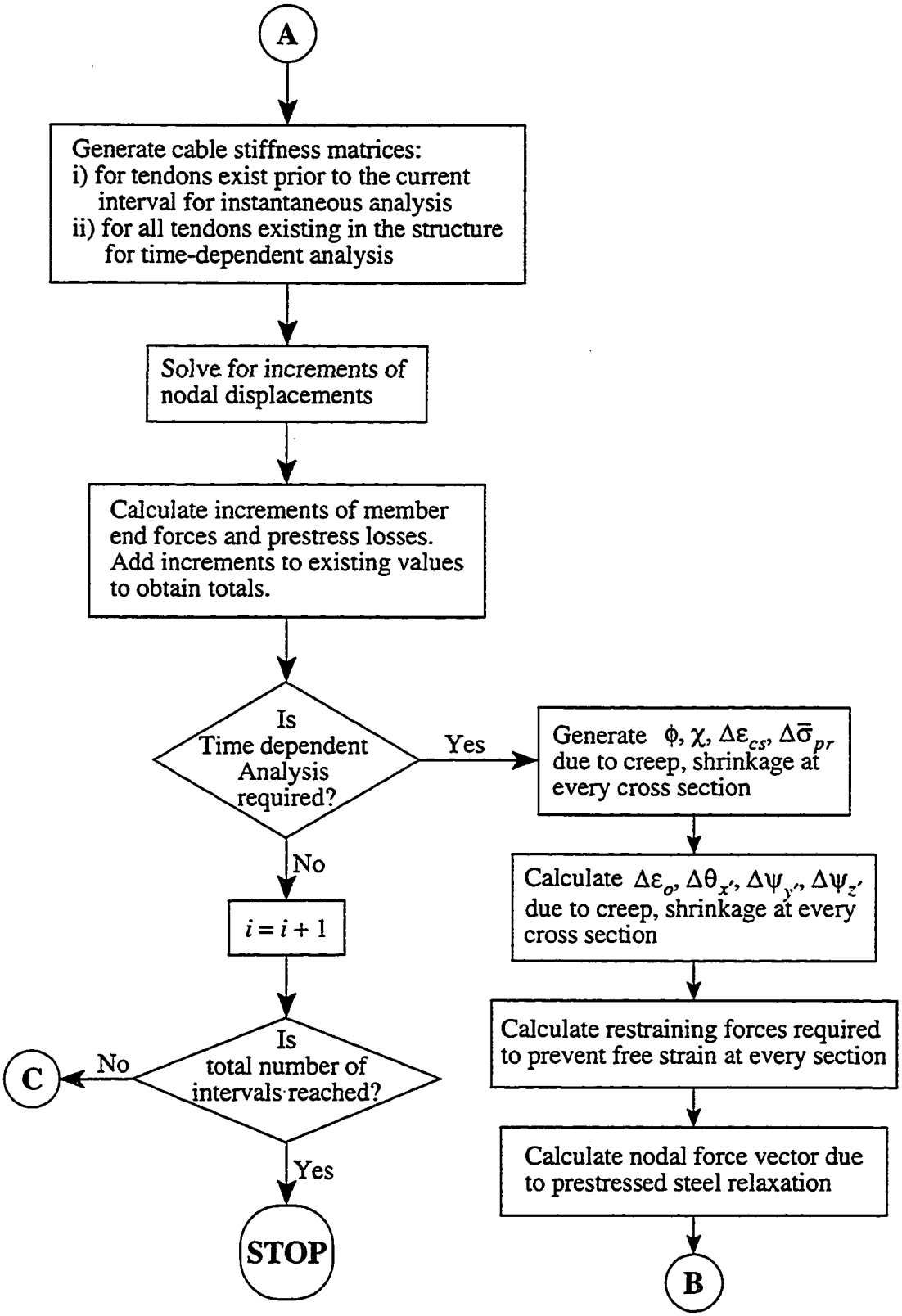

Figure 4.11 **Flow Chart for Computer Program TD-SFRAME (Cont'd)**

CHAPTER FIVE

Verification Examples and Application

5.1 Introduction

In the preceding chapters, a numerical procedure has been presented and a computer program, TD-SFRAME, has been described for the analysis of instantaneous and time-dependent behaviour of segmental prestressed concrete curved bridges. In this chapter, Program TD-SFRAME is employed for the analysis of a number of numerical examples, the purpose of which is to verify the validity of the method of analysis and to demonstrate the applicability of the program.

In Section 5.2, two verification examples are presented. In the first, two-span continuous beams tested by Kountouris (1970) for the effects of settlement of supports are analyzed. In the second example, a comparison is made between the analysis by TD-SFRAME and a method developed by Dezi and Tarantino (1991) for the analysis of the effects of change of statical system on the time-dependent behaviour of structures built in stages. A simple example of a structure made up of two cantilevers which are made continuous after a period of time is considered.

In Section 5.3, Program TD-SFRAME is applied for the analysis of a three span continuous curved prestressed concrete box-girder bridge built by the cantilever construction method. Stresses and deformations are calculated due to dead loads and prestressing during construction and due to superimposed load after completion of construction. In Section 5.4, TD-SFRAME is used to investigate the effects of restraints provided by the supports on the time-dependent behaviour of continuous curved concrete bridges.

5.2 Verification Examples

5.2.1 Example 1: Effects of Support Settlement in Continuous Beams

In statically indeterminate structures, movement of supports produces changes in the reactions and hence in internal forces. To allow for differential settlement in the design of continuous structures it is necessary to know the settlement-time relationship, the creep function and the changes in the properties of the structure during the period over which the settlement takes place. Sudden movement of a support produces instantaneous changes in reactions; subsequently these reactions decrease gradually with time due to the effect of creep. In other words, relaxation takes place. In the majority of structures, the settlement of supports takes place gradually over a long period of time so that settlement and relaxation occur concurrently. The variation in the reactions in this case is much smaller than when the settlement occurs suddenly. Since the maximum variation in the reactions is important for the design, ignoring the effect of the interaction of relaxation and settlement is definitely uneconomical (Neville, Dilger and Brooks, 1983).

To illustrate the time-dependent effects of support settlement on the reactions and internal forces in continuous structures, consider a two-span continuous beam subjected to a downward movement of the central support as shown in Figure 5.1. The reaction F caused by downward settlement δ is investigated for two cases. When δ is sudden, a force of magnitude F_{sudden} is instantaneously induced. If subsequently δ is maintained constant, creep of concrete causes relaxation of the reaction as shown by curve I. If the settlement is introduced gradually from zero to full value over a period of time (t_1, t_0), the reaction force develops also gradually until it reaches a maximum value F_{max} at t_1 which is generally much smaller than F_{sudden} and then decreases gradually with time as shown by curve II.

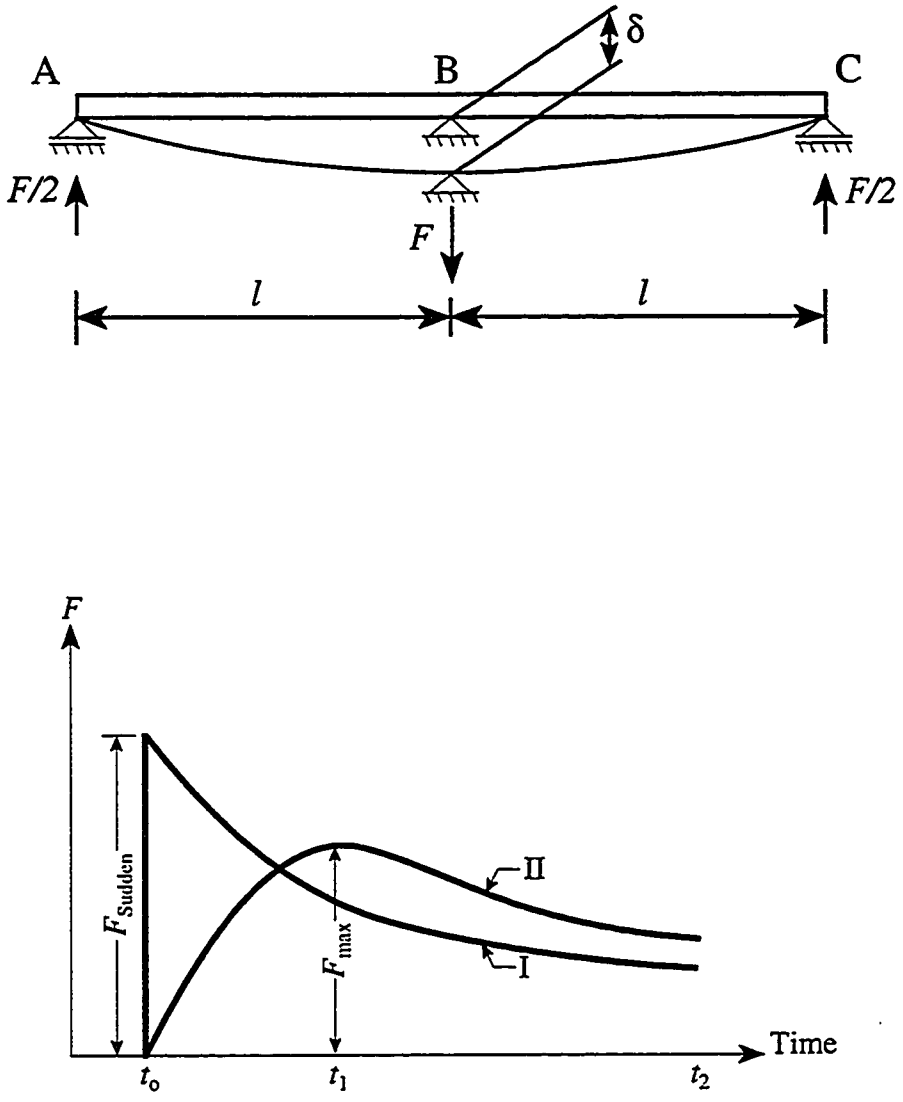

Figure 5.1 **Time-dependent Reaction due to Support Settlement in a Two-span Continuous Beam. I, Sudden Settlement; II, Gradual Settlement.**

For the analytical treatment of the forces induced by differential settlement, four cases can be considered:

1. Instantaneous settlement,

2. Settlement occurring at the same rate as creep,

3. Settlement following a standard time-consolidation curve,

4. Settlement occurring at a rate not included in (1) to (3).

The first two cases can be solved conveniently by the aging coefficient approach. The third case can be analyzed by using standardized charts developed by many researchers and available for use in several text books. The general case where settlement of support follows an arbitrary curve is best analyzed by the step-by-step procedure described in the preceding chapters and incorporated in Program TD-SFRAME.

Kountouris (1970) analysed a group of four two-span continuous beams for the effect of creep on the reaction and internal forces induced by settlement of the central support. Experimental tests were conducted on the four beams and the measured data was compared with the analytical solution. The four beams were subjected to different settlement profiles. All the beams had the same configuration, a cross section of 100×200 mm, two equal spans of 910 mm each and stressed by post-tension unbounded bar with initial prestressing force of 147 kN and cross-section area of 285 mm^2. The prestressing bar was located at the centroid of the cross-section of the beam and was mainly used to provide sufficient compressive stress to prevent cracking of the beam since the analysis done was only concerned with uncracked members.

In the present work, Program TD-SFRAME is used to analyze two of the four beams tested by Kountouris. The first beam is subjected to a sudden settlement of 76 mm

introduced in its full value at age 11 days and kept constant thereafter. The beam was monitored up to age 300 days. The second beam was subjected to a total settlement of 89 mm introduced in seven equal increments at ages 13, 18.25, 25, 35, 49, 64 and 96 days. The increments were applied instantaneously and maintained constant thereafter.

The development of the reaction at the central support with time to age 300 days is plotted in Figures 5.2 and 5.3 for the two beams respectively. The experimental values and those predicted by the program TD-SFRAME are compared in the figures. The program calculates the reaction values just before and just after the application of the support movement and at age 300 days. Creep functions given by CEB-FIP (1990) were adopted in the analysis. The agreement between the experimental and the analytical values indicates that TD-SFRAME is capable of predicting the behaviour of continuous structures subjected to support settlements with good accuracy. The results obtained from the analysis by Program CPF developed by El-Badry (1988) are also shown in Figures 5.2 and 5.3.

5.2.2 Example 2: Effect of Change of Statical System

Dezi and Tarantino (1991) introduced a new relation between the integral-type term (ξ-function) and the creep function to evaluate the redundant reactions in viscoelastic structures subjected to changes of statical system. The method of Dezi and Tarantino states that such redundant reactions can be obtained by multiplying the associated elastic solution by an integral-type term.

This method of analysis was applied to a simple structure shown in Figure 5.4. Two symmetric cantilevers, each of length l and having the same age, are loaded simultaneously at age t_0 = 14 days with a uniformly distributed load q per unit length. They were then left to behave freely till age t_1 = 90 days, the time at which they were joined together to form a

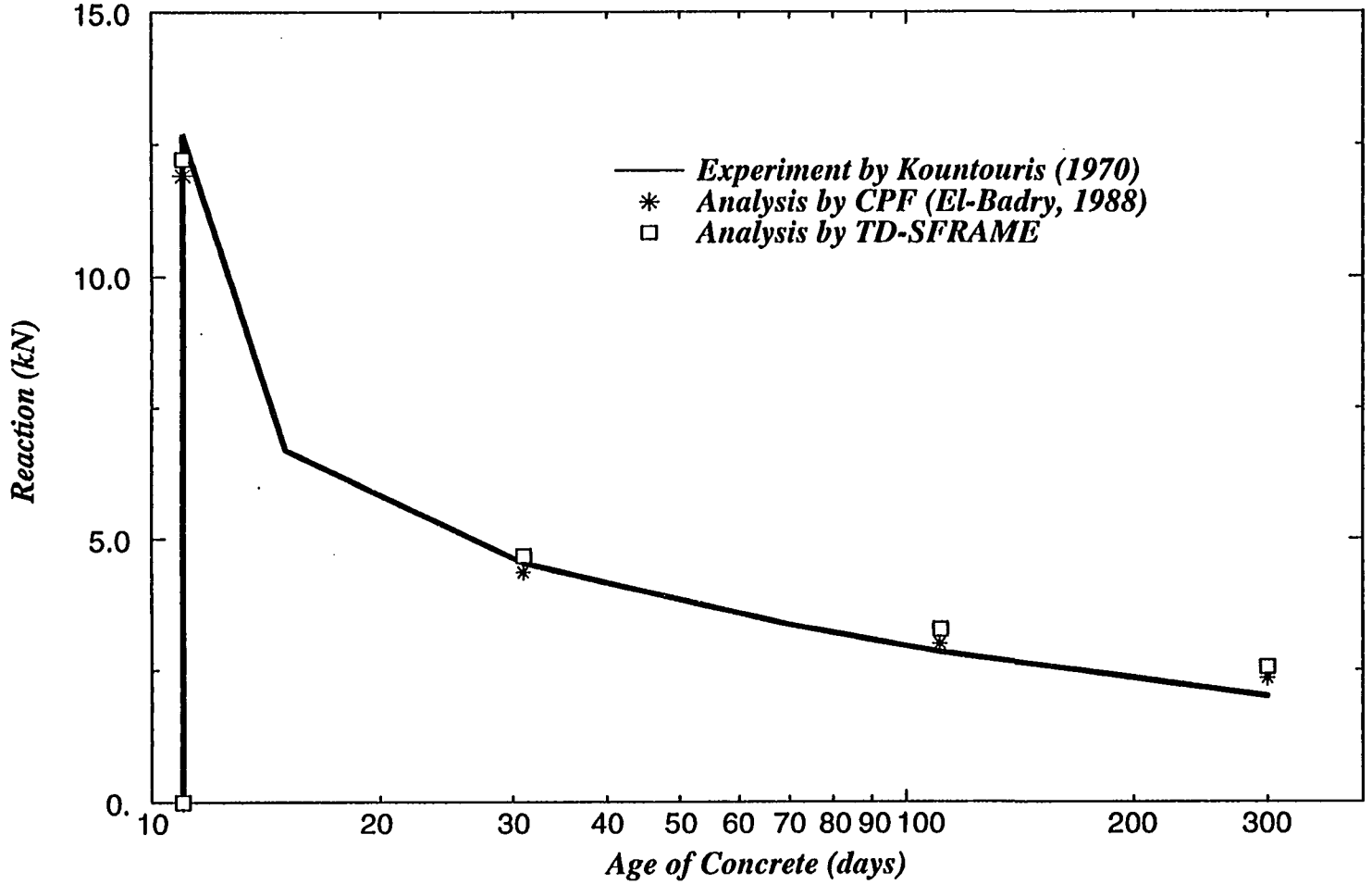

Figure 5.2 **Variation of the Reaction at the Central Support with Time in a Two-span Beam Subjected to Sudden Settlement Introduced at day 11.**

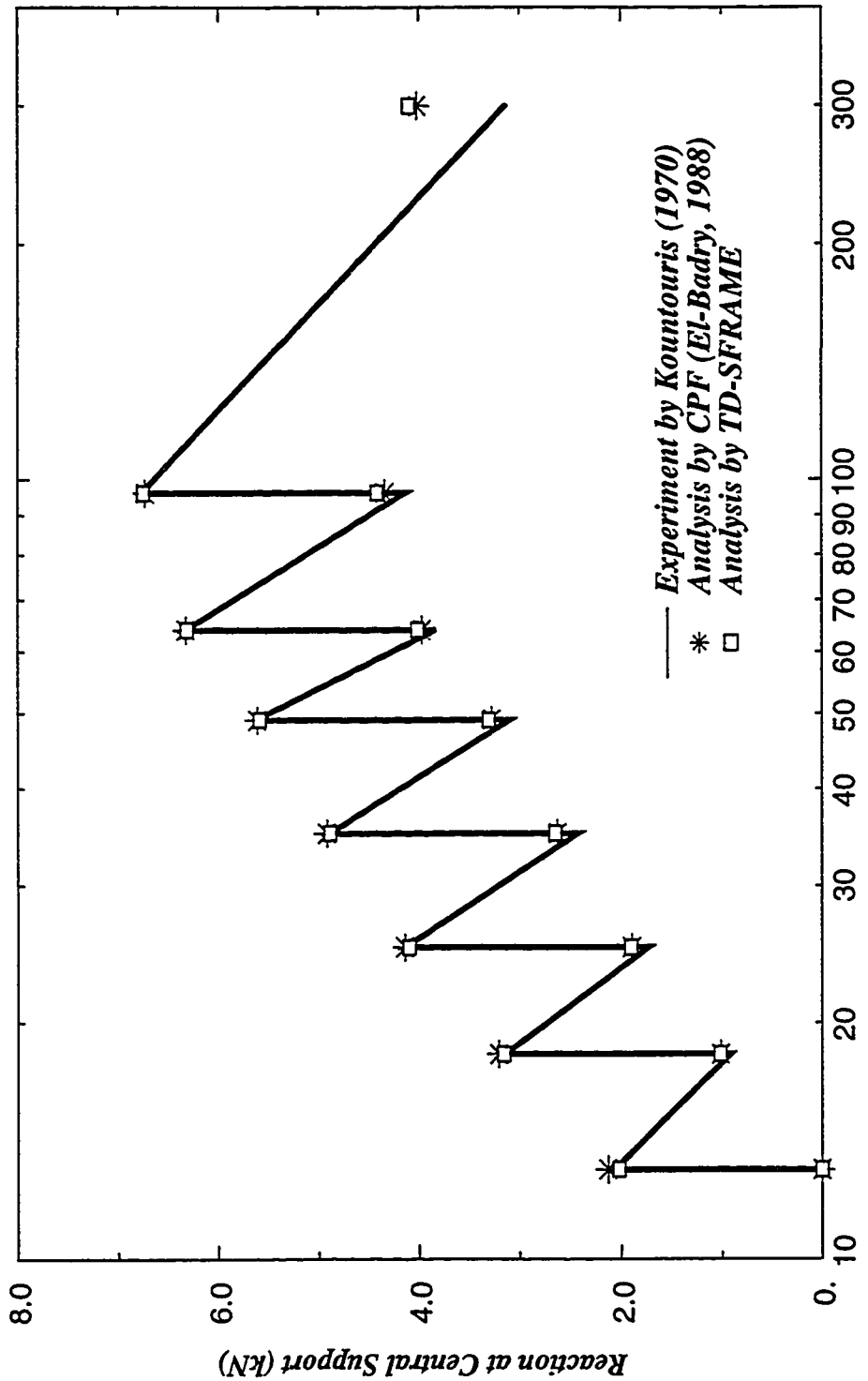

Figure 5.3 **Variation of the Reaction at the Central Support with Time in a Two-span Beam Subjected to Gradual Settlement introduced in 83 days.**

beam fixed at its two ends. The redundant reaction which in this case is the bending moment M at mid-span, is calculated simply by multiplying the elastic solution for the current structure ($M = ql^2/24$) by the value of the integral-type function. Table 5.1 shows the values presented for this function for different ages of the beam after closure.

The structure was analysed by the computer program TD-SFRAME developed for the present analysis. Material properties and ultimate creep coefficient were taken the same as used by Dezi and Tarantino. The concrete compressive strength at 28 days, f_{ck}= 25 MPa, and ultimate creep coefficient, Φ_u = 3. The CEB-FIP (1990) creep function is adopted in the analysis. Comparison between the results obtained from TD-SFRAME and Dezi and Tarantino for the mid-span bending moment M is shown in Figure 5.5. Good agreement is obtained.

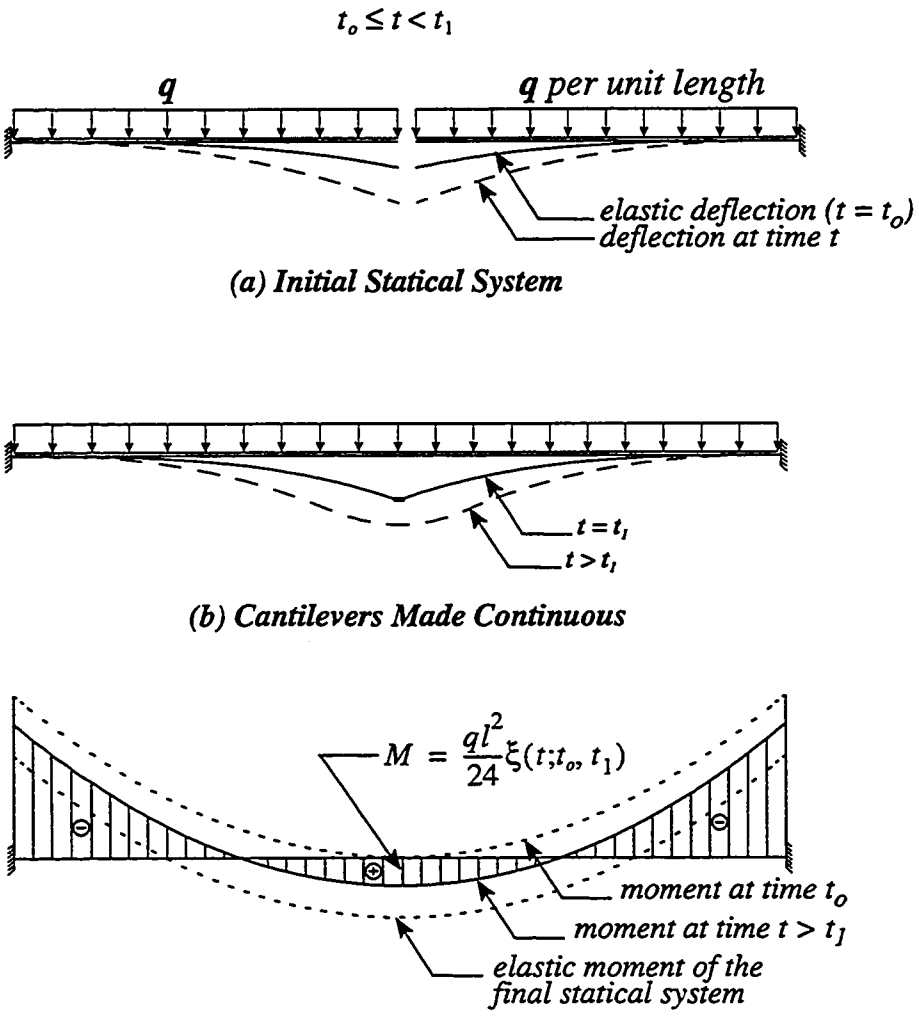

Figure 5.4 **Variation of the Bending Moment at Mid-span with Time due to Change in Statical System.**

Table 5.1 **Time Development of ξ Function as Presented by Dezi and Tarantino (1991).**

t, days	$\xi(t; 14,90)$
90	--------
100	0.0387
500	0.2879
1000	0.3420
5000	0.4165
10000	0.4346

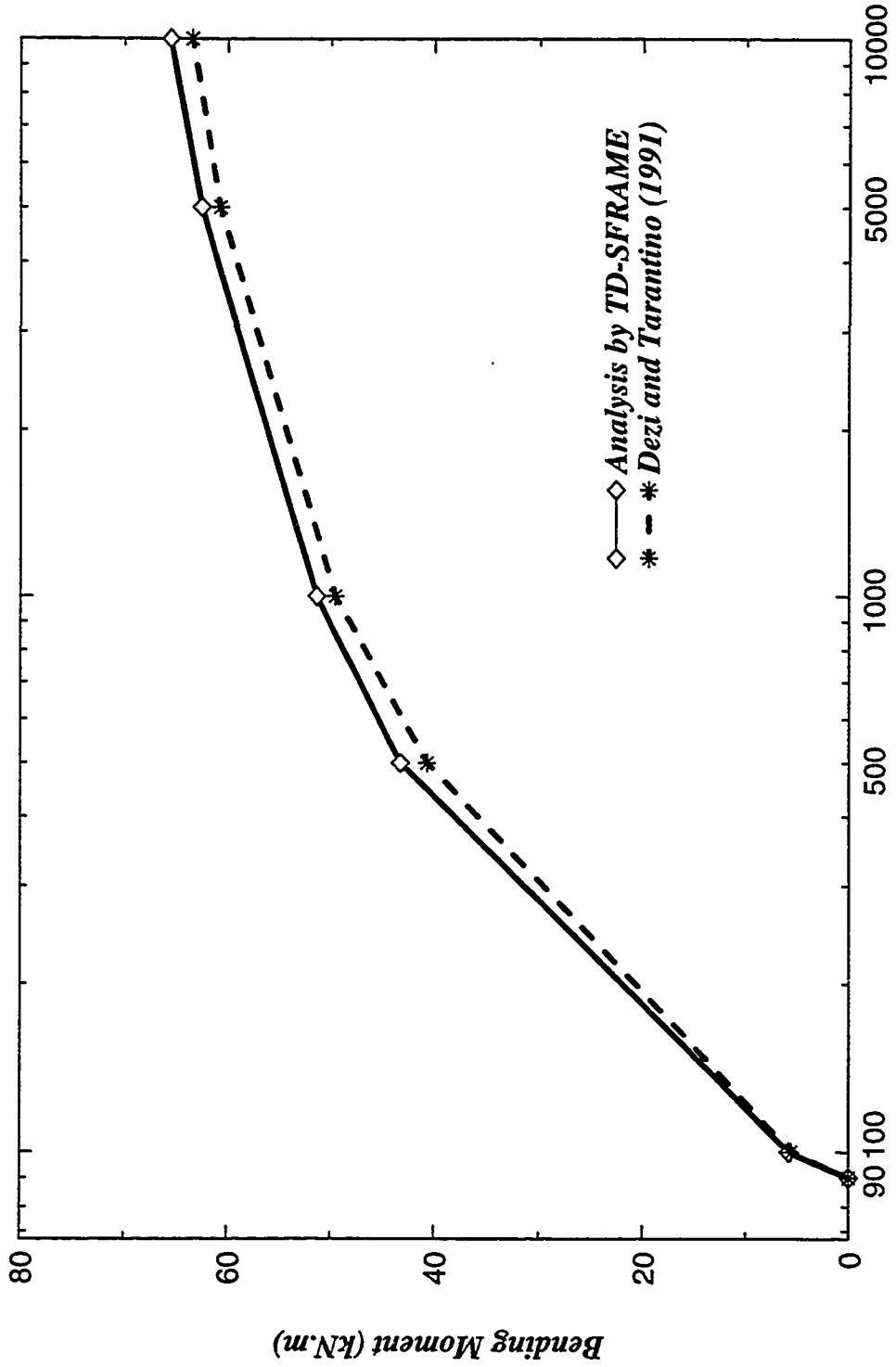

Figure 5.5 Variation of the Bending Moment at Mid-Span with Time after Continuity

5.3 Demonstration Example

In 1979, Van Zyl developed a computer program that predicts the time-dependent behavior of prestressed box-girder curved bridges. The program was based on the straight beam finite element with skew ends developed by Bazant and El-Nimeiri (1974). Van Zyl analyzed a fictitious bridge in order to demonstrate the capabilities and flexibility of his program. In the present research, due to the sever lack of data and experimental work available on curved bridges, the fictitious bridge of Van Zyl will be analyzed using TD-SFRAME for demonstration purpose.

The bridge selected is a three-span continuous box-girder bridge with variable depth over its length. Figures 5.6 and 5.7 show an elevation and a plan of the bridge. The overall length of the bridge is 168 m and the main span is 72 m. One end span of the bridge, span AB, is straight in plan and is 42 m long. The two spans BC and CD are curved in plan and of length 72 and 54 m, respectively. The radius of the curved part BCD is 150 m with a central angle of 48.13 deg. The cross section of the bridge consists of a single box section. Both the top and bottom widths of the cross-section (upper and lower slabs) vary linearly over the entire length of the bridge while the depth of the cross section and the thickness of the bottom slab vary as shown in Figures 5.8 and 5.9. The thicknesses of the top slab and the webs are constant. Figure 5.8 shows the cross-section dimensions at different locations of the bridge.

The bridge is built in segments using the balanced cantilever technique. The bridge segments are longer and the number of prestressing tendons is smaller than normally accepted in practice. The reason behind this choice is to reduce the computation time and to simplify the example for clarity of presentation. Erection of the bridge starts at the left

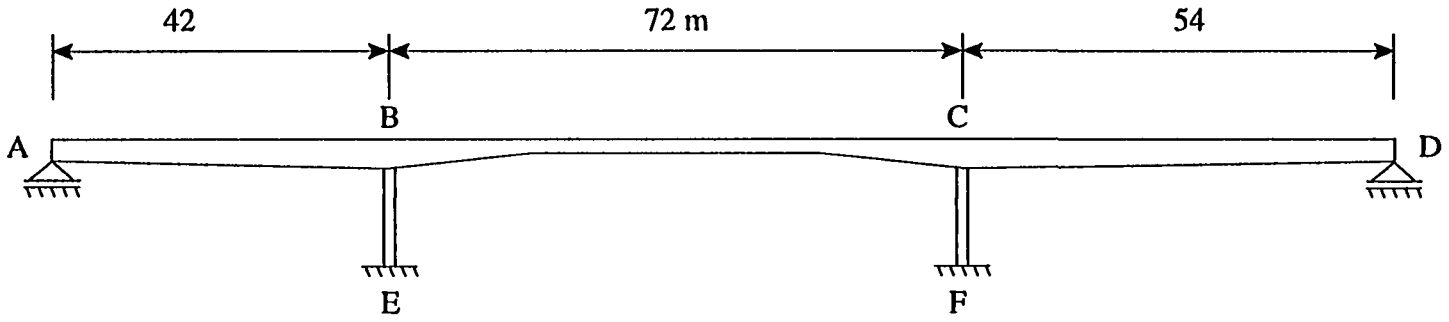

Figure 5.6 **Developed Elevation of the Bridge used in the Demonstration Example**

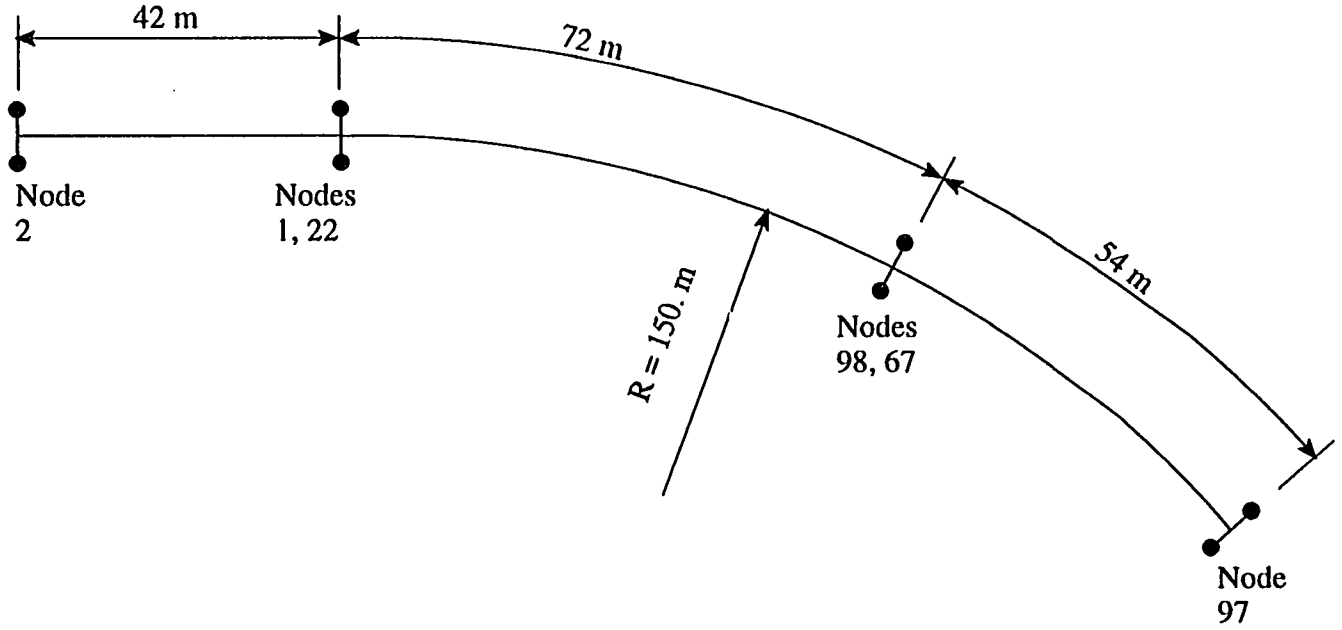

Figure 5.7 **Span Arrangement of the Bridge used in the Demonstration Example**

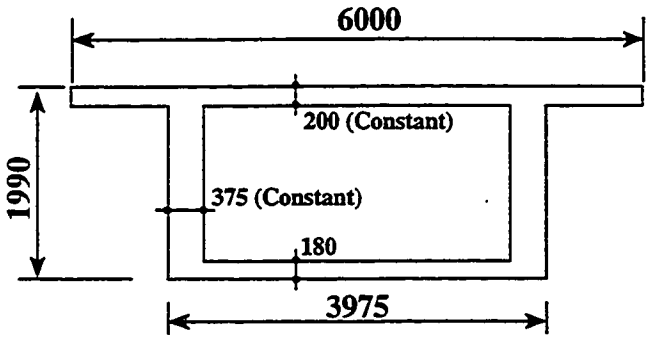

Cross section at node 2 (Left abutment)

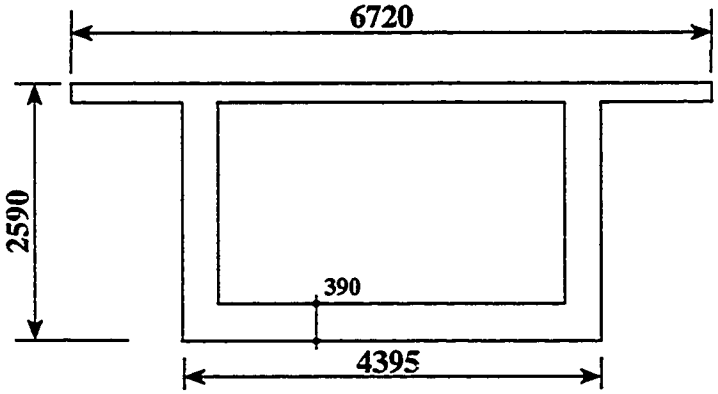

Cross section at node 22 (Top of left pier)

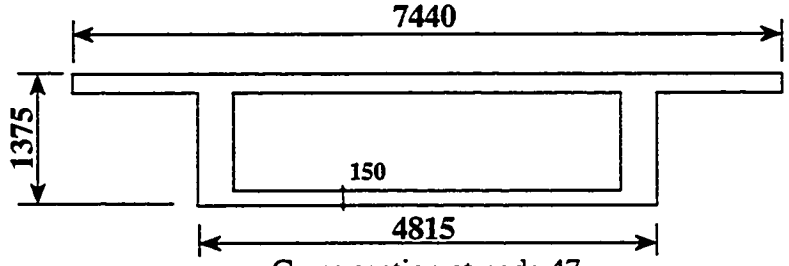

Cross section at node 47

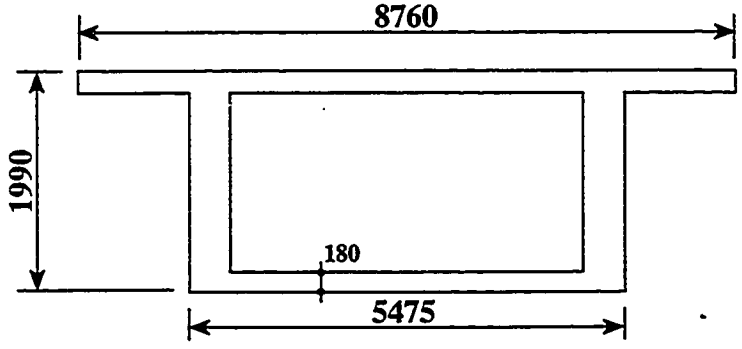

Cross section at node 97

Figure 5.8 **Cross Sectional Dimensions for Bridge used in Demonstration Example**

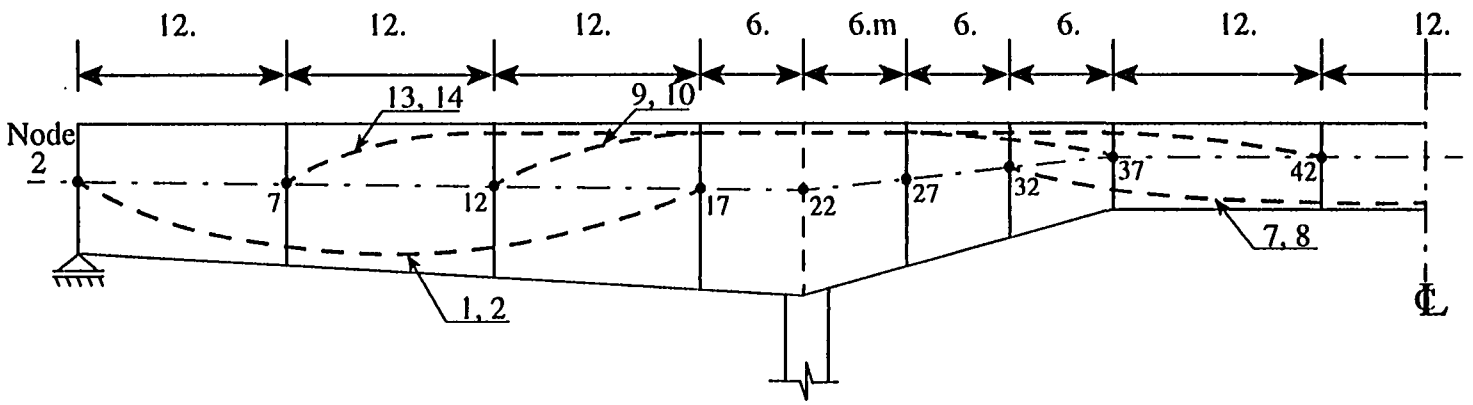

a) Left Half

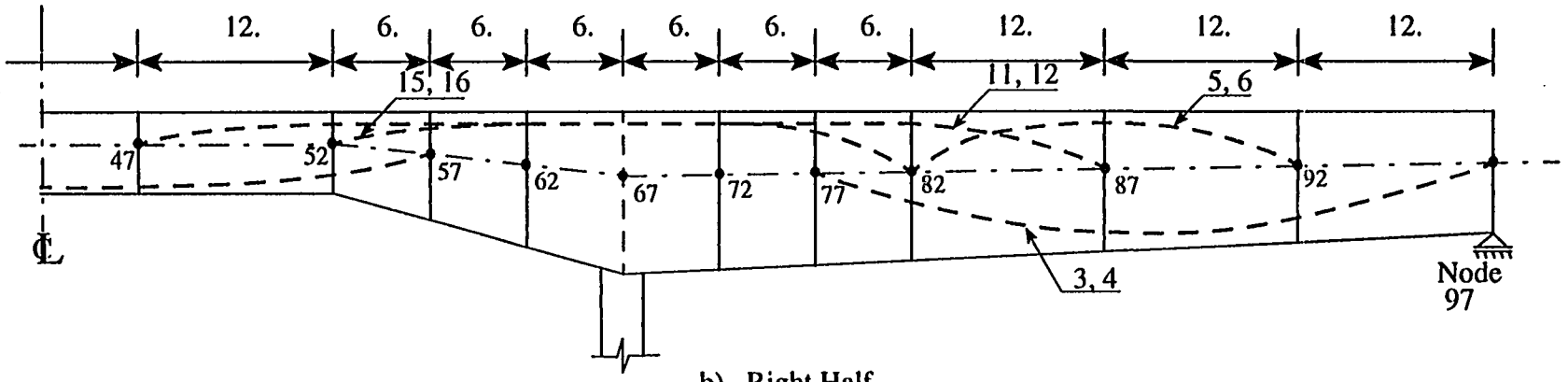

b) Right Half

Figure 5.9 **Longitudinal Configuration of the Bridge, Node Numbering and Tendons Layout.**

pier where segments are successively placed and tied together by post-tensioning. Figure 5.9 depicts the arrangement of segments and the prestressing tendon layout along the bridge length. The construction period is divided into nine stages (time intervals). Addition of new segments, prestressing tendons, loads, and/or boundary condition are all considered as new construction stages. Figure 5.10 shows the construction process for all the nine stages indicating the newly introduced segments, loads, boundary conditions in each stage. Table 5.2 summarizes the erection sequence and Tables 5.3 to 5.5 list the history of casting the concrete segments, the prestressing tendons data, and the tendon layout data, respectively.

Concrete properties used in the analysis are the same as those used by Van Zyl. The compressive strength at 28 days, f_{ck}= 27.6 MPa, Poisson's ratio = 0.18. Unit weight of 25.14 kN/m^3 which was used to calculate the dead load due to own weight of the structure during construction.

During the construction process, the following points were the major corner stone for the analysis:

- Erection of the L.H.S. portion of the structure was carried out first and completed at stage 3. The R.H.S. portion was then constructed in stages 4 to 8 during which the L.H.S. cantilever was left under its own weight and time-dependent effects.

- At the beginning of stage 7, the right cantilever of the R.H.S. portion of the bridge reached unacceptable length as a free cantilever which required introduction of a temporary support to prevent excessive deflection and stresses. This support was shortly removed in stage 8 when the above mentioned cantilever was connected to the right abutment and Span CD was completed.

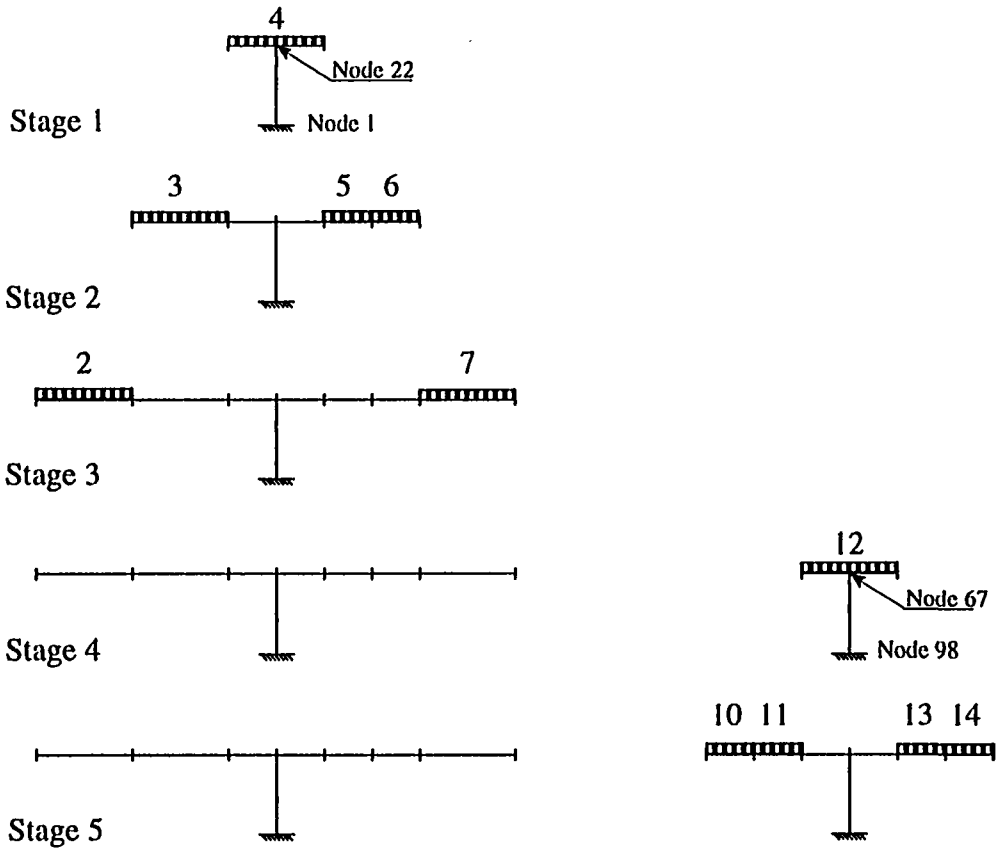

Figure 5.10 **Construction Process for Bridge used in the Demonstration Example (Developed Elevation)**

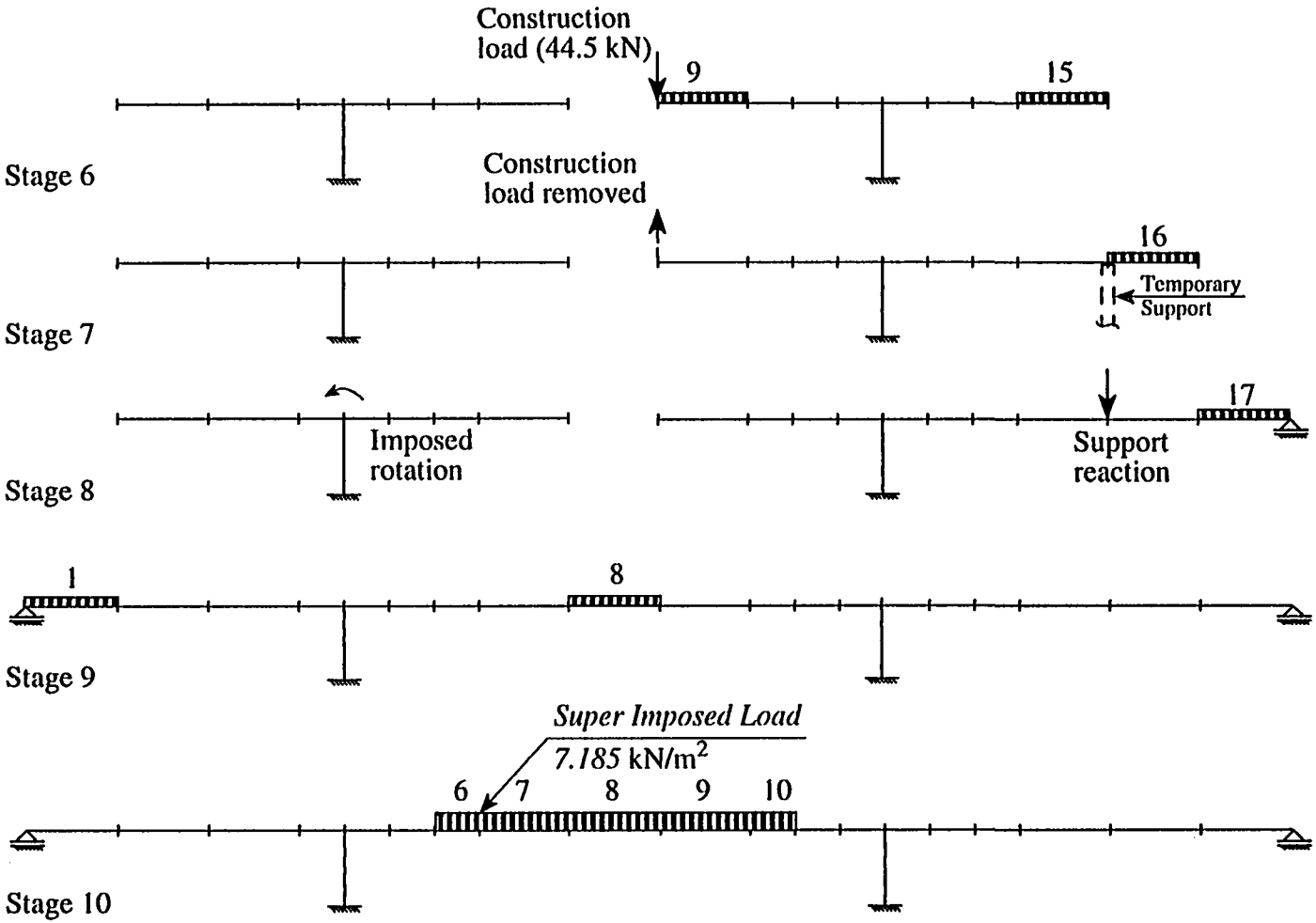

Figure 5.10 **Construction Process for Bridge used in the Demonstration Example (Cont'd)**

Table 5.2 **Construction Operation and Sequence for the Demonstration Example**

Stage No.	Time in days	Segments added	Tendons stressed	Loads	Support Conditions and Changes	Imposed displacement	Remarks
1	30	Left Pier, 4	---		Fixed base at left pier		
2	35	3, 5, 6	9,10				
3	40	2,7	13,14				Left frame completed
4	50	Right pier, 12	---		Fixed base at right pier		
5	55	10, 11, 13, 14	11,12				
6	60	9,15	15,16	44.5 kN at node 47			Right frame completed
7	70	16	5,6	Remove load at node 47	Add temporary shoring at Node 87		
8	75	17	3,4		Remove temporary shoring at Node 87 & add roller support at D (Node 97)	0.0017 radians rotation CCW at Node 22	Right abutment reached
9	91	1,8	1,2,7,8		Add roller support at A (Node 2)		Structure completed
10	150	----	---	Super imposed load			End of analysis at 1000 days

Table 5.3 **Segment Casting History**

Segment No.	1	2	3	4, 5, 6, 7, 10, 11	8	9	12,13, 14,15	16, 17
Age when Introduced	91.	35.	25.	15.	61.	25.	5.	10.

Table 5.4 **Prestressing Tendons Data**

Tendon No.	Area (mm^2)	Initial Force (MN)
1, 2	1395	1.335
7, 8	2787	2.670
3, 4	2787	3.115
13, 14	3716	4.450
9, 10	9290	11.125
15, 16	4645	5.562
11, 12	11148	13.350

Table 5.5 **Tendons Profiles Data**

Tendon No.	Drop of the 1st parabola mm	Drop of the 2nd parabola mm	Inflection of tendons at nodes
1, 2	698	---	---
7, 8	314	---	---
3, 4	960	---	---
13, 14	183	92	12, 37
9, 10	216	92	17, 27
15, 16	92	198	52, 82
11, 12	104	223	62, 72

- Completion of Span AB and closure of Span BC was done at stage 9 by adding segments 1 and 8 respectively. The L.H.S. portion of the structure was previously rotated by an angle equal to 0.0017 radians at stage 8 in order to match the vertical levels of the two tips of the inner cantilever parts which form the middle span. The value of the rotation angle was predicted by Van Zyl through a separate analysis, it was noticed from the current analysis that this value is slightly smaller than needed.

- Superimposed load is introduced at the final stage 10. This load is distributed over a major portion of the middle span, specifically between nodes 32 and 57 (Figure 5.10). Major conflict between the results of Van Zyl and the current analysis was observed with respect to the deflection produced by this superimposed load.

The profile of all tendons follow parabolic curve except for some zones in particular tendons where the tendon follows a straight line. Data for tendon profiles are summarized in Table 5.5. The straight zones of the tendons lie at 150 mm depth from the top surface of the bridge at all nodes.

Each tendon is stressed from both ends simultaneously. For all tendons, the material properties and data for friction and anchor slip losses are constant as follows:

1- Young's modulus, E_{ps} = 191.6 GPa

2- Wobble coefficient = 0.0002, friction coefficient = 0.2.

It should be mentioned here that in the analysis of Van Zyl, there were no consideration for prestressed steel relaxation.

Results of the analysis:

The results of the current analysis were not verified extensively, but a few equilibrium checks were made. Figure 5.11, depicts the deflected shape of the structure as

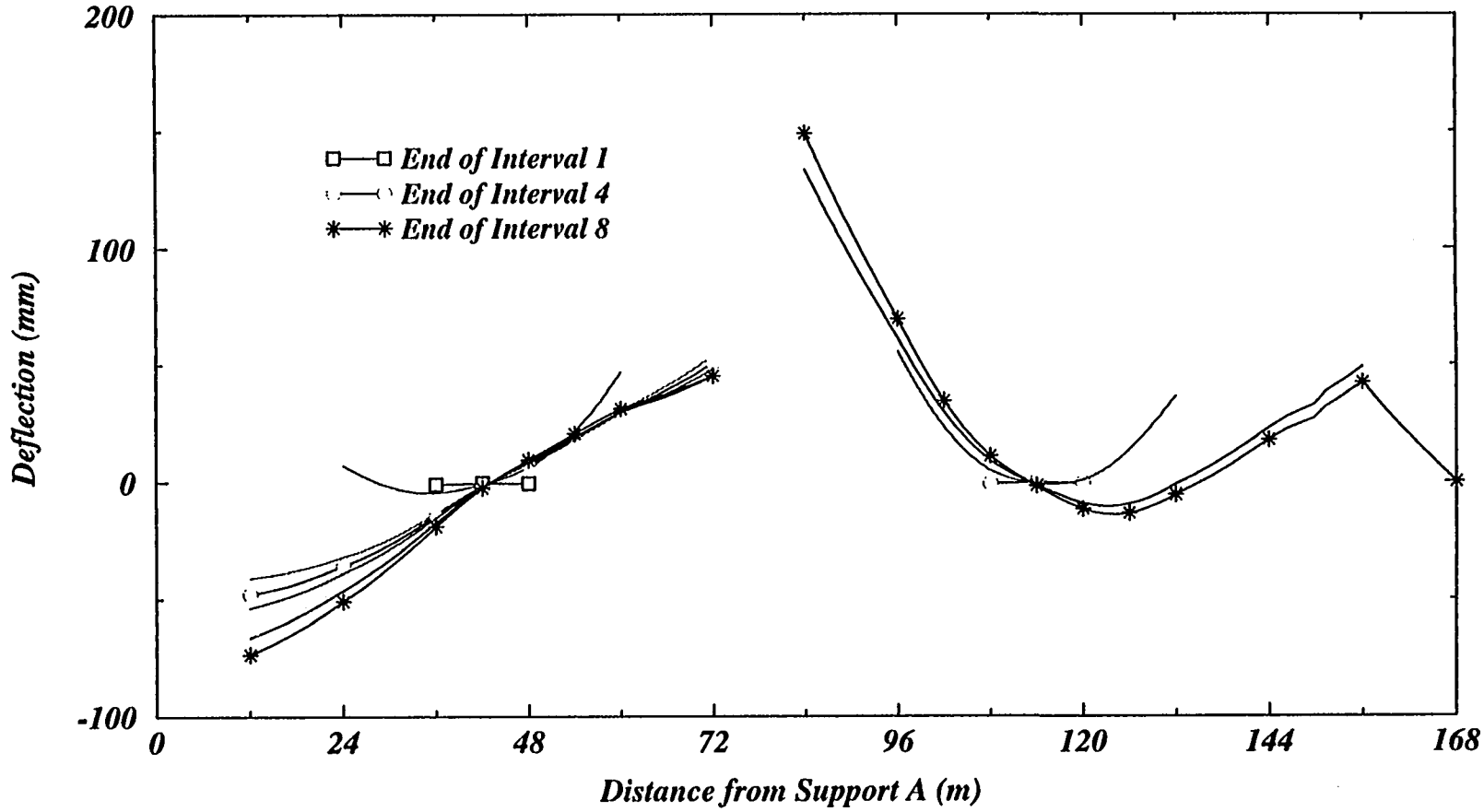

Figure 5.11 **Deflected Shape of the Bridge During Construction**

obtained from the current analysis at the end of each time interval (stage) up to the time of completion of construction. The deflection curves plotted in this figure are measured from one horizontal datum assuming no pre-camber is provided, i.e. each new segment is attached during construction to the previously erected segments so that it is tangent the existing deflection profile.This produces discontinuities in the girder profile at nodes 7 and 92 and nodes 42 and 47 just before the closure segments (segments 1, 8 and 17) are placed in position. Such discontinuities can be eliminated by building in camber while casting the cantilever segments or by application of imposed rotation at the tip of the cantilever as done here in this example at the beginning of stage 8. The deflection curves in Figure 5.11 can be used to calculate the required camber. Figure 5.12 shows the deflected shape of the completed structure starting from the instant of closure up to the end of the analysis at day 1000. Unfortunately, a significant difference in values of deflections for both cases was found between the results reported by Van Zyl and the current analysis. This difference can be attributed to the following:

1- The analysis of Van Zyl was carried out using two different structural discretization, the first one was done using 56 elements while the second employed only 14 elements. Surprisingly, the deflection results were plotted only for the second analysis which was described by Van Zyl in page 246 of his thesis as

"The analysis of the present method using the element configuration of Fig. 7.31 yielded results which do not satisfy statics at all".

2- In the dissertation of Van Zyl, the bending moment due to the superimposed load was plotted and compared to that obtained from analysis by the commercial software "SAP". The two results were not of good agreement. Also, the maximum ordinate of the

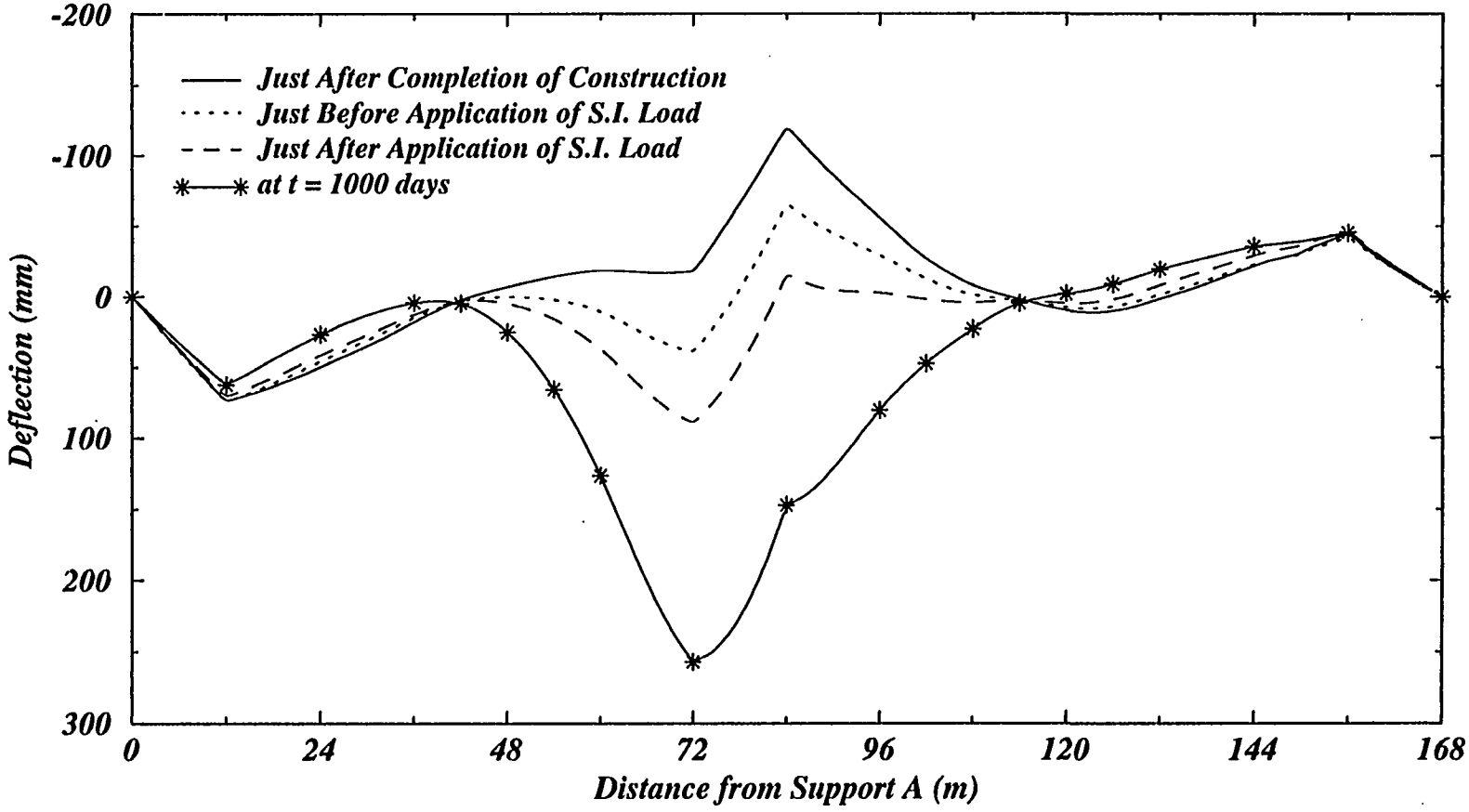

Figure 5.12 **Deflected Shape of the Completed Structure**

parabola of the bending moment obtained by Van Zyl failed to be of a reasonable value which should be in the neighbourhood of $ql^2/8$ where q is a value of the superimposed load per unit length. Figure 5.13 shows the bending moment by Van Zyl as given in his thesis.

Figure 5.14 depicts the bending moment diagram at the time of completion of construction, just before and just after application of the superimposed load on Span BC and at the end of analysis at t=1000 days. It should be noted that these bending moments include the primary moments due to prestressing. It can also be noted that the time-dependent effects on the bending moment are not as pronounced as they are on the deflection. Variation of the prestressing force in tendon No. 9 (introduced at stage 2) is plotted in Figure 5.15. Significant loss was reported near the ends of the tendon where large strains are developed while smaller losses took place near the support (left pier) where the tendon can be described as partially restrained. Figure 5.16 shows the variation of the torsional moment over the bridge with time since the instant of completion of construction, the results indicate higher influence of the time dependent effects of torsion than on bending moment. The curved part of the bridge experienced higher variation especially in the zone around the left pier were its effect is pronounced.

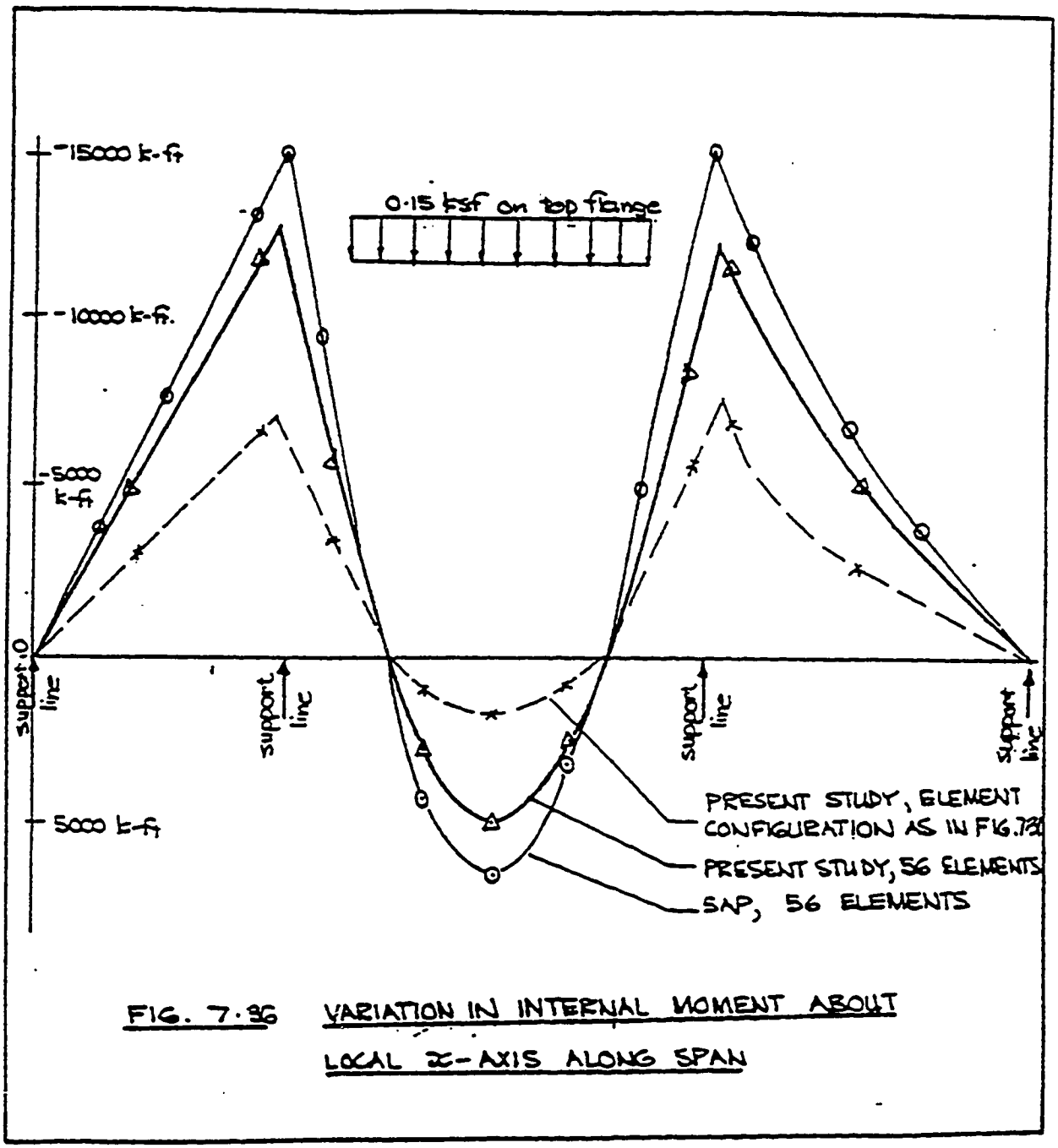

FIG. 7.36 VARIATION IN INTERNAL MOMENT ABOUT LOCAL x-AXIS ALONG SPAN

Figure 5.13 Bending Moment as Obtained by Van Zyl (1979)
Using different Structural Discretization

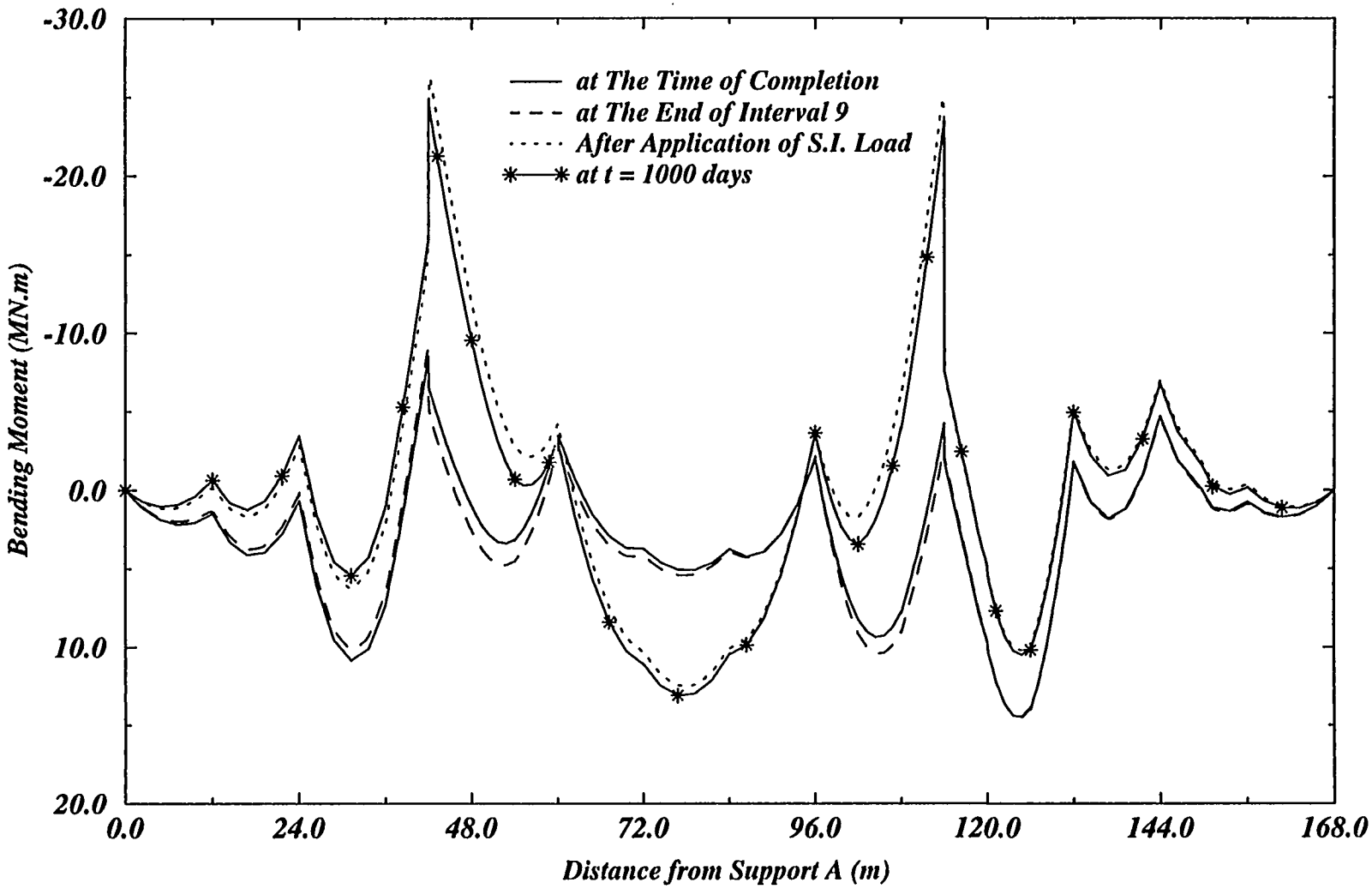

Figure 5.14 **Variation of the Bending Moment over the Bridge Since completion**

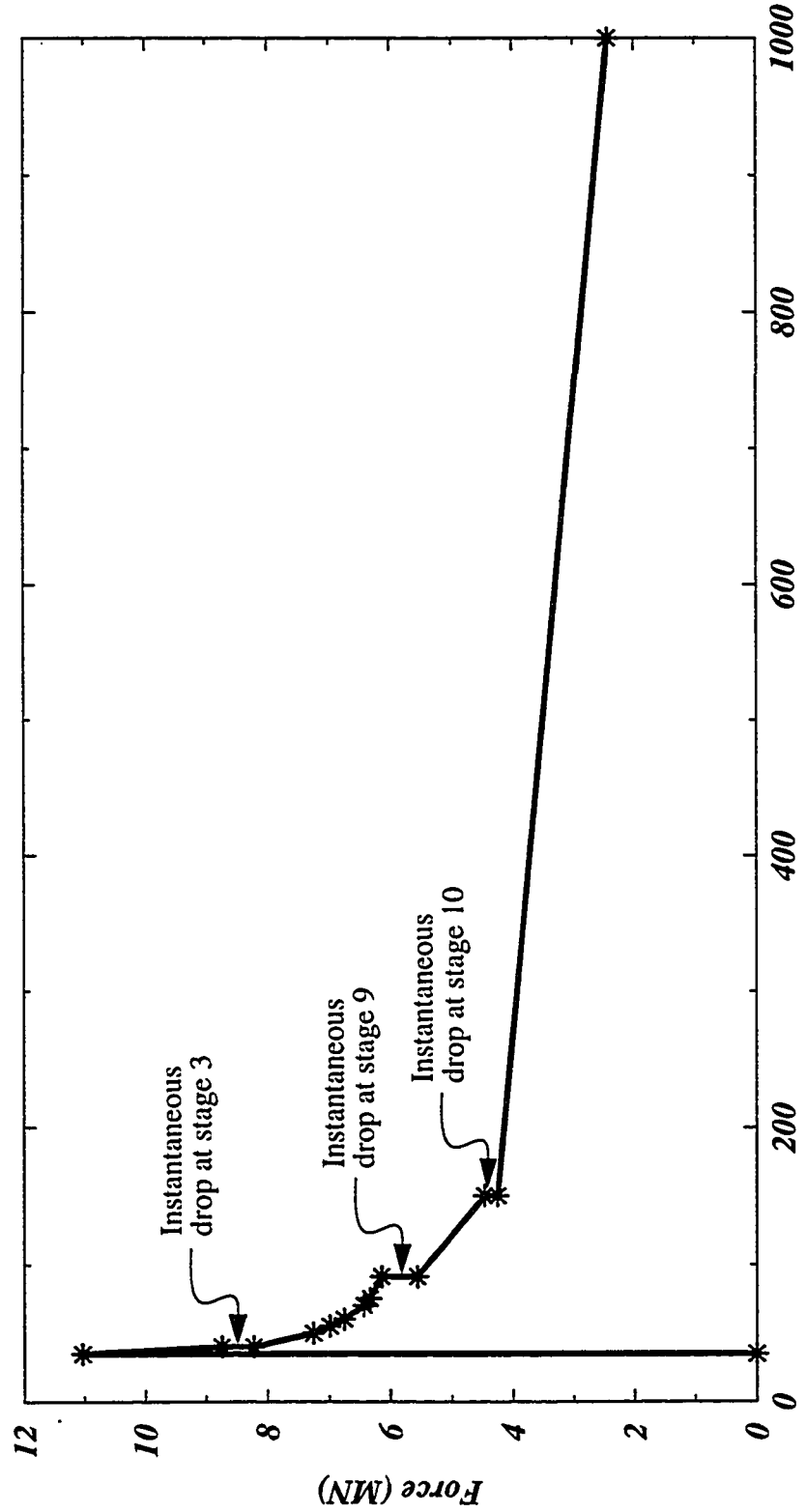

Figure 5.15 **Variation of the Force in Cable No. 9 with Time (at Section 55.2 m from A)**

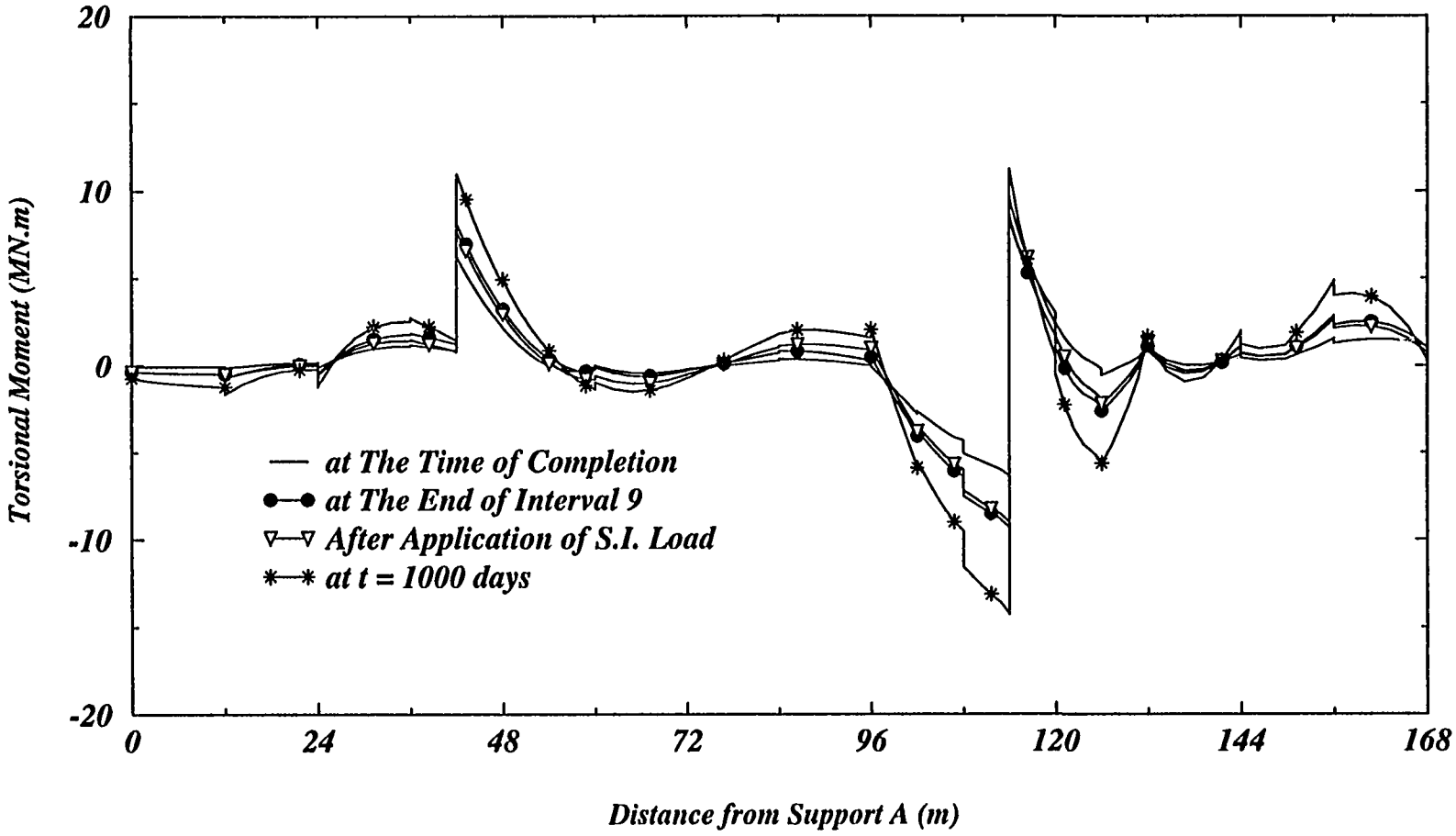

Figure 5.16 **Variation of the Torsional Moment over the Bridge Since completion**

5.4 Application: Effect of Skew Supports on Time-Dependent Stresses and Deformations

5.4.1 Description of the Problem:

As explained in section 1.7 of this thesis, movements at the supports in curved bridges must be permitted in some horizontal directions to allow for expansion or contraction of the superstructure due to temperature variations. The current design specifications (AASHTO, 1990) require that in horizontally curved bridges, movement at each roller support be allowed in the direction from a fixed (hinged) support to the roller support and that movement perpendicular to this direction be restrained at one support at least. An alternate design practice suggests that movements be restrained in the radial direction at the two ends of multi-span curved bridges as well as in the tangential direction at one of the interior supports. All other intermediate supports must be free to move in all directions as floating points (ball bearing) that prevent only vertical displacement. Figures 5.17 a and b show the directions of unrestrained movements and hence the alignments of skew supports in a typical three-span continuous curved bridge according to AASTHO recommendations and the alternate design practice, respectively.

The two systems of skew support alignment of Figure 5.17 have been used recently by Lai (1995) to study the effects of skew support alignments on the seismic response of horizontally curved girder bridges. A three-dimensional finite element analysis using the commercial software STAAD-III was performed to test the effects of the two alignments under different seismic loads.

In the present research, where the development of time-dependent stresses and deformations in curved bridges is the main concern, the effects of construction sequence

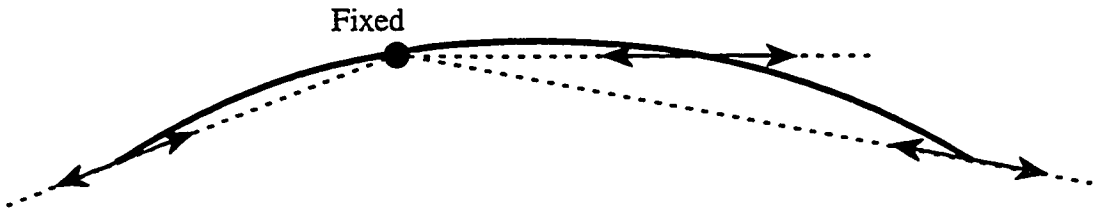

(a) AASHTO Criterion

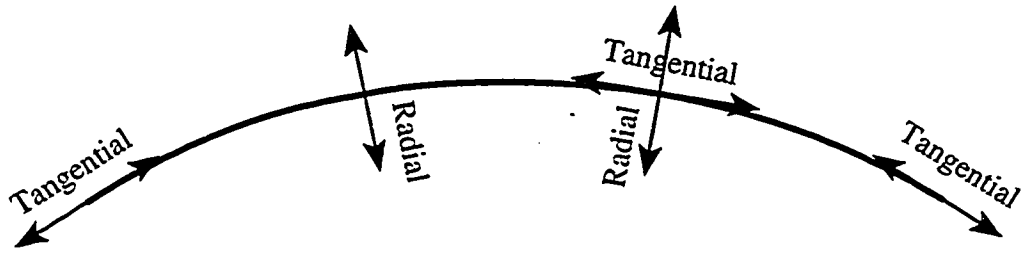

(b) Alternate Criterion

Figure 5.17 **Unrestrained Horizontal Movement and Alignments of Skew Supports in Curved Bridges Adopted in the Present Study**

and load history as well as changes in the statical system or boundary conditions have been included in the analysis. During the literature survey for this research, it was found that no previous research was done to evaluate the effects of skew support alignment on the time-dependent response of curved bridges. The common trend in all previous work was to assume the direction of skew supports in the orthogonal radial or tangential directions.

In this section, the effects of the two skew support alignments of Figure 5.17 on the time-dependent behavior of curved bridges are investigated. For this purpose, a three- span curved box-girder bridge (Figure 5.18) is analyzed. The span length, radius, cross-section dimensions and prestressing cable profile and forces are adopted from an existing box-girder curved bridge built over the Bow River in Calgary, Alberta in 1980. The actual bridge consists of a total of 9 continuous spans arranged in two straight parts connected with a three-span circular portion. The bridge was built using the span-by-span technique with cast-in-place single box-section. In the present study, only the curved part of the bridge is considered as shown in Figure 5.18. The prestressing cable profile is shown on a developed elevation of the bridge in Figure 5.19 and Table 5.6.

In the present analysis, the effects of multi-stage construction are not considered. It is assumed that the bridge is cast monolethically and built in one stage. The bridge is analyzed for the effects of its self-weight, an additional superimposed dead load of 20kN/m, and prestressing force of 30.40 MN. The time-dependent stresses and deformations are observed for a period of 5000 days and calculated at t = 500, 1000, 5000 days. The modulus of elasticity of concrete, the creep and aging coefficients and shrinkage strains are calculated automatically by TD-SFRAME according to the CEB-FIP recommendations based on compressive strength at 28 days, $f'_c(28) = 30$ MPa and relative

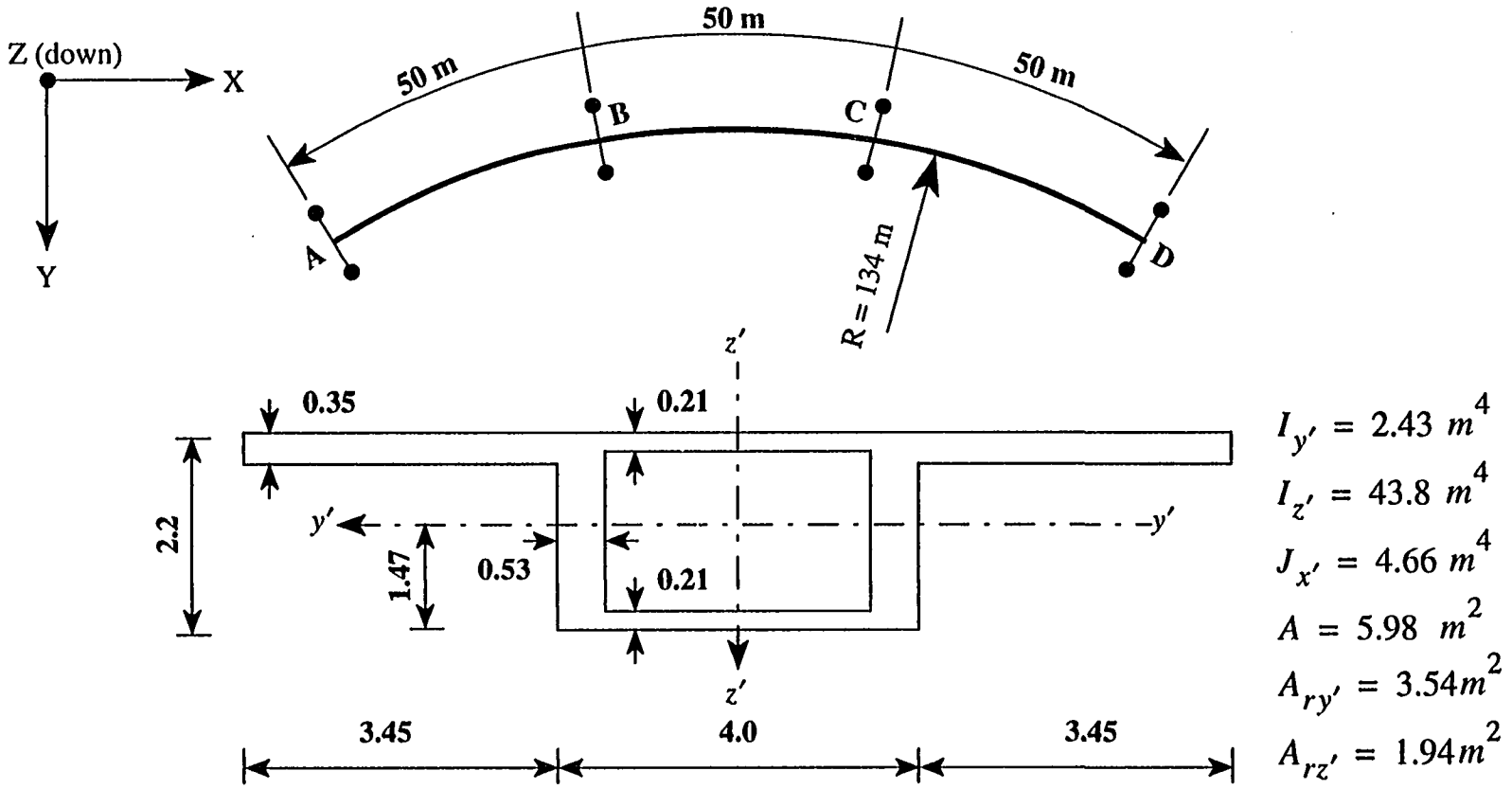

Figure 5.18 **Three-Span Curved Bridge, Plan and Cross Sectional Dimensions**

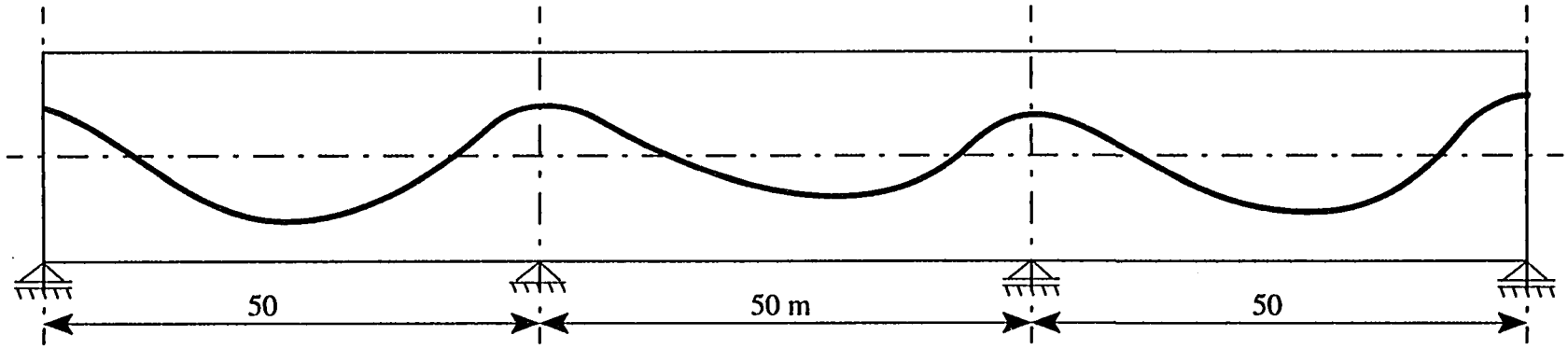

Figure 5.19 **Developed Elevation for the Curved Bridge**

Table 5.6 **Cable Eccentricities Along the Length of Each Span with Respect to the Local Axes of the Cross-Section**

Length	0.	2.	4.	6.	8.	10.	12.	14.	16.	18.	20.	22	24.
$e_{z'}$	-636	-589	-450	-263	-75	114	299	460	593	700	780	834	861
$e_{y'}$ *	1840	1833	1811	1779	1757	1750	1754	1779	1825	1859	1870	1870	1870

24.	26.	28.	30.	32.	34.	36.	38.	40.	42.	44.	46.	48.	50.
861	861	838	793	724	633	518	381	221	38	-167	-396	-576	-636
1870	1870	1870	1870	1870	1870	1870	1870	1870	1868	1860	1850	1842	1840

* Absolute values for tendons on both sides of the local z' axis (vertical axis)

humidity of 40%. Other data include the elasticity modulus of prestressing steel, E_{ps} = 190 GPa, area of prestressing cables, A = 0.0211 m^2. The intrinsic relaxation is calculated according to the CEB-FIP equations based on characteristic strength f_{ptk} = 1860 MPa. The friction coefficient of prestressed steel = 0.15, the wobble coefficient = 0.0025 and anchor slip = 4.2 mm.

Figures 5.20 to 5.23 show the instantaneous and time-dependent development of stress resultants along the bridge length for both systems of skew support alignment. It should be noted here that the stress resultants shown in these figures include the primary effects of prestressing. For example, the bending moment $M_{y'}$ includes the values $P \cdot e_{z'}$ and $M_{z'}$ includes $P \cdot e_{y'}$, etc. Figures 5.24 to 5.26 depict the variation of displacements in the three global directions for both alignments.

Two other parameters are believed to have influence on the time-dependent stresses and deformations in conjunction with the alignment of skew supports in curved bridges; these are: the magnitude of the prestressing force including creep and the radius of curvature of the bridge. Therefore, the bridge of Figure 5.18 is reanalyzed for an increase in the prestressing force to 40 MN and again for a reduction in the bridge radius to 100 m. Figure 5.27 and 5.28 show the results of these two analyses.

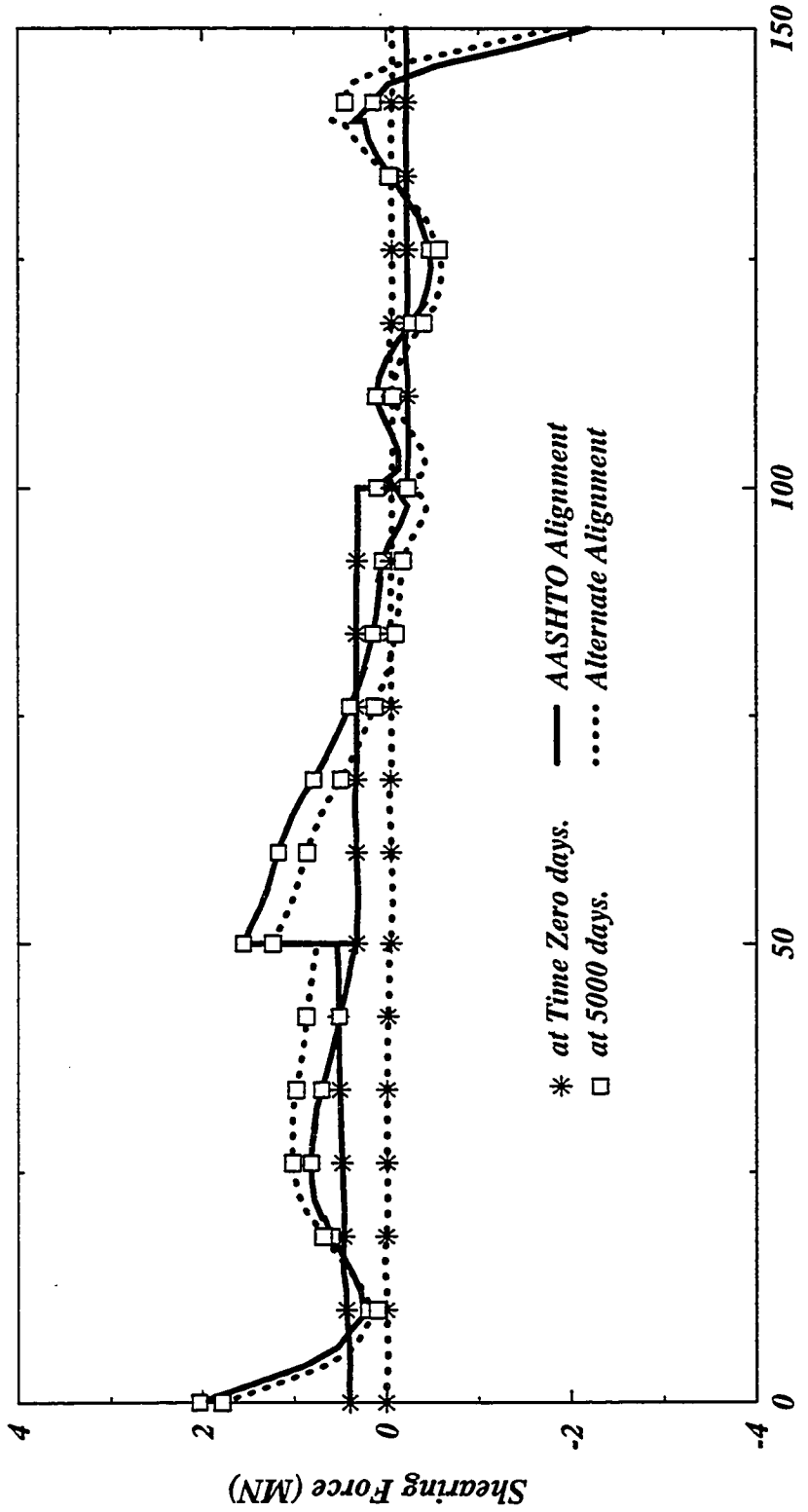

Figure 5.20 **Shearing Force in the Local y' Direction (Transverse Shear), (Prestressing Force = 30.4 MN; Radius = 134 m).**

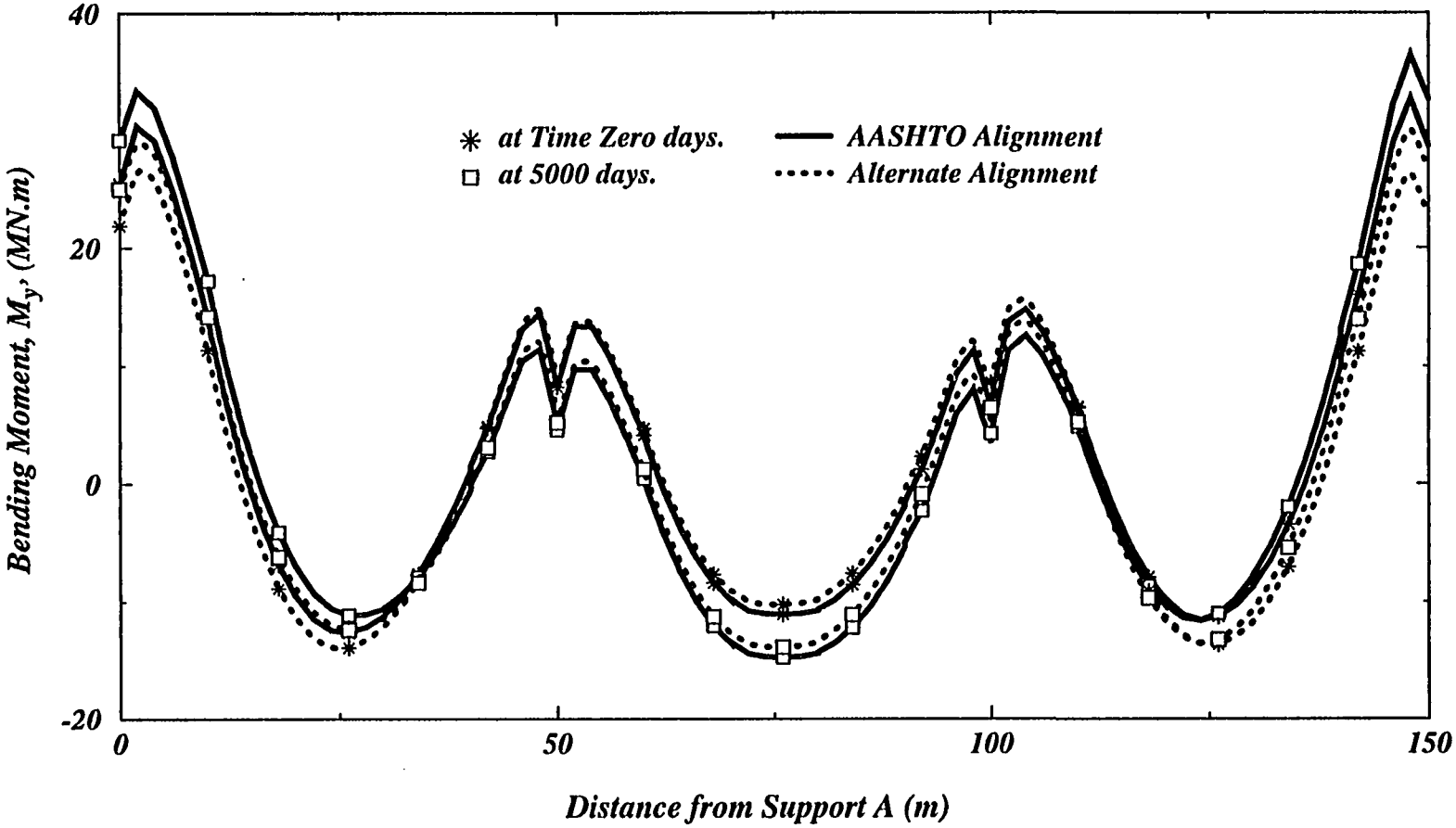

Figure 5.21 **Bending Moment about the Local y' Direction, (Prestressing Force = 30.4 MN; Radius = 134 m).**

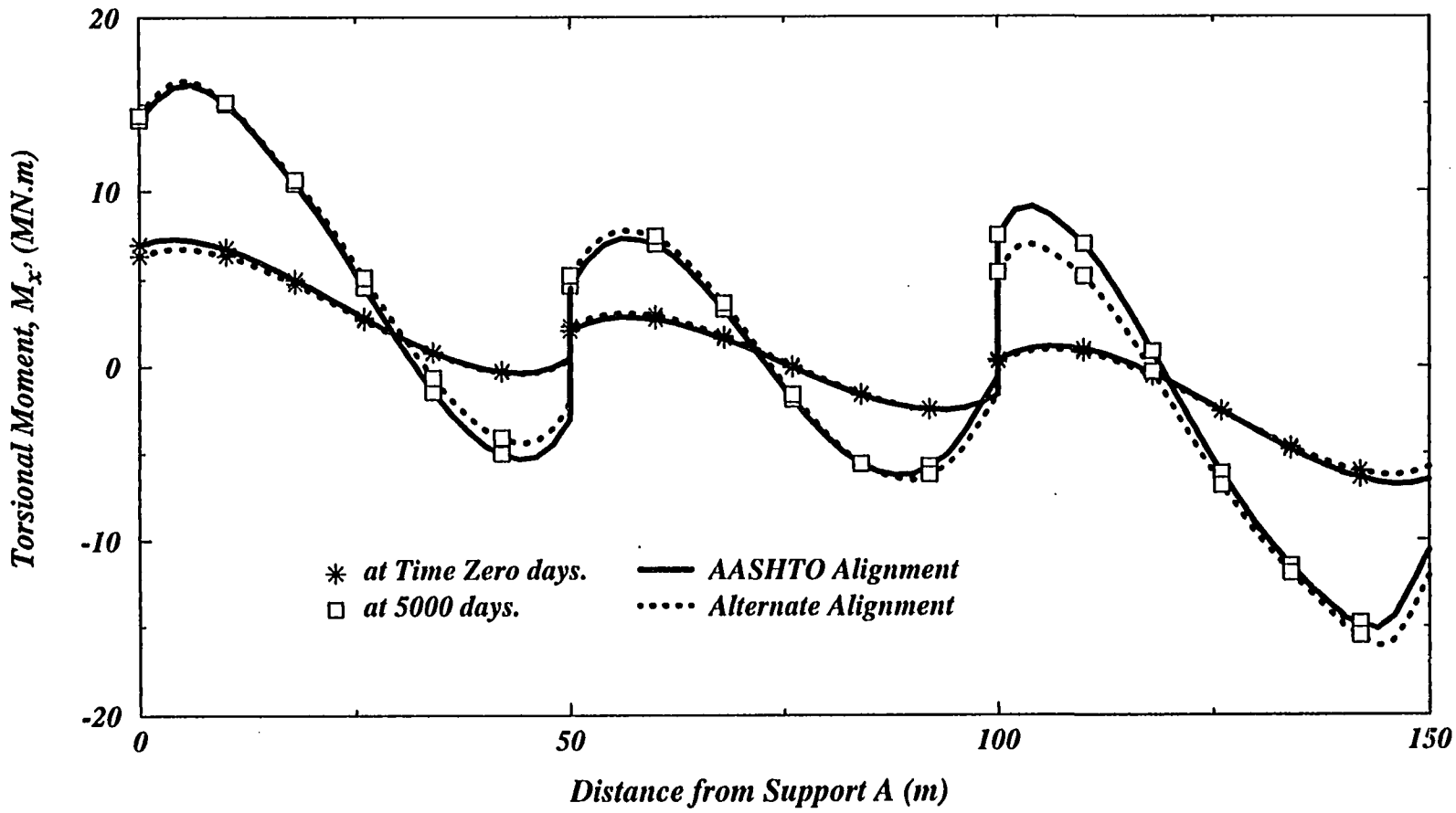

Figure 5.22 **Torsional Moment about the Local x' Direction, (Prestressing Force = 30.4 MN; Radius = 134 m).**

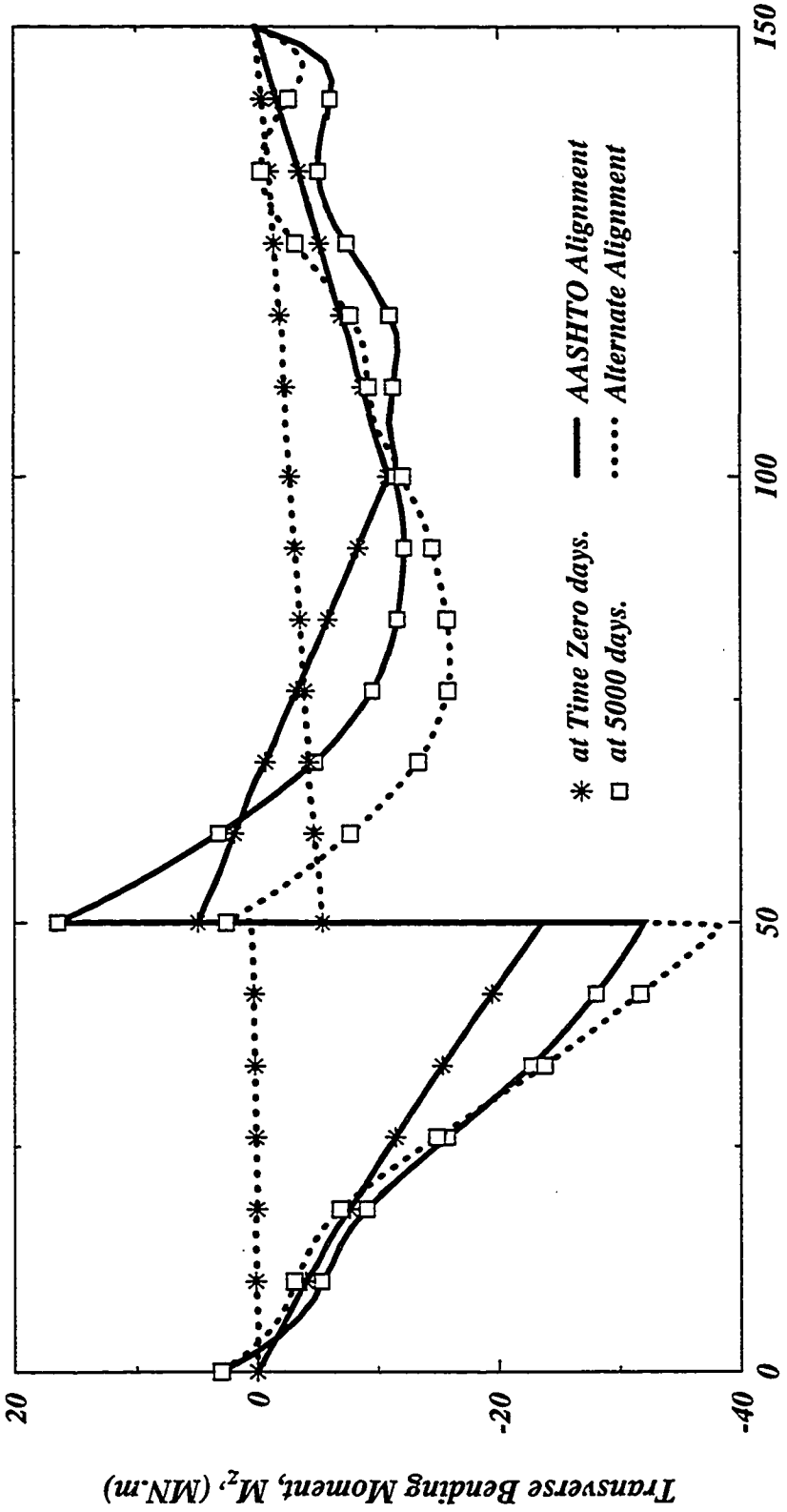

Figure 5.23 **Transverse Bending Moment about the Local z' Direction, (Prestressing Force = 30.4 MN; Radius = 134 m).**

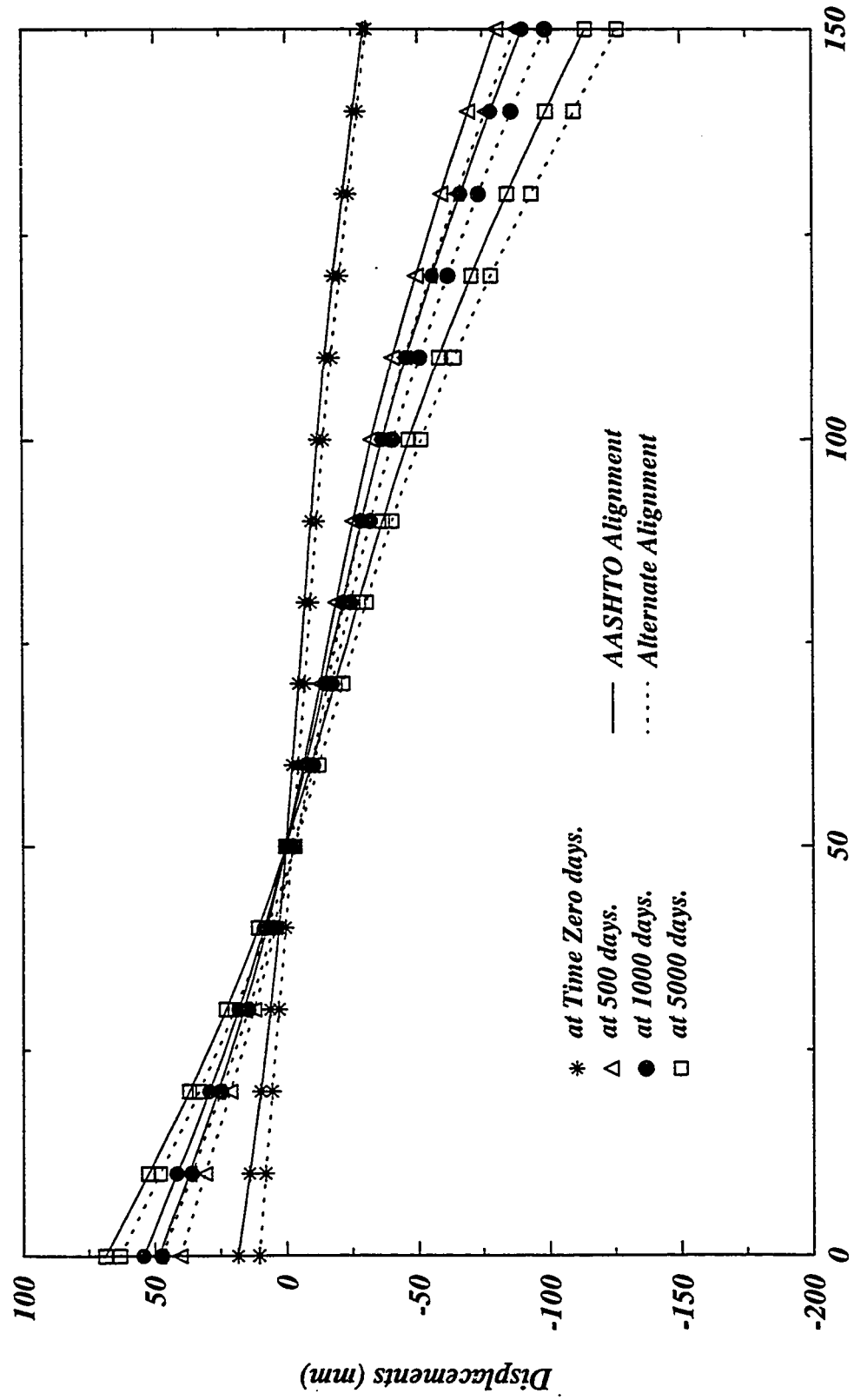

Figure 5.24 **Development of Displacement in the Global *x*-Direction (Prestressing Force = 30.4 MN; Radius = 134 m).**

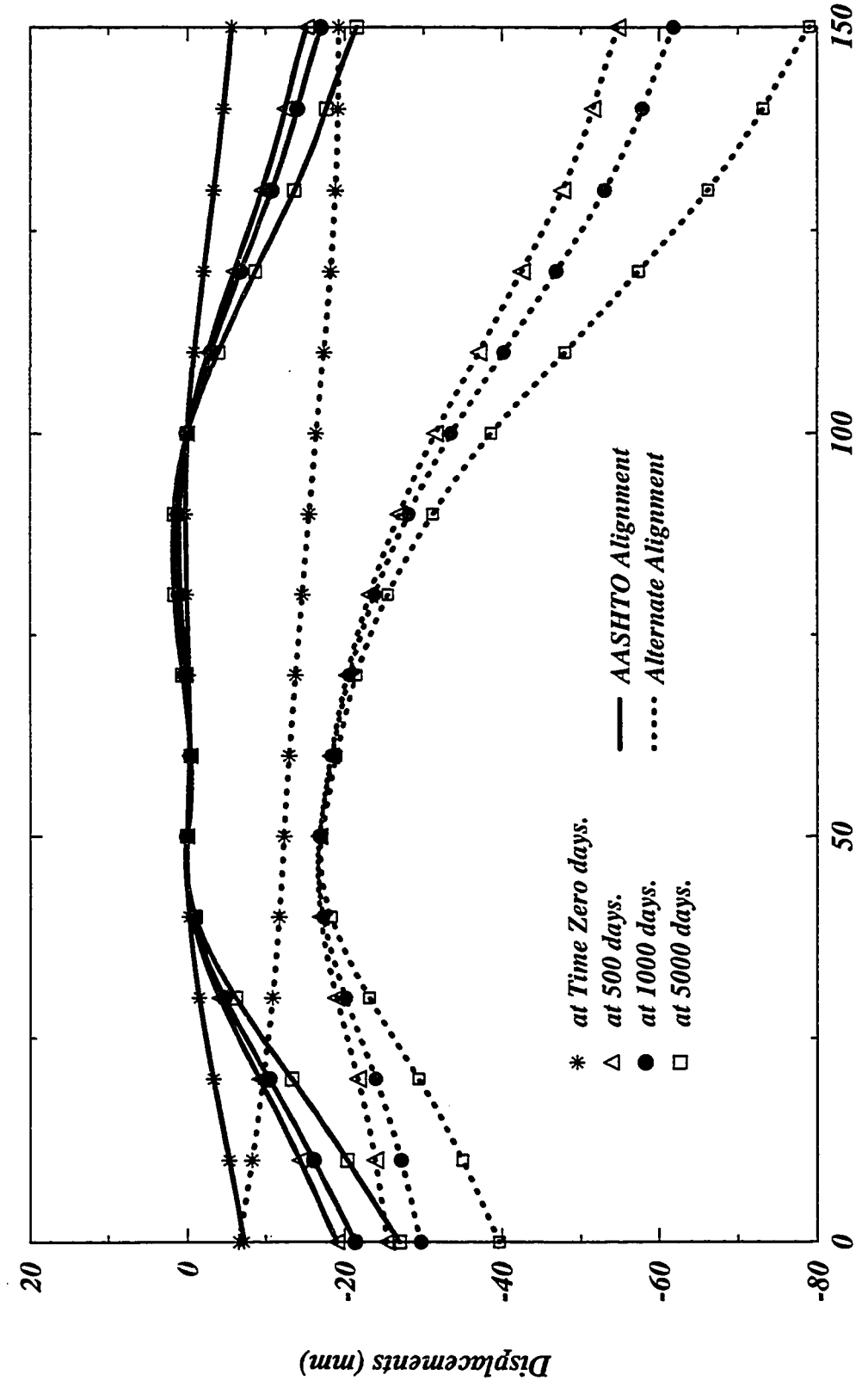

Figure 5.25 Development of Deflection in the Global y-Direction (Prestressing Force = 30.4 MN; Radius = 134 m).

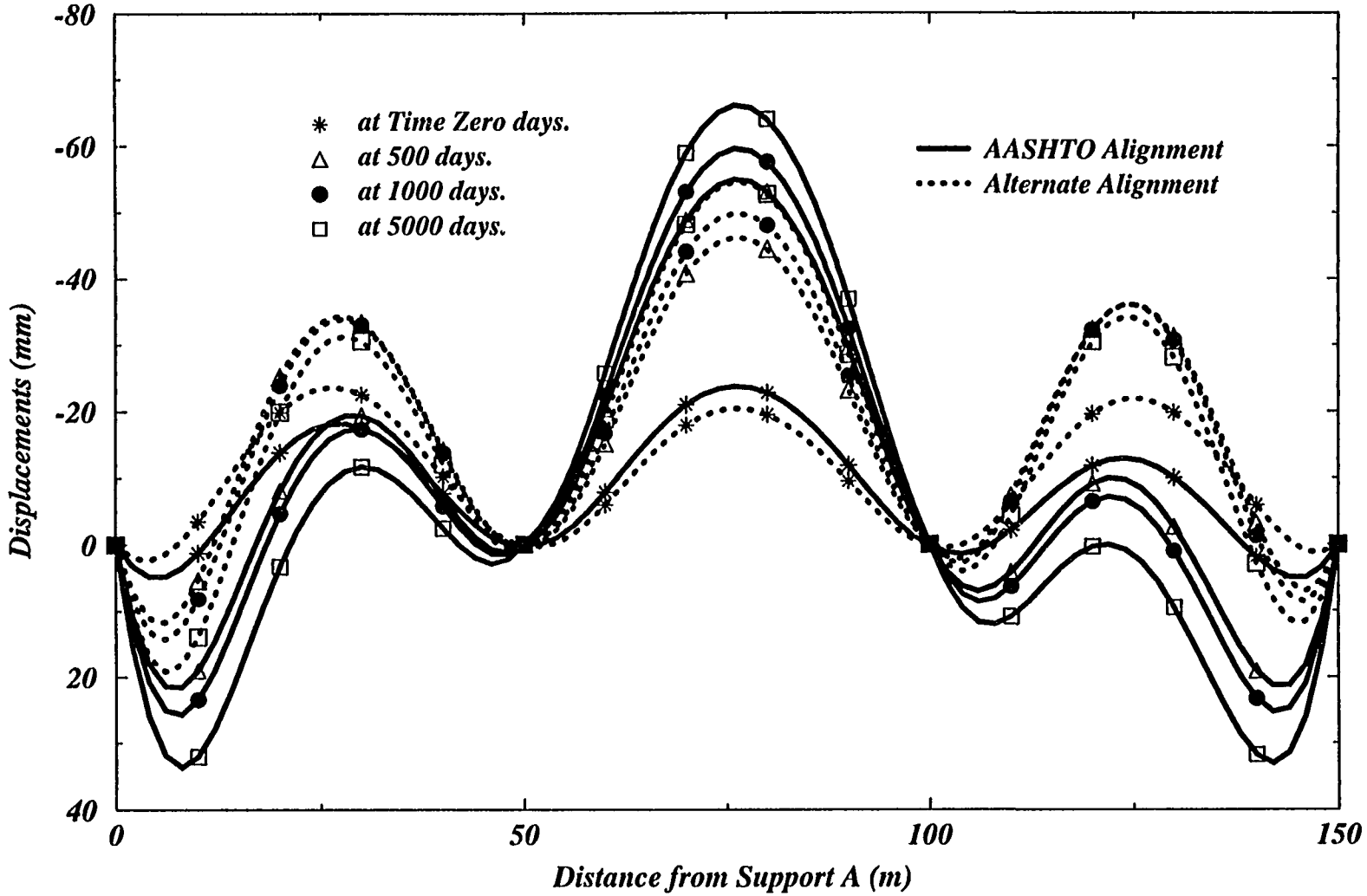

Figure 5.26 **Development of Deflection in Global *z* Direction (Prestressing Force = 30.4 MN; Radius = 134 m).**

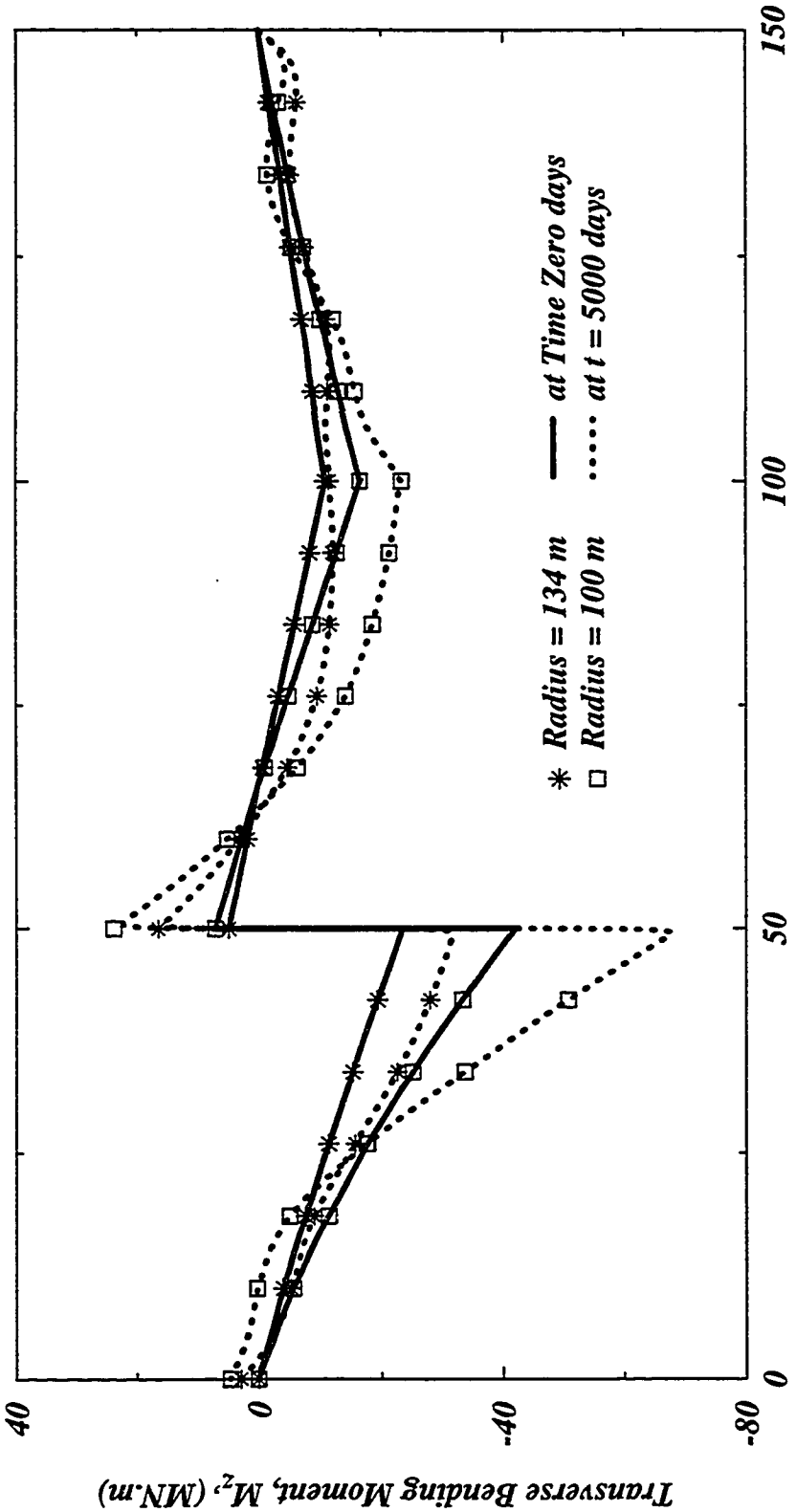

Figure 5.27(a) Transverse Bending Moment about the Local z' Direction, AASHTO Support Alignment (Prestressing Force = 30.4 MN).

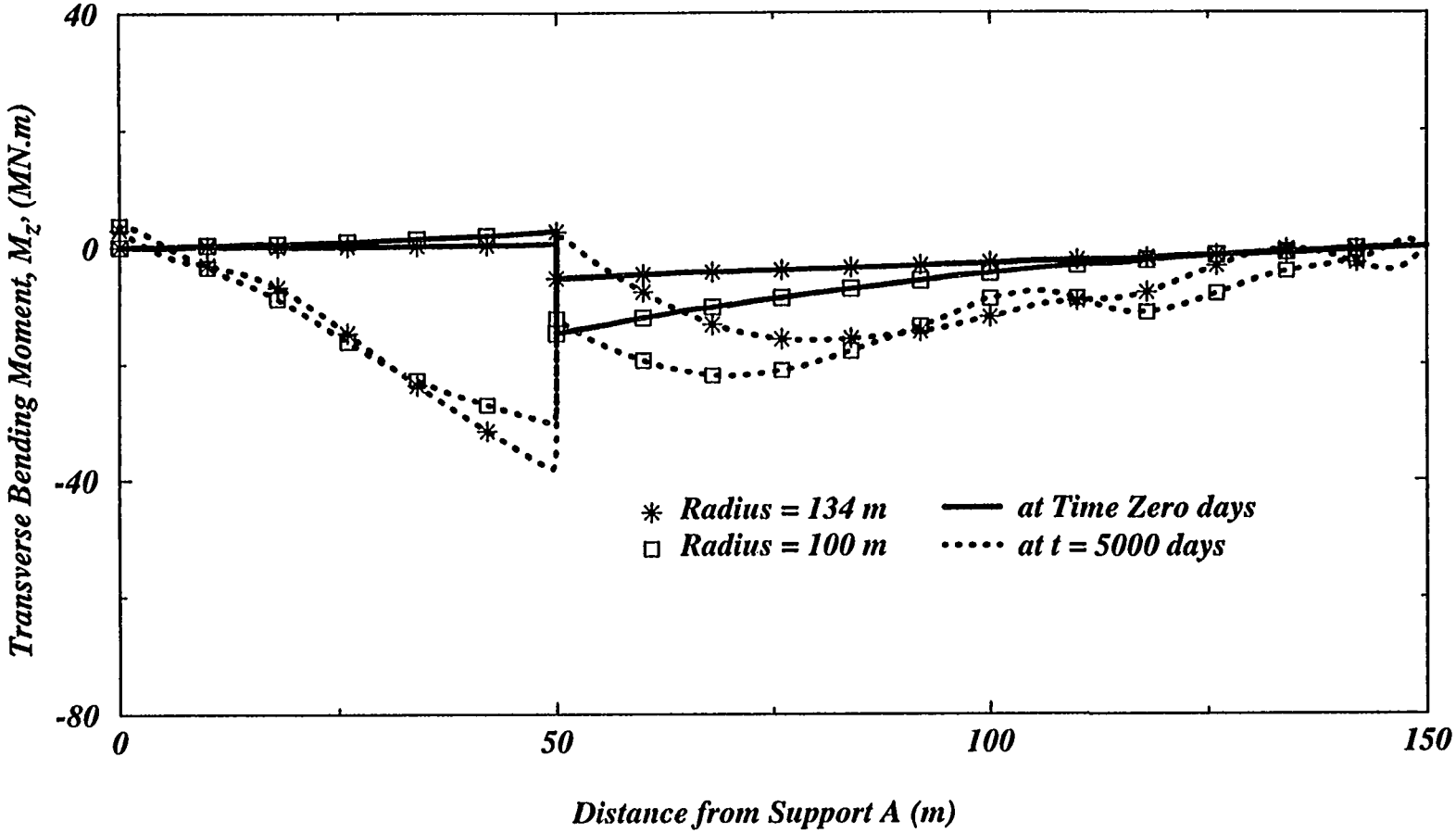

Figure 5.27(b) **Transverse Moment about the Local z' Direction, Alternate Support Alignment (Prestressing Force = 30.4 MN).**

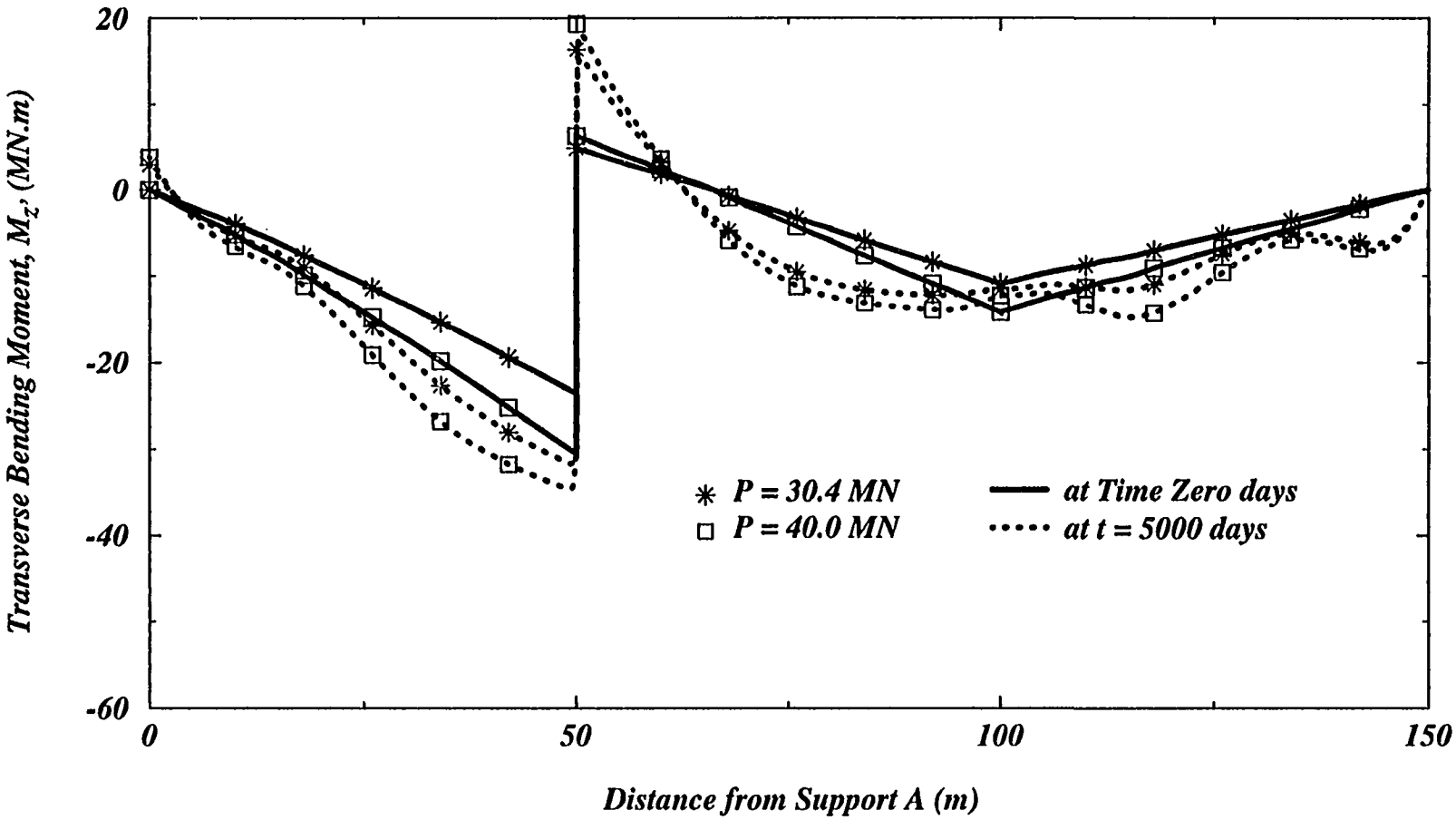

Figure 5.28(a) **Transverse Moment about the Local z' Direction, AASHTO Support Alignment.**

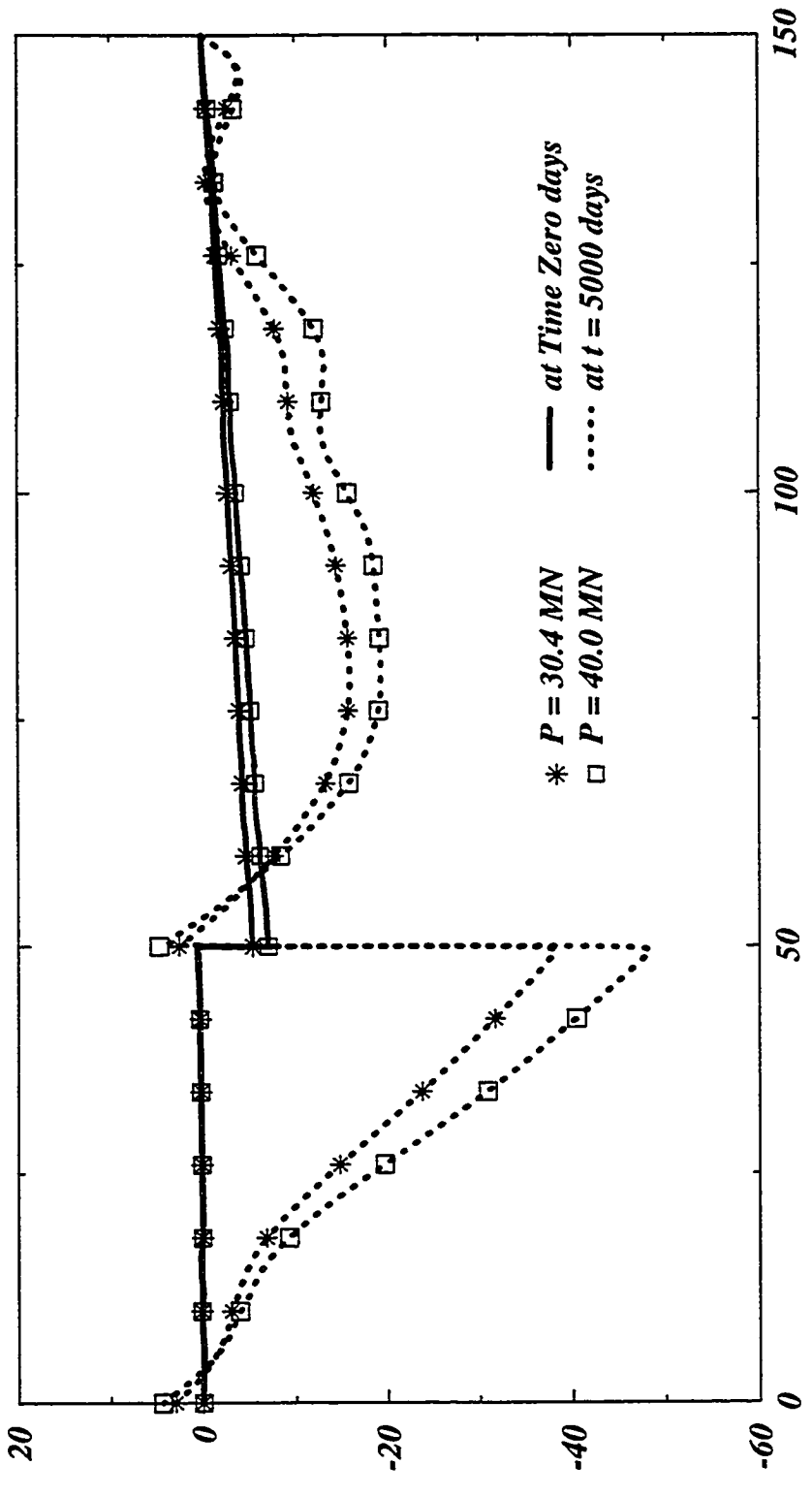

Figure 5.28(b) **Transverse Moment about the Local z' Direction, Alternate Support Alignment.**

5.4.2 Results of the Analysis

I- With Respect to the Stresses

In a comprehensive review of the results obtained from the two different skew alignment systems, which will be referred to as cases one and two, the following conclusions can be drawn:

- Shearing forces in local y' direction (Radial direction of the Bridge), developed with almost the same behaviour in the two cases. The forces were noticed to develop in greater values in short zones near the two ends of the bridge in the two cases. The time-dependent behaviour of the two structures has no distinct difference (Figure 5.20).

- Shearing forces in local z' direction (vertical global direction) were noticed to have very slight difference between the two cases. This can be explained as the vertical component of the reaction are not affected at all by the orientation of the other two components of reactions in the horizontal plan. Since the bridge is curved horizontally, only the geometry of the bridge and load distribution can affect the values of the vertical reactions obtained. Magnitude of shearing forces were also slightly changed from the original values at time zero days. The behavior of the bending moment about the local y' direction (Figure 5.21), as expected, follows the same behavior and rate of change as the shearing force in vertical global direction. In the second case, a slight drop in the bending moment curve was obtained, i.e., increase in negative moment and decrease in positive moment.

- The change in the torsional moment along the bridge length due to time-dependent effects is more pronounced in both cases of support alignment. Using the AASHTO alignment, the change in torsional moment was slightly less than that of the alternate

solution (Figure 5.22).

- The transverse bending moment about the local z'-direction is noticed to be highly affected by the skew support alignment. For the first case, even though the initial moment had greater values, it changed due to time-dependent effects by a ratio smaller than for the second case (Figure 5.23).

- The transverse bending moment was also studied under the effect of other parameters such as the amount of prestressing and the curvature of the bridge in plan. The bridge was reanalyzed using a radius of 100 m. For this smaller radius, the change in moment due to time-dependent effects was higher. This change also was noticed to be greater in the case where the AASHTO support alignment is used. This was a result of the higher restraint to the structure in the transverse direction using that alignment (Figure 5.27). The same conclusion was also drawn when higher prestress force was applied to the bridge. Higher prestress force produced higher time-dependent moments following the same aforementioned behaviour and having a greater effect in the case of the alternate alignment (Figure 5.28).

II- With Respect to the Deformations

- Movement of the bridge in the global x' direction, as shown in Figure 5.24, indicates higher effect in second case over the first one. The initial displacement of the nodes in that direction were almost the same for both alignments. On the other hand, development of this displacement with time was higher in the case of the alternate skew support alignment. Although the difference between the two alignments is small (about 16%), the AASHTO support alignment is recognized to give more accepted behaviour.

- Deformations of the bridge in the global y'-direction (Figure 5.25) were noticed to

be greatly affected by the support alignment. while in the AASHTO alignment the second support to the left is hinged and the second to the right is restrained in global y direction, it is realized that the alternate alignment does not restrain the movement in that direction at any point. This led to a small displacements in the first case than in the second one.

- The vertical deflection (global z'-direction) is shown in Figure 5.26. The bridge using the AASHTO alignment experienced smaller values of downward deflections in the outer spans than in the bridge with the alternate alignment. The change due to time-dependent effects was almost the same for both alignments.

5.4.3 Closing Remarks

The present study conducted on two suggested alignments of skew support in horizontally curved box-girder bridges, namely the AASHTO and an alternate alignments, has successfully highlighted the main characteristics and merits of each. Differences in their effects on the bridge both in the instantaneous and the time-dependent behaviour were obtained. The AASHTO support alignment showed more acceptable performance than the alternate one. Development of time-dependent stresses in most of its components, were of a smaller rate and values. Deformation of the structure on the long range were more accepted in magnitude using this alignment.

5.5 Conclusion

Throughout the present chapter, several examples and verification problems were presented to investigate and explore the behavior of segmentally erected structures under time-dependent effect. The study of a two-span continuous beam under the effect of incremental settlement of the central support showed excellent results in comparison with previous theoretical and experimental research work. A girder totally fixed at both ends

built from two cantilevers connected together at a later time was analyzed using the developed program TD-SFRAME. The results of the development of the mid-span positive bending moment was compared to the theoretical formula suggested earlier by Dezi and Tarantino (1991). Very good agreement was obtained between the two results.

The capabilities of the computer program TD-SFRAME was demonstrated by an example of a three-span post-tensioned prestressed segmental curved box-girder bridge. The bridge was built in 9-stages using the balanced cantilever method of construction. The analysis involved evaluation of both instantaneous and time-dependent stresses and deformations in each construction stage or time-interval. For every stage, addition of new element, prestressing cables and/or boundary condition was successfully performed. TD-SFRAME was able to determine the development of every parameter involved in the investigation of such structures and hence can be used for the prediction of the behavior of any similar structure during and after construction.

Finally, TD-SFRAME was utilized for a study into the effect of alignment of the skew supports on the development of time-dependent stresses and deformations in curved bridges. The study was conducted over a part of an existing prestressed single box-girder bridge. Two systems of skew support alignment, the AASHTO recommended alignment and an alternate alignment were used in the study. The results obtained showed an advantage of the first alignment over the second one.

CHAPTER SIX

Conclusions and Recommendations

6.1 Summery

In today's modern highway bridge systems, prestressed concrete box-girders have become the most frequently used type of bridges. Among these bridges, curved bridges are very common as a practical solution for complicated roadway alignments and crossing problems. Such structures, particularly those of medium and long spans, are normally built over a long period of time and, therefore, need to be constructed in stages. A continuous bridge can be cast span-by-span or assembled from precast or cast-in-place segments. In each stage of construction, units or segments of the bridge are cast or placed in the appropriate position and tied together by post-tensioned prestressing tendons.

During the construction process, the structure undergoes continuous changes in geometry, in the statical system or support conditions and in the distribution and magnitude of applied loads and prestressing. This leads to significant and continuous variations in the stresses and deformations during the construction period and after completion of the structure. Such variation occur because of the effects of creep and shrinkage of concrete and relaxation of prestressed steel.

Imposed deformations due to temperature variation in continuous structures also produce changes in the reactions and the internal forces. Development of these time-dependent and thermal stresses and deformations in curved bridges depends primarily on the restraint provided at each support. The analysis of such stresses and deformations is a

complex problem and is an essential step to predict the behaviour of these structures in order to achieve better design and performance.

The present investigation is concerned with the development of a rational numerical procedure and a reliable computer program that are capable of predicting the time-dependent stresses and deformations in curved prestressed concrete segmentally erected box-girder bridges. The analysis accounts for the effects of aging, creep and shrinkage of concrete and relaxation of prestressed steel, for the effects of sequence of construction, loading and prestressing and changes in geometry, the statical system and support conditions during construction and for the effects of temperature variation and support movements.

The structure is idealized as a space frame in which the concrete segments are modelled using multi-node isoparametric elements or two-node prismatic straight elements. Post-tensioned prestressing tendons of arbitrary profile in space are also included in the curved concrete elements and are defined by their eccentricities with respect to the nodal points. The stiffness method of structural analysis is employed to determine the instantaneous and time-dependent changes in displacements, reactions and stress resultants.

The analysis is performed step-by-step for which the time is divided into intervals. In each interval two analysis, instantaneous and time-dependent may be carried out. An instantaneous analysis is performed at the start of a time interval only when a new event takes place. Such events include addition or removal of new members, prestressing, loads or support conditions. In the time-dependent analysis for any time-interval, the hypothetical free strain due to creep and shrinkage of concrete is calculated at individual sections using the stress history of all previous intervals. This free strain is used to calculate nodal

restraining forces for each element of the structure. Relaxation of prestressed steel is treated as an initial stress.

The numerical procedure is implemented in a computer program, TD-SFRAME (Debaiky and El-Badry, 1997) which is a modified version of program SFRAME developed by Maher (1985). The time variation of concrete properties such as the modulus of elasticity, creep and shrinkage, can be calculated automatically by TD-SFRAME from equations given either by the CEB-FIP 1990 Model Code or the ACI Committee 209. Relaxation of prestressed steel can be calculated based on CEB-FIP recommendations. These material parameters can be also specified by the analyst as input to the program.

The computer program has been tested using analytical and experimental results previously published by other investigators. The applicability of the program has been demonstrated by studying the behaviour during erection and after completion of construction of a three-span continuous curved prestressed concrete box-girder bridge built segmentally by the cantilever construction method. Finally, the program has been employed in an investigation into the effects of skew support alignments on the development of the time-dependent stresses and deformations due to creep, shrinkage and relaxation in curved concrete bridges.

6.2 Conclusions

The main conclusions drawn from the present investigation are:

1. The numerical procedure presented in this thesis enables the analysis of the instantaneous and the time-dependent stresses and deformations that develop in segmentally erected prestressed concrete curved box-girder bridges due to the effects of loads, prestressing, sequence of construction, changes of geometry and

boundary conditions and the effects of creep and shrinkage of concrete and relaxation of prestressed steel during and after construction.

2. The computer program TD-SFRAME has been shown to be useful and valuable tool for the analysis of the time-dependent effects on segmentally erected bridges of arbitrary geometry.
3. The results of analysis of the bridge examples presented in this thesis show the significance of the time-dependent deformations and internal forces on the serviceability of curved bridges. For example,
   a) Prediction of stresses and deformations in segmentally erected curved bridges can be considerably in error if the effects of creep, shrinkage and relaxation are ignored. Considerable discontinuity can develop during construction due to the time-dependent deformations at the ends of two joining parts of a bridge. Such deformations can be accurately predicted by the present method of analysis and can be used to determine the adjustment in the formwork and the pre-camber required to eliminate the discontinuity.
   b) The orientation of movement of skew supports in curved bridges has a significant influence on the time-dependent internal forces. The study conducted in this thesis has shown that the AASHTO recommendation for skew support alignment is more advantageous than an alternate alignment which allows movements in the tangential and radial direction.

6.3 Recommendations for Future Research

Through the progress of the present study and the development of the computer program several points were observed and believed to be of great importance. Detailed

simulation of concrete bridges with arbitrary geometry can not be achieved unless refinements are made to the current version of the computer program. Such refinements may include but not limited to the following:

1. It is well established that the presence of non-prestressed (reinforcing) steel in concrete structures has a great effect on their time-dependent behaviour. This steel restrains the free strain that takes place in concrete due to creep and shrinkage and, thus, produces a redistribution of stresses in individual cross sections. Therefore, it would be useful to modify TD-SFRAME to include modelling of non-prestressed steel within the concrete elements and to account for its effects on the time-dependent behaviour of curved bridges.
2. In the present study, a concrete member or segment is assumed to be precast or cast in place in a single stage. In most cast-in-place bridges, box-girder cross-sections are often built-up in three casts in which the bottom slab is cast first, followed by the webs and then the top slab. Also, in girder-type bridges, the deck slab is normally cast some time after placing the precast girders or casting the cast-in-place girders. This type of construction creates cross-sections with parts of different ages and time-dependent properties. TD-SFRAME can be modified to account for this type of multi-stage construction.
3. As outlined in Chapter 4, the formulation of the isoparametric curved element of Jirousek is based on the linear behaviour of both concrete and steel. The material nonlinearity and the effects of cracking of concrete and yielding of steel are beyond the scope of this study. Cracking of concrete is known to have significant effects such as a reduction in stiffness and, hence, increase in deflections, high

concentration of stresses in the compression zones and large strains in both concrete and non-prestressed steel. Incorporation of the non-linear behaviour of the material into the present program and studying its effects is highly recommended.

4. Time-dependent analysis presented in this study is based on the evaluation of the hypothetical free strain in any time-interval from the stress history during all the preceding time-interval (Chapter 3). With this approach, a relatively large computer storage is required, particularly for the analysis of an actual complicated structure in which large number of cross-sections, prestressed tendons, time intervals, and boundary conditions are involved. Thus, a technique for reduction of the computer storage required for the analysis is desirable.

Finally, it is believed that the present research work can be considered as a solid corner stone to several future investigations for development of state-of-the-art software package useful for the analysis of curved segmental structures.

List of References

Abdel Halem, M., (1982), "Nonlinear Analysis of Segmental Concrete Bridge by Finite Element Method", Ph.D. Thesis, Pennsylvania State University, Pennsylvania, September 1982, 236 pp.

Abdel Karim, A.M., (1991), "Analysis and Design of Precast/Prestressed Concrete Sliced-Girder Bridges", Ph.D. Thesis, University of Nebraska at Lincoln, Nebraska, November 1991, 279 pp.

ACI Committee 209 (1992), Prediction of Creep, Shrinkage and Temperature Effects in Concrete Structures, American Concrete Institute

Bazant, Z.P., (1972), "Prediction of Concrete Creep Effects Using Age-Adjusted Effective Modulus Method", Journal of the American Concrete Institute, ACI Proceedings, Vol. 69, No. 4, April 1972, PP. 212-217.

Bazant, Z.P. and El-Nimeiri, M. (1974), "Stiffness Method for Curved Box Girders at Initial Stress", Journal of the Structural Division, ASCE Proceedings, Vol. 100, No. ST10, October 1974, pp. 2071-2090.

Bazant, Z.P. and Najjar, L.T., (1973), "Comparison of Approximate Linear Methods for Concrete Creep", Journal of the Structural Division, ASCE Proceedings, Vol. 99, No. ST9, September 1973, pp. 1851-1874

Bell, L.C. and Heins, C.P., (1970), "Analysis of Curved Girder Bridges", Journal of the Structural Division, ASCE Proceedings, Vol. 96, No. ST8, August 1970, pp. 1657-1973.

Brown, R.C., Jr., Burns, N.H. and Breen, J.E., (1974), "Computer Analysis of Segmentally Erected Precast Prestressed Box Girder Bridges", Centre for Highway Research, University of Texas at Austin, Austin, Texas.

CEB-FIP, (1978), Model Code for Concrete Structures, Comité Euro-International du Béton - Federation International de la Precontrainte, Paris, 1978, 348 pp.

CEB-FIP, (1990), Evaluation of Time Dependent Behavior of Concrete, Comite Euro-International du Beton, Bulletin d'information No. 199, Paris, Aout 1990.

Cook, R.D., (1992), "Concepts and Applications of Finite Element Analysis", 3rd Edition, John Wiley and Sons, New York, 1989, 630 pp.

Debaiky, A. El-Badry (1997), User's Manual and Computer Program TD-SFRAME: Time-Dependent Analysis of Space FRAMEs, Research Report, School for Building,

Concordia University, Montreal, Quebec.

Dezi, L. and Tarantino, A.M., (1991), "Time Dependent Analysis of Concrete Structures with a Variable Structural System", Journal of the American Concrete Institute, ACI Material Journal, Vol. 88, No. 3, May-June 1991, pp. 320-324.

Dischinger, F., (1937), "Untersuchungen über die Knicksicherheit, die elastiche Verformung das Kriechen des Beton bei Bogenbrücken", Der Bauingenieur, 18, No. 33-4, 1937, pp. 487-520.

El-Amin, F.M. and Brotton, (1976), "Horizontally Curved Beam Finite Element Including Warping", International Journal for Numerical Methods in Engineering, Vol. 10., pp. 1397-1408.

El-Badry, M.M., (1988), "Serviceability of Concrete Structures", Ph.D. Thesis, Department of Civil Engineering, The University of Calgary, Calgary, Alberta, November 1988, 294 pp.

El-Badry, M.M. and Ghali, A. (1985), User's Manual and Computer program CPF: Cracked Plane Frame in Prestressed Concrete, Research Report No. CE85-2, Department of Civil Engineering, The University of Calgary, Calgary, Alberta, January 1985, (Revised August 1990)

El-Badry, M.M. and Ghali, A., (1989), "Serviceability Design of Continuous Prestressed Concrete Structures", Prestressed Concrete Institute, PCI Journal, Vol. 34, No. 1, January-February 1989, pp. 54-91.

Engel, S., (1967), "Structural Analysis of Circular Curved Beams", Journal of Structural Division, ASCE Proceedings, Vol. 93, No. ST1, January 1967, pp. 221-234.

England, G.L. and Illiston, J.M., (1965), "Method of Computing Stress in Concrete from a History of Measured Strain", Civil Engineering and Public Works Review, London, Vol. 60, April 1965, pp. 692-694.

Faber, O., (1927), "Plastic Yield, Shrinkage and Other Problems of Concrete and Their Effect on Design", Minutes of Proceedings of Institute of Civil Engineers, Vol. 225, Part I, London, 1927.

Ferguson, G.H. and Clark, R.D., (1979), "A Variable Thickness Curved Beam and Shell Stiffening Element with Shear Deformation", International Journal for Numerical Method in Engineering, Vol. 14, pp. 581-592.
Ghali, A. and Favre, R., (1994), Concrete Structures: Stresses and Deformations, Chapman and Hall, London and New York, 1994, 444 pp.

Ghali, A. and Neville, A.M., (1989), Structural Analysis: A Unified Classical and Matrix Approach, 3rd Edition, Chapman and Hall, London, 1989, 870 pp.

Ghali, A., Sisodiya, R.G. and Tadros, G.S., (1974), "Displacements and Losses in Multi-Stage Prestressed Members", Journal of Structural Division, ASCE Proceedings, Vol. 100, No. ST11, November 1974, pp. 2307-2322.

Ghali, A. and Trevino, J., (1985), "Relaxation of Steel in Prestressed Concrete", Prestressed Concrete Institute, PCI Journal, Vol. 30, No. 5, September-October 1985, pp. 82-94.

Glanville, W.H., (1930), 'Studies in Reinforced Concrete, III: The Creep Flow of Concrete Under Load", Building Research Technical Paper No. 12, Department of Scientific and Industrial Research, London, 1930, 39 pp.

Hsu, Y.T., Fu, C.C. and Schelling, D.R., (1990), "An Improved Horizontally-Curved Beam element", Computers and Structures, Vol. 34, No. 2, pp. 313-318.

Jirousek, J., Bouberguig, A. and Saygun A. (1979), "A Macro-Element Analysis of Prestressed Curved Box Girder Bridges", Computers and Structures, Vol. 10, pp. 467-482.

Jirousek, J., (1981), "A Family of Variable Section Curved Beam and Thick-Shell or Membrane-Stiffening Isoparametric Elements", International Journal for Numerical Methods in Engineering, Vol. 17, pp. 171-186.

Kabir, A.F., (1976), "Nonlinear Analysis of Reinforced Concrete Panels, Slabs, Shells for Time-Dependent Effects", Ph.D. Thesis, Division of Structural Engineering and Structural Mechanics, University of California, Berkeley, UC-SESM Report No. 76-6, December 1976.

Kashima, S. and Breen, J.E., (1975), "Construction and Load Tests of Segmental Precast Box Girder Bridge Model", Centre for Highway Research, University of Texas at Austin, Austin, Texas, 261 pp.

Ketchum, M.A., (1986), "Redistribution of Stresses in Segmentally Erected Prestressed Concrete Bridges", Report No. UCB/SESM-86/07, Division of Structural Engineering and Structural Mechanics, University of California at Berkeley, Berkeley, California, May 1986, 238 pp.

Khalil, M.S., (1979), "Time Dependent Non-Linear Analysis of Prestressed Concrete Cable-Stayed Girders and Other Concrete Structures", Ph.D. Thesis, Department of Civil Engineering, University of Calgary, Calgary, Alberta, April 1979, 246 pp.

Kim, J.K., (1990), "Prediction of Time-Dependent Deformations of Concrete and Bridge Deflection Probability", Ph.D. Thesis, Department of Civil Engineering, Northwestern University, Evanston, Illinois, December 1990, 182 pp.

Kountouris, C.L., (1970), "Time-Dependent Forces Induced by Settlement of Supports in Continuous Prestressed Concrete Structures", M.Sc. Thesis, Department of Civil

Engineering, The University of Calgary, Calgary, Alberta, April 1970, 103 pp.

Lai, L.Y., (1995), "Seismic Analysis of Horizontally Curved Girder Bridges", 7th. Canadian Conference on Earthquake Engineering, Montreal, Quebec, 1995, pp. 747-754.

Lacey, G.C. and Breen, J.E., (1969), "Long Span Prestressed Concrete Bridges of Segmental Construction, State of the Art Report", Centre for Highway Research, University of Texas at Austin, Austin, Texas.

Lin, T.Y., (1963), "Load Balancing Method for Design and Analysis of Prestressed Concrete Structures", Journal of the American Concrete Institute, ACI Proceedings, Vol. 60, No. 6, 1963, pp. 719-741.

Maher, P.G., (1985), "Torsion Control in Curved Prestressed Bridges", M.A.Sc. Thesis, University of Calgary, Calgary, Alberta, 1985, 202 pp.

Maslov, G.N., (1940), "Thermal Stress State in Concrete Masses with Account to Creep of Concrete", Izvestia Nauchno-Issledovatelskogo Institute VNII Gidrotekhniki, Gosenergoizdat. USSR, Vol. 28, 1940, pp. 175-188.

McHenry, D., (1943), "A New Aspect of Creep in Concrete and Its Application to Design" Proceedings of the American Society of Testing Materials (ASTM), Vol. 43, 1943, pp. 1069-1084.

Menn, C., (1990), "Prestressed Concrete Bridges", Birkhauser Verlag, Berlin, 1990, 535 pp.

Müller, H.S. and Hilsdrof, H.K., (1982), "Comparison of Prediction Methods for Creep Coefficients of Structural Concrete with Experimental Data", Fundamental Research on Creep and Shrinkage of Concrete, Edited by Wittmann, Martinus Nijhoff Publications, The Hague, 1982, pp. 269-278.

Neville, A.M., Dilger, W.H. and Brooks, J.J., (1983), Creep of Plain and Structural Concrete, Construction Press, London and New York, 1983, 361 pp.

Nielsen, L.F., (1970), "Kriechen und Relaxation des Betons", Beton und Stahlbetonbau, 65, 1970, pp. 272-275.

Rao, R.S., (1976), "Creep Prediction and Creep Analysis for Concrete Structures - A Critical Appraisal of the Literature", M.Sc. Thesis, Civil Engineering Department, University of Calgary, Calgary, Alberta, 1976.

Reddy, M.N. and Tuma, J.J., (1967), "Analysis of Laterally Loaded Continuous Curved Beams", Journal of Structural Engineering, ASCE Proceedings, Vol. 93, No. ST1, January 1967, pp. 495-513

Ross, A.D., (1958), "Creep of Concrete Under Variable Stress", Journal of the American Concrete Institute, ACI Proceedings, Vol. 54, No. 3, March 1958, pp. 739-758.

Rozvany, G.I.N., (1963), Discussion to "Load Balancing Method for Design and Analysis of Prestressed Concrete Structures", Journal of the American Concrete Institute, ACI Proceedings, Vol. 60, No. 12, 1963, pp. 1862-1870.

Rüsch, H., Jungwirth, D. and Hilsdrof, H., (1973), "Kritische Sichtung der Einflüsse von Kriechen und Schwinden des Betons auf das Verhalten der Tragwerke", Beton and Stahlbetonbau, Vol. 68, Nos. 3, 4 and 5, 1973.

Scordelis, A.C., (1966), "Analysis of Simply Supported Box Girder Bridges", Research Report No. UCB/SESM 66-17, University of California at Berkeley, Berkeley, California, 1966.

Scordelis, A.C., (1967), "Analysis of Continuous Box Girder Bridges", Research Report No. UCB/SESM 67-25, University of California at Berkeley, Berkeley, California, 1967.

Tadros, M.K., Ghali, A. and Dilger W.H., (1980), User's Manual and Computer program, "Analysis of Stresses and Deformation in Segmental Construction", Research Report No. CE80-11, University of Calgary, Calgary, Alberta, 1980. 48 pp.

Tadros, M.K., Ghali, A. and Dilger W.H., (1979), "Long Term Stresses and Deformations of Segmental Bridges", Prestressed Concrete Institute, PCI Journal, Vol. 24, No. 4, July-August 1979, pp. 66-87.

Thornton, W.A. and Master, B.G., (1977), "Direct Stiffness Formulation for Horizontally Curved Beams", Journal of Structural Division, ASCE Proceedings, Vol. 103, No. ST1, January 1977, pp. 284-289.

Timoshenko, S.P. and Gere, J.M., (1961), Theory of Elastic Stability, Second Edition, McGraw-Hill, New York, 521 pp.

Trost, H., (1967), "Auswirkungen des Superpositionsprinzips auf Kriech und Relaxationsprobleme bei Beton und Spannbeton, Beton und Stahlbetonbau 62, No. 10, 1967, pp. 230-238 and No. 11, 1967, pp. 261-269.

Van Zyl, S.F. (1978), "Analysis of Curved Segmentally Erected Prestressed Concrete Box Girder Bridges", Ph.D. Thesis, SESM Report No. 78-2, University of California at Berkeley, Berkeley, California, 1978.

Vlasov, V.Z., (1961), "Thin Walled Elastic Beams", Israel Program for Scientific Translations, Jerusalem, Israel, 1961.

Wang, T.M. and Merrill, T.F., (1988), "Stiffness Coefficients of Noncircular Curved Beams", Journal of Structural Engineering, ASCE Proceedings, Vol. 114, No. 7, July

1988.

Whitney, C.S., (1932), "Plain and Reinforced Concrete Arches", American Concrete Institute, Journal of the American Concrete Institute, ACI Proceedings, Vol. 28, 1932, pp. 479-519.

Ziadat, G., (1988), "Time-Dependent Analysis of Prestressed Concrete Segmental Bridges", Ph.D. Thesis, University of Bristol, Bristol, U.K., November 1988, 320 pp.